Russian Chemical Reviews **71** (5) 347 – 381 (2002) © 2002 Russian Academy of Sciences and Turpion Ltd

DOI 10.1070/RC2002v071n05ABEH000717

Structure of X-ray photoelectron spectra of lanthanide compounds†

Yu A Teterin, A Yu Teterin

Contents

I.	Introduction	347
II.	Lanthanide trifluorides	348
III.	Lanthanide oxides	363
IV.	General rules for the formation of the XPS spectral structure of lanthanide compounds	371
V.	Conclusion	378

Abstract. The results of the X-ray photoelectron spectroscopy studies of the electronic structures of trifluorides, oxides and other compounds of Sc, Y and lanthanides (Ln) from La to Lu, except for Pm, in the binding energy range from 0 to 1350 eV are generalised. The established dependences of the Ln4*f* binding energies and the relative intensities of lines on the atomic number *Z* do not contradict the theoretical data stating that the Ln4*f* atomic orbitals (AO) participate markedly in the formation of molecular orbitals (MO) in the lanthanide compounds. It is established that inner valence molecular orbitals (IVMO) composed of the metal Sc3*p*, Y4*p*, Ln5*p* AO and the ligand L(O,F)2*s* AO are formed in these systems in addition to the outer valence molecular orbitals (OVMO). It is shown that the spectral fine structure caused by multiplet splitting, many-body perturbation and dynamic effects is correlated with the lanthanide oxidation state, the spin state of ions and the mechanisms of the secondary electronic processes accompanying the photoemission and can serve as a characteristic for identification of lanthanide compounds. Charge induction is discussed using titanium and niobium double oxides as examples. The bibliography includes 206 references.

I. Introduction

The lanthanide (Ln) group includes elements with atomic numbers (Z) in the $58 \leqslant Z \leqslant 71$ range. Together with scandium, yttrium, and lanthanum, they form the class of rare earth elements (REE) and can be divided into two subgroups, namely, cerium [(La), Ce, Pr, Nd, Pm, Sm, Eu] and yttrium (Gd, Tb, Dy, Ho, Er, Tm, Yb, Lu) subgroups. The electronic configurations of lanthanide atoms can be expressed by the general formula $\{Xe\}4f^n5d^m6s^2$, where $0 \leqslant n \leqslant 14$, $m = 0, 1$. In the ground state, lanthanides, except for lanthanum, gadolinium, lutetium and, possibly, terbium, contain no Ln5*d* electrons ($m = 0$); however, transition of one or two electrons from the Ln4*f* to the Ln5*d* shell does not require much energy. In compounds, lanthanides can exhibit different valences, II, III and IV, the trivalent state being the most typical.[1–4]

Metallic lanthanides, their chemical compounds and alloys are extensively used in various branches of science and engineering. Thus the rare earth element alloys of the $SmCo_5$ type are used to produce permanent magnets possessing tremendous energy.[5,6] Samarium, europium and gadolinium, characterised by high absorption ratios for thermal neutrons, and their compounds are used in nuclear industry. Oxides of these lanthanides are parts of protective ceramic coatings of nuclear reactors; they are suitable for the manufacture of control rods.[5] Lanthanide additives are used in catalysis.[7,8] Yttrium, lanthanum and other lanthanides are employed to produce high-temperature superconductors. The development of efficient processes for the isolation of pure lanthanides and for the preparation of their compounds possessing specified physicochemical properties requires the knowledge of their electronic structures and types of chemical bonding. For this purpose, rare earth metals are actively studied by X-ray photoelectron spectroscopy (XPS).[9–17]

Currently, XPS studies of the electronic structures of substances are performed using expensive spectrometers operating with both X-ray and synchrotron exciting radiations. However, the use of these spectrometers for the investigation of lanthanide compounds is associated with a number of problems because, due to the presence of unpaired Ln4*f* electrons and specific features of chemical bonding in these compounds and to secondary electronic processes which accompany electron photoemission, the X-ray photoelectron (XPS) spectra of these compounds in the binding energy (E_b) range from 0 to 1350 eV (in which the XPS spectra are normally recorded) contain complex fine structures. This hampers the quantitative elemental analysis of lanthanide compounds and makes difficult the determination of their oxidation states on the basis of the traditional characteristics of the XPS spectra (line intensities and chemical shifts). Therefore, the efforts of researchers are concentrated on the interpretation of the fine structure of the spectra of lanthanide compounds, elucidation of the reasons for its appearance and identification of the relationship between the spectral structure characteristics and the physicochemical properties of compounds.[5,18]

Thus the effect of the degree of occupancy of the Ln4*f* shell of lanthanide compounds on the structure of their spectra and the giant Coster-Kronig electron transition phenomenon (dynamic effect) within the core and valence electron shells have been studied by XPS.[19,20] In addition, the degree of participation of relatively low-lying occupied orbitals of neighbouring atoms in

Yu A Teterin, A Yu Teterin Institute of General and Nuclear Physics, Russian Research Centre 'Kurchatov Institute', pl. Kurchatova 1, 123182 Moscow, Russian Federation. Fax (+7 095) 742 5868. Tel. (7-095) 196 92 52. E-mail: teterin@ignph.kiae.ru (Yu A Teterin) Tel. (7-095) 196 90 28 (A Yu Teterin)

Received 14 March 2002
Uspekhi Khimii **71** (5) 403 – 441 (2002); translated by Z P Bobkova

† Dedicated to I V Kurchatov on occasion of his 100th birthday.

the formation of inner valence molecular orbitals (IVMO) has been determined.[18] Since an increase in the atomic number (Z) of lanthanides in the range of $57 \leqslant Z \leqslant 71$ entails an increase in the Ln5$p_{3/2}$ electron binding energy [E_b(Ln5$p_{3/2}$)] in their oxides from 17.7 to 27.5 eV, while the oxygen O2s electron binding energy [E_b(O2s)] is an intermediate value, these compounds are convenient objects for investigating the influence of the difference between the energies of the Ln5p and O2s atomic orbitals (AO) on the efficiency of their participation in the IVMO.[18] For example, the Ln–O bond lengths (R) in the lanthanide oxides Ln_2O_3 are rather great ($\sim$0.240 nm); therefore, the formation of IVMO for lanthanide oxides of the beginning of the row is not very efficient. However, in the case of LnO oxides in the gas phase, the Ln–O distance is rather short ($\sim$0.180 nm);[21] therefore, participation of the Ln5p and O2s AO in the formation of IVMO can be substantial; this should be taken into account when investigating the interaction between the atoms contained in the monoxides.

Analysis of the fine spectral structure (besides line intensities and chemical shifts) extends substantially the scope of XPS in the study of lanthanides and their compounds. This is the most adequate technique for determination of the lanthanide oxidation states in compounds, which is widely used in practice.[6, 7, 12–17, 22–33] Considerable attention is also devoted to the theoretical examination of the multielectron processes which accompany the photoemission of electrons and account for the fine structure observed in the XPS spectra.[34–41]

In this review, we present the results of XPS investigations of the electronic structures of several series of stable compounds of lanthanides (except for Pm, which is difficult to obtain), Sc, Y and La. The correlations between characteristics of the XPS spectra, physicochemical properties of these compounds and the nature of chemical bonding in them are discussed. Attention is focused on lanthanide trifluorides and oxides. The lanthanide compounds under consideration are rather stable against oxidation in air, high vacuum and X-radiation. Since some of lanthanide oxides have a variable stoichiometric composition inconsistent with the general formula Ln_2O_3, analysis of the structures of the XPS spectra of these compounds is accompanied by comparison with analogous spectra of some LnL_3 complexes containing Ln^{3+} ions and organic ligands (L). These compounds can be regarded as clusters consisting of condensed molecules rather than as solids with a band electronic structure. Conversely, lanthanide oxides and niobates are solids in which the lanthanide ions occupy the crystal lattice points and are surrounded by oxygen atoms.

II. Lanthanide trifluorides

The lanthanide trifluorides LnF_3 (Ln = La–Lu, except for Pm) are relatively stable compounds; the metal ions Ln^{3+} in them are formally trivalent.[1–4] No noticeable changes were detected in the XPS spectra of these compounds during recording of the spectra using the sample preparation procedure proposed by Teterin *et al.*[42] In addition to this study,[42] data on the XPS spectra of some lanthanide fluorides can be found in other publications.[43–54]

The X-ray photoelectron spectra of lanthanide trifluorides in the binding energy range from 0 to 1350 eV exhibit fine structure for virtually all electron levels.[42, 52, 55] To analyse XPS spectra and elucidate the relationship between the structural characteristics and the properties of substances, it is convenient to distinguish three conventional spectral ranges.

1. Electron binding energy in the range from 0 to $\sim$15 eV. For lanthanide trifluorides, this range of XPS spectra exhibits a poorly resolved structure related to the electrons of outer valence molecule orbitals (OVMO), which are largely formed from the partially filled Ln5d, Ln6s and F2p AO. A structure caused by Ln4f electrons also arises in this region. Theoretical calculations suggest[54–59] significant participation of the Ln4f AO in the formation of the OVMO in lanthanide compounds. In this case, in analysis of the chemical bond, the Ln4f electrons cannot, generally speaking, be classified as core electrons (as was traditionally considered before).

2. Electron binding energy in the range from $\sim$15 to 50 eV. In this region, XPS spectra show relatively well resolved structure due to the electrons of the inner valence MO (IVMO),[18, 42, 52, 55, 60–63] which are mainly composed of low-energy occupied Ln5p, Ln5s and F2s AO of neighbouring atoms. The structure of the IVMO spectra can be used to characterise the structures of the compounds under study and even to estimate the bond lengths in them.

3. Electron binding energy of $>$50 eV. This XPS range is typical of electrons of inner (core) MO; specifically, for lanthanide trifluorides, the spectra of the core AO are mainly recorded. These include the Ln3$p_{3/2}$, Ln3d, Ln4s, Ln4p, Ln4d and F1s AO. Both the energy region of the binding energies of these electrons and the low-energy part of the XPS spectra of the compounds in question can be subject to various effects resulting in a more complex spectral structure.[18, 38–40] Since these effects can arise simultaneously in any binding energy region, when interpreting spectral structure corresponding to individual shells, one should also take into account the structure displayed in other spectral regions. Therefore, when investigating lanthanide compounds by the XPS method, it is expedient to measure the spectrum over the whole experimentally accessible range (Table 1). It should be noted that one or another mechanism giving rise to the fine structure shows itself with variable probability in the spectra of electrons of different shells; this markedly facilitates interpretation of the spectra.

To identify the structural features of the low-energy XPS spectra of lanthanide fluorides, the spectra of scandium and yttrium fluorides have also been studied.[52, 55]

1. The spectral region of electrons of the outer valence molecular orbitals

The spectra of the outer valence MO of scandium, yttrium and lanthanum trifluorides,[52, 55] which contain no 4f electrons, are largely due to the Mnd, M$(n+1)s^2$ and F2p electrons of the neighbouring metal (M) and fluorine atoms, respectively (Fig. 1). They are displayed as 3.7-, 3.3- and 2.9-eV wide bell-shaped lines with smeared structures characterised by weighted-mean electron binding energies of 8.9, 8.9 and 8.4 eV, respectively. Comparison of these values with the positions of the maxima of these broadened lines (see Table 1) shows that the line in the spectrum of YF_3 is the most symmetrical. The lines related to the F2p and F2s electrons are approximately 21 eV apart (see Table 1). In the spectra of lanthanide trifluorides containing Ln4f electrons, the line intensity markedly increases with an increase in the metal nuclear charge (Z) due to the increase in the number of these electrons (n_{4f}) (Fig. 2). With the assumption that the Ln4f electrons do not participate in the formation of chemical bonds in the trifluorides, the spectral structure should be mainly governed by the final state of the ion which arises after photoemission of an Ln4f electron.[43, 51, 53, 54, 64–67]

In the XPS spectra of LnF_3 for lanthanides at the beginning of the row, the Ln4f lines are located at lower binding energies than the OVMO lines (Fig. 3, see also Fig. 2). As the atomic number (Z) of lanthanides and, correspondingly, the n_{4f} number increase (the relationship between these values is considered below), the binding energy of the Ln4f electrons noticeably increases, and their spectrum overlaps with the line of the OVMO electrons.[37, 67, 68]

Ln^{3+}	n_{4f}	Z	Ln^{3+}	n_{4f}	Z	Ln^{3+}	n_{4f}	Z
La^{3+}	0	57	Sm^{3+}	5	62	Ho^{3+}	10	67
Ce^{3+}	1	58	Eu^{3+}	6	63	Er^{3+}	11	68
Pr^{3+}	2	59	Gd^{3+}	7	64	Tm^{3+}	12	69
Nd^{3+}	3	60	Tb^{3+}	8	65	Yb^{3+}	13	70
Pm^{3+}	4	61	Dy^{3+}	9	66	Lu^{3+}	14	71

Table 1. Electron binding energies (E_b, eV) for the basic lines and satellites in the XPS spectra of lanthanide trifluorides.[42]

Compound	OVMO	Ln5$p_{3/2}$	Ln5$p_{1/2}$	F2s	Ln5s	Ln4$d_{5/2,3/2}$	Ln4$p_{3/2,1/2}$ (see [a, b])	Ln4s	Ln3$d_{5/2}$ (see [b])	Ln3$d_{3/2}$	F1s
LaF_3	−; 8.1	18.6	20.8	29.3	36.4	104.4; 107.5; 120.3; 134.6; 137.7	198.1; 203.4; 213.1; (231.5)	276.9	837.3; (841.6)	854.1; (858.3)	685.1
CeF_3	3.4; 8.4	19.4	22.4	29.5	38.0	110.7; 112.8; 125.7; 135.7; 143.2	208.2; 223.9; 243.5; 250.1	289.4; 291.0	884.7; (888.2)	903.3; (906.3)	685.4
PrF_3	5.2; 8.3	20.1	23.8	29.6	39.4; 40.5	118.4; 137.2; 147.6; 151.8; 169.6	219.1; 233.4; −; (251.4)	306.5; 309.5	934.4	955.2	685.3
NdF_3	6.5; 8.0	20.7	24.4	29.4	40.4; 41.7	122.8; 139.4; 136.3; 154.0; 160.0	229.6; 246.4; 259.9; (266.0)	319.0; 321.8	982.6	1005.6	685.1
SmF_3	7.5; 9.2	22.1	26.4	29.7	43.1; 45.5	132.3; 134.5; 137.3; 154.1; 164.0	251.8; 269.0	348.2; 352.1	1084.4; (1099.4)	1111.4	685.2
EuF_3	8.3; 11.8	22.4	unknown	29.2	43.8; 46.4	137.1; 142.6; 152.0 158.7; 168.2	261.9	365.5; 370.2	1135.3	1164.8; (1167.5)	685.0
CdF_3	−; 9.8	22.9	the same	29.2	45.4; 48.5	143.4; 148.6; 159.3 172.0; 183.0	272.7; 278.7; 289.4	379.8; 388.1	1187; (1200.2)	1219.8	684.8
TbF_3	4.2; 9.4	23.9	"	29.1	46.8; 49.5	147.5; 151.2; 155.0; 167.0; 178.8	288.5; 306.6; −; (322.6)		1242.6	1277.3	685.1
DyF_3	5.9; 9.7	24.5	"	29.4	49.2; 51.5	155.1; 157.3; 162.1; 173.6; 183.9	297.3; 301.3; −; (336.9)	415.4; 421.1	1297.6	1335.6; (1351.0)	685.2
HoF_3	8.0; 11.1	26.2	33.0	30.4	50.3; 52.3	163.1; 168.1; 177.2; 187.0; 191.4	309.9; 315.0; 322.6; (347.0)	433.7; 438.2	1356.5; (1346.1)	unknown	685.2
ErF_3	7.7; 10.8	26.1	32.9	29.7	53.8; 55.1	170.2; 173.6; 185.1; 194.1; 197.7	321.3; 327.3; −; (366.7)	452.1; 455.6	unknown	the same	685.4
TmF_3	7.5; 10.8	26.8	34.0	29.8	55.0; 56.0	177.9; 201.0; 185.8; 192.4; 204.1	334.4; 339.6; −; (392.4)	470.9; 472.4	the same	"	685.4
YbF_3	8.8; 12.6	27.2	34.7	29.6	57.0; 57.7	186.3; 189.3; 194.1 200.7; 206.2	347.2; 351.2; −; (399.0)	489.3; 491.3	"	"	685.2
LuF_3	−; 10.2	28.4	35.7	unknown	59.0	197.3; 207.3	361.1; 414.3	508.9	"	"	685.5
YF_3	−; 8.9	26.1 [c]	unknown	29.9	47.1 [d]	159.4; 161.3 [e]	302.5; 314.5 [f]	397.0 [g]	−	−	685.2
ScF_3	−; 8.7	33.9 [h]	the same	29.4	55.3 [i]	unknown	405.0; 409.3 [j]	503.9 [k]	−	−	685.6

Note. The binding energies are presented for the peaks with respect to the C1s binding energy for hydrocarbons on the sample surface [E_b(C1s) = 285.0 eV]. [a] Weighted-mean energies for electrons in a complex structure. [b] The values in parentheses are satellite or shoulder energies. [c] The Y4$p_{3/2,1/2}$ line. [d] The Y4s line. [e] The Y3$d_{5/2,3/2}$ lines. [f] The Y3$p_{3/2,1/2}$ lines. [g] The Y3s line. [h] The Sc3$p_{3/2,1/2}$ line. [i] The Sc3s line. [j] The Sc2$p_{3/2,1/2}$ lines. [k] The Sc2s line.

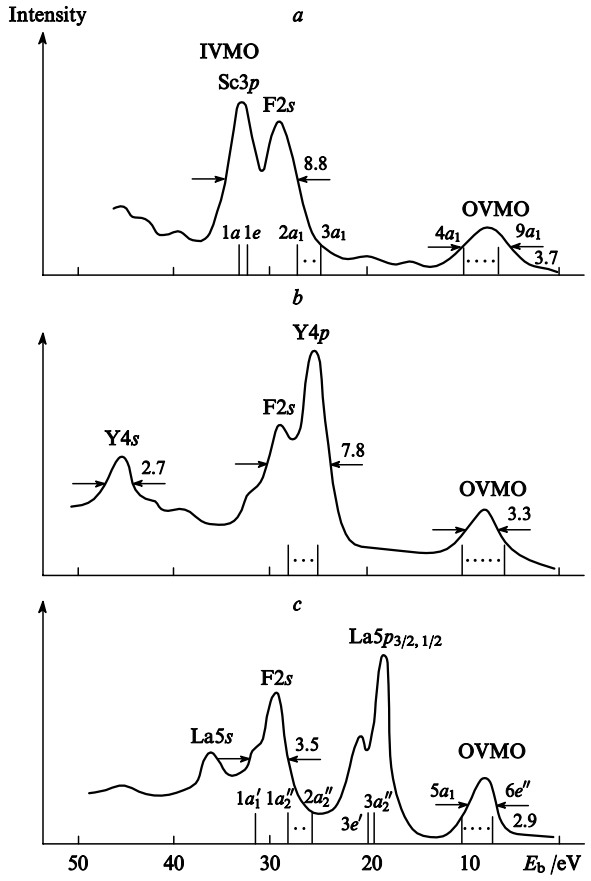


Figure 1. XPS spectra of scandium (*a*), yttrium (*b*) and lanthanum (*c*) trifluorides.[5] The vertical segments show the MO energies for the ScF_6^{3-} (C_3 symmetry), YF_9^{6-} (asymmetrical) and LaF_{11}^{8-} (D_{3h} symmetry) clusters calculated in the self-consistent field (SCF) X_α-DV (discrete variation) approximation.[63]

Starting from terbium, the spectrum of Ln4*f* electrons starts exhibiting an extra line located at a lower binding energy than the most intense component. As the Ln4*f* shell is being filled, this line grows approaching in intensity the high-energy component (see Fig. 2). In the Tb4*f* spectrum of TbF_3, this line is located at a distance of 5.2 eV from the second component. The observed splitting can be qualitatively considered using Tb^{3+} as an example.[43] The Tb^{3+} ion occurs in the $(4f\uparrow)^7(4f\downarrow)^1$ state, which implies the $^7F_6$ term, *i.e.*, the Tb4*f* shell is occupied by more than half. Photoemission of one Tb4*f* electron gives rise to two final states: $(4f\uparrow)^7$ — ^8S term and $(4f\uparrow)^6(4f\downarrow)^1$ — the $^{2s+1}L_J$ term. Since the former can be attained in only one way and the latter, in seven ways, the intensity ratio of the two components arising in the Tb4*f* spectrum is expected to be 1 : 7; this is close to the experimental value (see Fig. 2).

The photoemission of an electron with the β(↓) spin is known [43, 69] to require less energy than the removal of an electron with the α(↑) spin. The results of SCF X_α-DV (discrete variation) calculations (with allowance for spin polarisation)[69] for exchange splitting in the Ln4*f* spectra of REE compounds for the second half of the lanthanide row are in qualitative agreement with the corresponding experimental values (Fig. 4); for LnF_3, they are in accord with published data.[43]

Indeed, photoemission of an Ln4*f* electron gives rise to a more complex final state, resulting in a further complication of the spectra of the Ln4*f* electrons. The structure of these spectra is in satisfactory agreement with the set of levels derived from theoretical considerations of the multiplet splitting of the Ln4*f* line for the Ln^{3+} cations.[66, 70] The results of these calculations are reflected in Fig. 2 as vertical segments below the Ln4*f* spectra. The structure

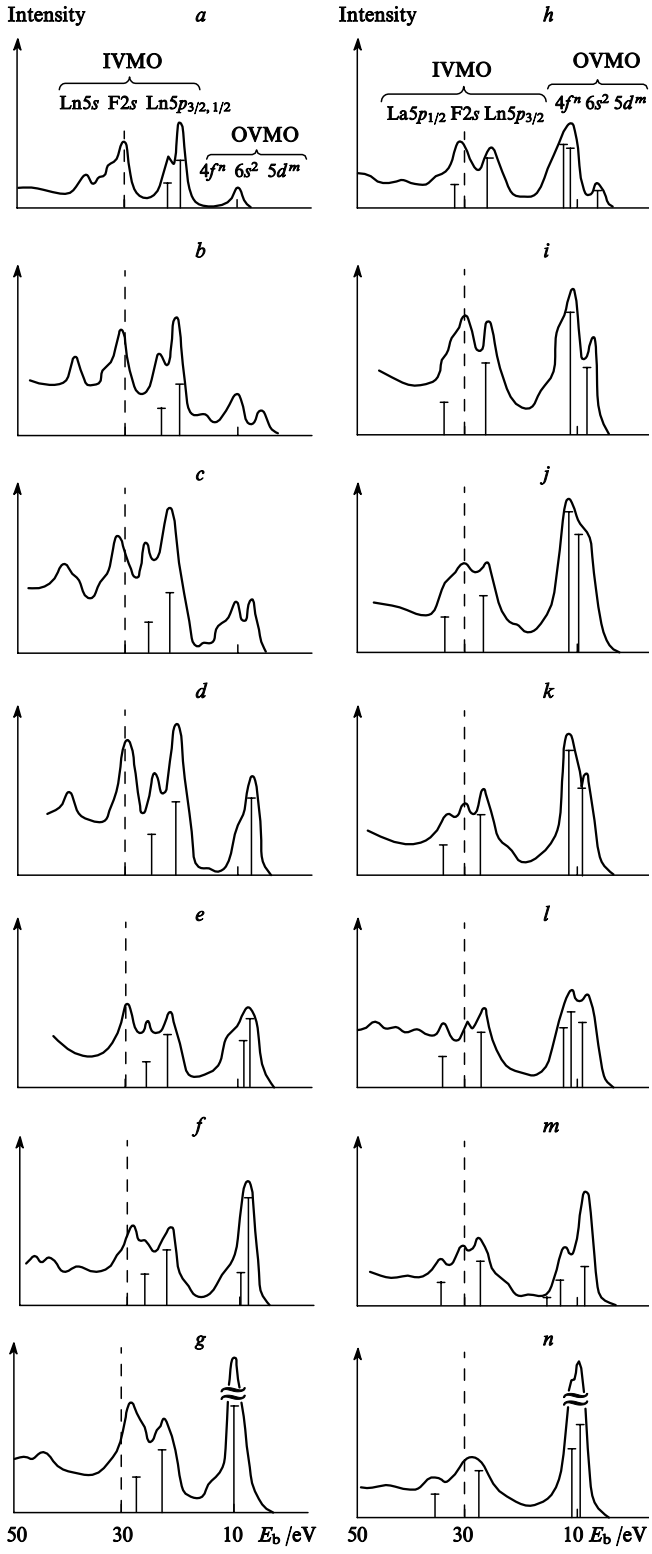


Figure 2. XPS spectra of low binding-energy electrons of lanthanide trifluorides.[42] (*a*) LaF_3, (*b*) CeF_3, (*c*) PrF_3, (*d*) NdF_3, (*e*) SmF_3, (*f*) EuF_3, (*g*) GdF_3, (*h*) TbF_3, (*i*) DyF_3, (*j*) HoF_3, (*k*) ErF_3, (*l*) TmF_3, (*m*) YbF_3, (*n*) LuF_3. The vertical segments in the OVMO energy range show the Ln4*f* lines found in the ionic approximation,[66] and those in the IVMO energy range are the lines of the Ln5*p* and F2*s* atomic spectra.[22] The dashed lines show the positions of the F2*s* lines of fluorine.

of the spectra of these electrons can characterise the lanthanide oxidation state in the compounds. As was to be expected, in the case of Lu^{3+} in LuF_3, the line of Lu4*f* electrons is split due to the

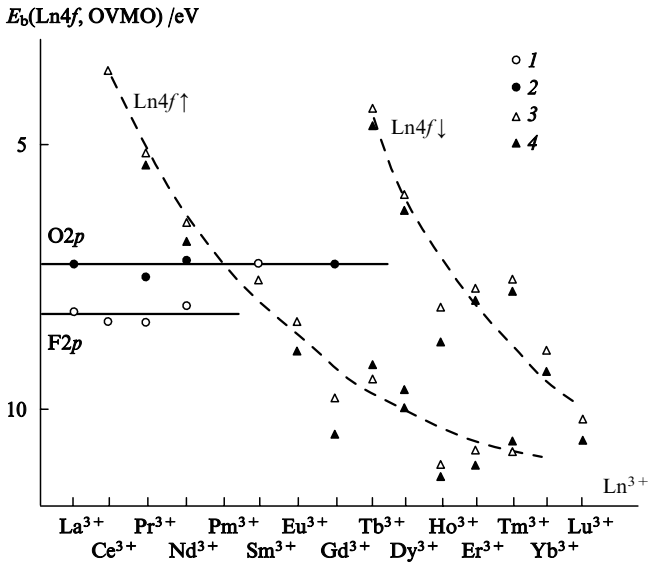


Figure 3. Binding energy (E_b) of the OVMO (*1*, *2*) and Ln4*f* (*3*, *4*) electrons *vs*. the number of electrons in the $La^{3+}-Lu^{3+}$ series. (*1*, *3*) LnF_3 (see Table 1); (*2*, *4*) Ln_2O_3.[37]

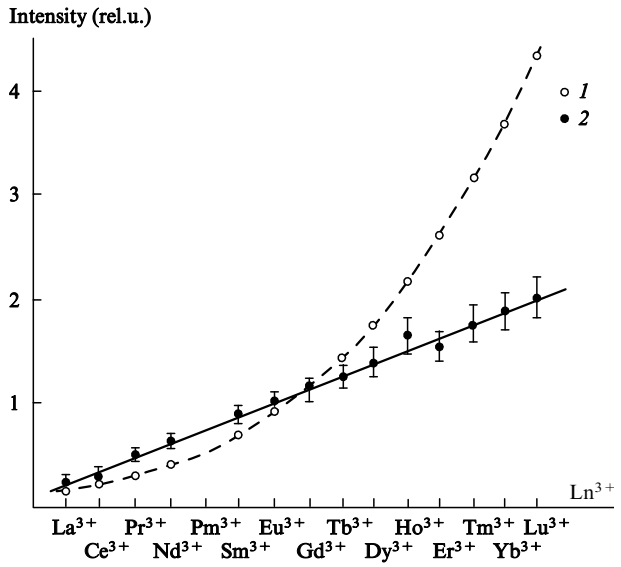


Figure 5. Relative intensity of the Ln4*f* line *vs*. the number of 4*f* electrons in the $La^{3+}-Lu^{3+}$ series; (*1*) theoretical dependence [Eqn (5)]; (*2*) experimental data for LnF_3 [Eqn (1)].[68]

spin–orbit coupling into only two components, the difference between their binding energies (ΔE_{so}) being 1.2 eV in magnitude. A similar effect could be expected for the Yb4*f* spectrum of Yb^{2+} in YbX_2 (the electronic configuration of Yb^{2+}, like that of lutetium, is $4f^{14}$); this is the case for the Yb atom [71] and for the Yb metal.[72,73] However, the structure of the spectrum of these electrons in the ytterbium fluoride (see Fig. 2) corresponds to the Yb^{3+} electronic configuration ($4f^{13}$). The structures of the spectra of the Ln4*f* electrons of other lanthanide ions are also unique and characterise the particular metal ion. When the energy of the exciting X-radiation increases, the intensities of the lines for the metal Ln4*f* electrons grow.[74,75] Figure 5 shows the experimental values for the total relative intensity (I_{exp}) of the OVMO and the Ln4*f* line, found as the ratio of the total area of these spectral lines to the total area of the Ln5*p* and F2*s* lines, depending on the number of Ln4*f* electrons (n_{4f}) in lanthanide fluorides. The I_{exp} values are described approximately by the linear relation

$$I_{exp} = 0.128n_{4f} + 0.20, \quad (1)$$

derived using the least-squares method. Equation (1) reflects the experimental dependence of the relative intensity of the Ln4*f* spectral line on the number of these electrons in the LnF_3 molecules. The absolute term in Eqn (1), equal to 0.20, characterises the relative intensity of lines for the OVMO electrons, which are partially due to Ln5*d* and F2*p* AO. It is noteworthy that this value is somewhat greater than the corresponding theoretical value calculated without allowance for the contribution of occupied Ln4*f* states. This suggests that an Ln4*f* electron involved in the chemical bond does not lose the *f* nature (traditionally, it has been considered that the Ln4*f* electron passes preliminarily to the Ln5*d* orbital), and in the case of LaF_3, La4*f* states are formed in its outer valence shell. However, verification of this hypothesis requires a more accurate experimental determination of the relative line intensities than that performed by Teterin *et al*.[37,67,68] It is significant that such data can, in principle, provide an answer to the question discussed. The difference between the relative intensities for LnF_3 containing Ln4*f* electrons and the absolute term in Eqn (1) (0.20) is proportional to the number of Ln4*f* electrons, which slightly participate in the chemical bond, and can be used to estimate the oxidation state of lanthanides in fluorides.

The theoretical dependence of the relative intensity (I_{theor}) of the Ln4*f* line in the spectra of LnF_3 on the number of electrons (n_{4f}) can be derived using the data on photoionisation cross-sections for low-energy subshells.[76,77] In this case, the expression for I_{theor} can be written in the form

$$I_{theor} = \frac{\sigma(4f)n_{4f} + \sum_i \sigma_i(\mathrm{OVMO})n_i}{\sigma(5p)n_{5p} + 3\sigma(\mathrm{F2}s)n_{\mathrm{F2}s}} = \quad (2)$$

$$= \frac{\sigma(4f)n_{4f}}{\sigma(5p)n_{5p} + 3\sigma(\mathrm{F2}s)n_{\mathrm{F2}s}} + \frac{\sum_i \sigma_i(\mathrm{OVMO})n_i}{\sigma(5p)n_{5p} + 3\sigma(\mathrm{F2}s)n_{\mathrm{F2}s}},$$

where $\sigma(nl)$ is the photoionisation cross-section of the *nl* shell (*n* and *l* are the principal and orbital quantum numbers, respectively); n_{nl} is the number of electrons; the summation involves

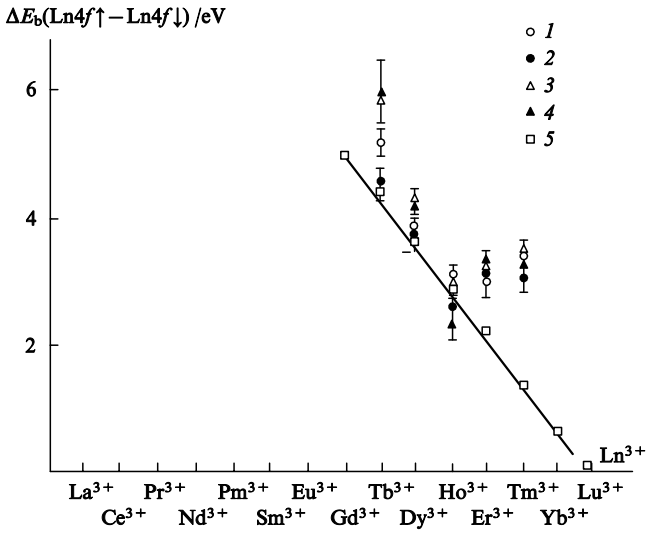


Figure 4. Splitting [ΔE_b(Ln4*f*↑ − Ln4*f*↓)] of the spectral line for the Ln4*f* electrons *vs*. the number of electrons in the $La^{3+}-Lu^{3+}$ series. (*1*) LnF_3 (see Table 1); (*2*) Ln_2O_3; (*3*) LnL^1_3 (L^1 is the *o*-methoxybenzoic acid residue);[67] (*4*) LnL^2_3 (L^2 is the diphenylacetic acid residue); (*5*) SCF X_α-DV calculations for $LnVO_4$.[69]

occupied OVMO.[37, 67, 68] The first term in this expression was found under the assumption that the Ln4*f* electrons do not participate directly in the chemical bond. To estimate the second term, the expression in the numerator was replaced by the sum of terms characterising valence AO,

$$\sum_i \sigma_i(\mathrm{OVMO})n_i \approx \sigma(5d)n_{5d} + \sigma(6s)n_{6s} + 3\sigma(\mathrm{F}2p)n_{\mathrm{F}2p}\,. \quad (3)$$

In this rather rough approximation, the second term of Eqn (2) for LaF_3 was found to be 0.17, which is smaller than the absolute term (0.20) in Eqn (1). The corresponding values for GdF_3 and LuF_3 are 0.16 and 0.15, respectively. In particular, relation (2) can be written in the form

$$I_{\mathrm{theor}} = \frac{\sigma(4f)n_{4f}}{\sigma(5p)n_{5p} + 3\sigma(\mathrm{F}2s)n_{\mathrm{F}2s}} + 0.17. \quad (4)$$

Assuming that the Ln atoms involved in the chemical bonds in LnF_3 have the configuration $4f^n5d^16s^2$, using the atomic photoionisation cross-sections of the Ln4*f* shell [52] and taking into account Eqn (4), one can obtain the following expression for I_{theor}:

$$I_{\mathrm{theor}} = 0.01\, n_{4f}^{2.24} + 0.17. \quad (5)$$

The plotted function I_{theor} and the corresponding experimental data are presented in Fig. 5.

The substantial difference between the theoretical and experimental values considered can hardly be explained by errors brought about by rough calculations of some terms of Eqn (5) or by the change in the Ln4*f* line intensity caused by different scattering of low-energy electrons upon photoemission. Note that the use of the photoionisation cross-sections of the outer 3*d* electrons for Period 4 elements and various low-lying inner electron levels for any other elements reported in Refs 76 and 77 to determine the relative intensities of their lines provides, as a rule, satisfactory agreement between theoretical and experimental data within the experimental error. Among other reasons, the observed discrepancy may be due to participation of the Ln4*f* electrons in the chemical bonds.

2. The energy region of Ln5p and F2s electrons

When investigating the structures of XPS spectra of low-energy electrons in the binding energy range from 0 to 50 eV, in particular, in the spectra of lanthanide compounds, researchers noted that some lines in this range are often substantially broader than the corresponding lines for the core electrons.[78, 79] Indeed, it follows from the uncertainty relation $\Delta E\Delta\tau \approx h/2\pi$ (ΔE is the atomic level width, $\Delta\tau$ is the lifetime of the 'hole' formed upon photoemission of an electron, and h is Planck's constant) that the lines for the low-lying electrons should be the broadest because the parameter $\Delta\tau$ decreases with an increase in the magnitude of the atomic level energy. However, for example, in LaF_3, the width (Γ) of the F2*s* line is 3.5 eV (see Fig. 1), whereas the low-lying F1*s* electrons account for Γ(F1*s*) = 1.6 eV [5] (Table 2).

Whereas line broadening in the binding energy range from 0 to ~15 eV can be due to the MO formation and solid-state effects, the broadening of lines in the energy range from ~15 to 50 eV cannot be interpreted in terms of the well-known classical mechanisms of fine structure origination alone. Moreover, the XPS spectra in the Ln5*p* and F2*s* binding energy range have a more complex structure than that expected upon simple superposition of the lines due to the corresponding lanthanide and fluorine atomic shells (see Fig. 2).[52] Therefore, it has been suggested that this structure could arise due to the formation of the inner valence molecular orbitals largely composed of the Ln5*p* and F2*s* AO of neighbouring atoms.[18, 42] In addition, it was found that separate maxima can be distinguished in the spectra and attributed, in a certain approximation, to the Ln5$p_{3/2}$ and Ln5$p_{1/2}$ components of the doublet (see Fig. 2).

The overall atomic spectra of this region obtained by summation of the Sc3*p*, Y4*p*, Ln5$p_{3/2,\,1/2}$ and F2*s* lines for scandium, yttrium, and some lanthanide trifluorides are presented in Fig. 6. In the simulation of these spectra, the spin–orbit splitting ΔE_{so}(M*np*) was varied around the corresponding value for the metal,[80] and the FWHM (full line width at half maximum) Γ and

Table 2. Spectral parameters found by comparison of the approximate atomic (calculation) and experimental XPS spectra of metal fluorides: electron binding energies (E_b, eV), spin–orbit splitting [ΔE_{so}(M5*p*), eV], binding energy difference between the F2*s* and *F*1*s* electrons [ΔE_b(F2*s*–F1*s*), eV], line widths (Γ, eV)[55] and photoionisation cross-sections (σ) at 1487 eV.[76]

Compound	Ln5$p_{3/2}$			Ln5$p_{1/2}$		ΔE_{so}(M5*p*)		F2*s* (see [a])		Γ(F1*s*), experiment	ΔE_b(F2*s*–F1*s*)[b]	
	E_b (see [c])	Γ	σ (see [d])	E_b	σ	calculation	experiment [e]	E_b	Γ		calculation	experiment [e]
LaF_3	18.6	0.9	0.458	21.1	0.230	2.4	2.3	29.5	1.6	1.6	656.6	655.8
CeF_3	19.4	1.0	0.439	22.5	0.221	3.1	2.9	29.7	1.3	1.7	655.7	655.9
PrF_3	21.7	1.5	0.456	25.6	0.229	3.9	unknown	31.2	2.0	2.1	654.1	655.7
NdF_3	20.7	1.1	0.472	24.0	0.236	3.7	the same	29.6	1.4	1.5	655.5	655.7
SmF_3	22.1	1.4	0.501	26.2	0.249	4.1	"	30.0	1.5	1.5	655.2	655.5
EuF_3	22.4	1.7	0.515	27.0	0.255	4.6	"	29.7	2.0	1.7	655.3	655.8
GdF_3	22.9	1.8	0.568	29.3	0.279	6.4	"	28.6	2.2	1.6	656.2	655.6
TbF_3	23.9	1.6	0.539	30.1	0.265	6.2	6.2	29.0	1.9	1.8	656.1	656.0
DyF_3	24.5	1.7	0.551	32.0	0.270	7.5	6.4	29.4	1.7	1.8	655.8	655.8
HoF_3	26.2	1.9	0.562	33.5	0.274	7.3	6.7	30.6	2.1	2.5	654.6	654.8
ErF_3	26.1	1.1	0.572	33.2	0.277	7.1	6.7	29.9	1.9	2.1	655.5	655.7
TmF_3	26.6	1.1	0.583	34.0	0.281	7.4	6.8	29.7	1.3	1.7	655.7	655.6
YbF_3	27.1	1.4	0.592	34.7	0.284	7.6	6.9	29.9	1.6	1.6	655.3	655.6
LuF_3	28.4	2.5	0.645	35.7	0.304	7.3	7.0	28.7	3.2	2.1	656.8	unknown
YF_3 (see [f])	26.1	1.2	0.599	27.4	0.311	1.3	–	30.2	1.6	1.7	655.0	655.3
ScF_3 (see [g])	33.9	1.4	0.429	34.6	0.221	0.7	–	29.8	1.8	2.3	655.8	656.2

[a] For the F2*s* electrons, $\sigma = 0.210$. [b] The ΔE(F2*s*–F1*s*) values for MnF_2 and MnF_3 are 655.4 and 655.2 eV, respectively. [c] Comparison of the approximate atomic spectra of Ln, Y, Sc and F with experimental spectra of the fluorides was carried out for La–Er, Y and Sc relative to the Ln5$p_{3/2}$, Y3$p_{3/2}$ and Sc3$p_{3/2}$ energies, and for Tm–Lu, relative to the Ln5$p_{1/2}$ energies. [d] In relative units, 1 rel.u. = 13.600 barn. [e] The values for individual metals are given.[80] [f] The Y4$p_{3/2,\,1/2}$ energies are presented. [g] The Sc3$p_{3/2,\,1/2}$ energies are presented.

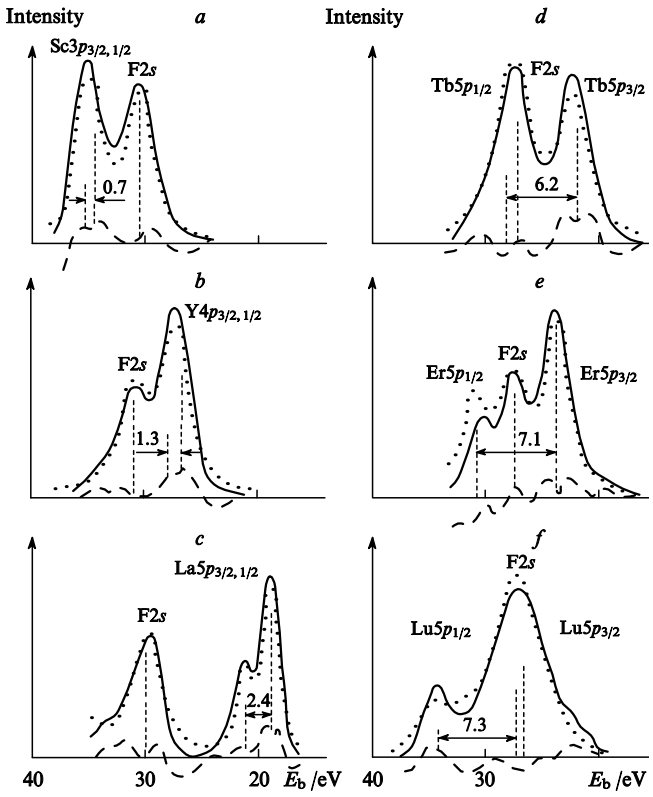


Figure 6. XPS spectra of the MF_3 fluorides in the Sc3*p* (*a*), Y4*p* (*b*), La5*p* (*c*), Tb5*p* (*d*), Er5*p* (*e*), Lu5*p* (*f*) and F2*s* binding energy ranges.[42] The continuous lines show the experimental spectra, the vertical dashed segments correspond to atomic spectra; the dots show the summarised spectra; and the dashed lines are the differences between the experimental and simulated spectra.

the F2*s* binding energies with allowance for photoionisation cross-sections[76,77] were varied until the best agreement with the experimental spectra was attained. It was assumed that the composition of the compounds considered corresponds to the stoichiometric formula MF_3, and the spectral lines for their electrons have a Lorentzian form. The spectral parameters found in this way and the corresponding experimental values are presented in Table 2 and in Fig. 7. These values characterise the main features of the considered spectra and barely reflect the complex structure of the spectra. Therefore, one should not expect too large a difference between the theoretical and experimental values (see Fig. 6, Table 2). Thus the general trend for the increase in the spin–orbit splitting [ΔE_{so}(M5*p*)] and FWHM (Γ) for Ln5*p* electrons can be followed, but the FWHM values for the F2*s* lines are markedly different (see Table 2).

The binding energy differences between the F2*s* and F1*s* electrons [ΔE_b(F2*s*–F1*s*)] for the metal fluorides studied differ somewhat from the corresponding values for 3*d*-metal compounds, in particular MnF_2 and MnF_3, in which the conditions for IVMO formation from the F2*s* and Mn3*p* AO are much less advantageous than those in LnF_3. It really follows from this comparison (see Table 2, Fig. 2) that the experimental spectra in the considered energy range do not consist of separate lines but have a more complex structure. The dependence of the Ln5*p* binding energy on the atomic number (Z) is relatively weak and is nearly linear for the whole lanthanide series (see Fig. 7). This pattern of the E_b–Z curve is not typical of the core shells the energy of which follows a quadratic dependence on Z.

The F2*s* XPS spectra for LaF_3, CeF_3, PrF_3, NdF_3 and SmF_3 exhibit a clear-cut shoulder removed from the basic line by ~2.2 eV towards higher electron binding energies. In the spectra of other lanthanide trifluorides, this region is superimposed by the

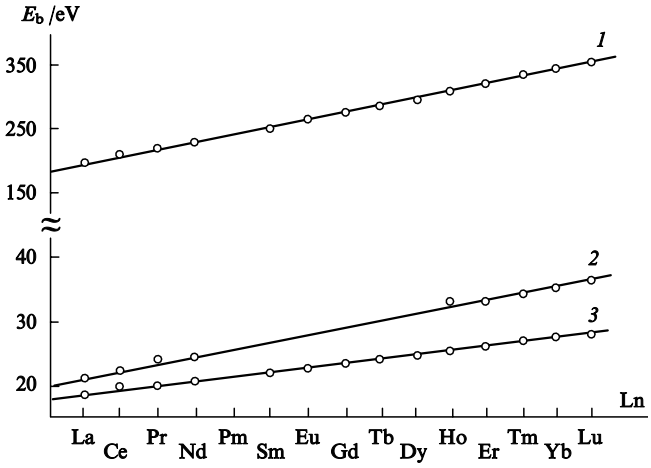


Figure 7. Binding energies (E_b) of the Ln4$p_{3/2}$ (*1*), Ln5$p_{1/2}$ (*2*) and Ln5$p_{3/2}$ electrons (*3*) of lanthanide trifluorides *vs.* the metal atomic number in the La–Lu series. The error in determination of the electron binding energies from the maxima of the corresponding lines is ±0.2 eV.[5]

Ln5$p_{1/2}$ line, which complicates the observation of this shoulder. This extra structure cannot be due to fluorine atoms having different oxidation states because the F1*s* line in the spectra of these compounds is rather narrow and symmetric. On passing from La to Sm, the Ln5$p_{3/2}$ and Ln5$p_{1/2}$ binding energies increase by 3.5 and 5.1 eV, respectively. Simultaneously, the shoulder at the basic F2*s* line shifts to a much lesser extent. The absence of the corresponding shoulder at the F1*s* line suggests that this shoulder is not due to many-body perturbation, *i.e.*, to the so-called shake-up (or shake-down) process, which implies transition of a valence electron to a higher (or lower) excited state simultaneously with photoemission of a core electron and gives rise to shake-up (or shake-down) satellites on the side of higher (or lower) electron binding energies of the basic spectral line. In other words, the observed shoulder is not a shake-up (shake-down) satellite.[5,42]

The same conclusion can be drawn by analysing and comparing the relative electron binding energies of satellites in the spectra of various core electrons of the fluorides studied. Complication of the structure of LnF_3 spectra in the Ln5*p* and F2*s* electron binding energy ranges in, for example, the spectra of LaF_3 and LuF_3 cannot be due to the multiplet splitting either, as these fluorides contain no unpaired Ln4*f* electrons and they are diamagnetic. This splitting should result, apparently, in some broadening of the Ln5*p* doublet lines for lanthanide trifluorides that contain unpaired Ln4*f* electrons, which is actually observed in the spectra of fluorides of light lanthanides (see Fig. 2). This is not at variance with the results of the estimation of the influence of this factor on the Ln5*p* spectra performed in the approximations of isolated Ln^{3+} ions[81] and atoms in the metals.[82]

On the basis of the foregoing data and with allowance for similar results for oxygen-containing lanthanide compounds,[57–59,78,79,83,84] it was suggested that one reason for structure complication in the Ln5*p* and F2*s* spectral range is the formation of IVMO, mainly from the Ln5*p* and F2*s* AO.[5,18,42,52] The spectral structure in this energy range can be qualitatively described by considering the diagram of the IVMO levels for the clusters that reflect the surrounding of the metal atoms by the ligands in the MF_3 trifluorides (Fig. 8).

Lanthanide (La to Sm) trifluorides form a tysonite hexagonal layered lattice characterised by the D^3_{6h} ($C6/mcm$) point group of symmetry.[2,85] The wavy layers of F atoms alternate in the lattice with the flat layers composed of Ln and F atoms, which form six-membered rings. The lanthanide atoms are surrounded by three fluorines. Therefore, a calculation of the electronic structure of the lanthanide trifluorides has been carried out for LnF_3 clusters with D_{3h} symmetry.[47] It has been noted[2] that the structures of

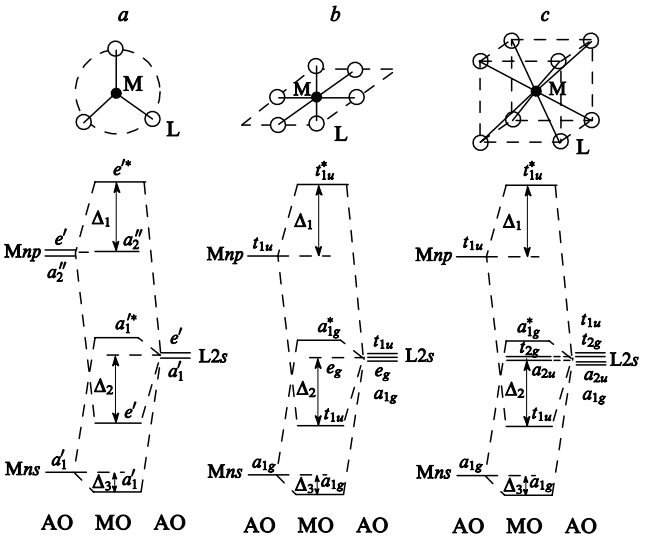


Figure 8. Diagram of IVMO formed by the metal M*np* and M*ns* AO and the ligand L2*s* AO of model clusters. (*a*) $ML_3^{n_1-}$ (D_{3h} symmetry); (*b*) $ML_6^{n_2-}$; (*c*) $ML_8^{n_3-}$ (O_h symmetry).[42]

lanthanide trifluorides from La to Ho can be regarded as a hexagonal LaF_3 (tysonite) structure, space group D_{3d}^4 ($P\bar{3}c1$). In this structure, each lanthanum atom is surrounded by nine fluorine atoms located at distances of 0.2416 to 0.2640 nm. At room temperature, lanthanide (Sm to Lu) trifluorides can also have the YF_3 structure[2] with an orthorhombic lattice, space group D_{2h}^{16} (*Pnma*). Each yttrium atom in the structure is surrounded by eight fluorine atoms located at distances of 0.225 to 0.232 nm. One more (ninth) fluorine is located at a distance of 0.260 nm.

To discuss qualitatively the spectral patterns in the Ln5*p*, Y4*p*, Sc3*p* and F2*s* energy ranges in terms of the IVMO concept, Teterin *et al.*[42] used, instead of the real structures, structural models of the local environment of the metal atoms in fluorides resembling most closely the real structures but which are more symmetrical.[42] Using group theory in a non-relativistic (NR) approximation for the chosen model clusters, one can describe schematically the structure and energy of the IVMO consisting of the M*ns*, M*np* and L2*s* AO of the neighbouring metal and ligand atoms (see Fig. 8). The IVMO structures corresponding to different local environments of the metal are significantly different. Thus, for the $ML_3^{n_1-}$ cluster (D_{3h} symmetry), two energy levels representing the a_2'' and e'^* IVMO are observed instead of one level representing the M*np* AO. In the case of $ML_6^{n_2-}$ and $ML_8^{n_3-}$ clusters (O_h symmetry), as for the metal atom, this energy range contains one level whose position can vary (see Fig. 8). The relative intensities of lines of the theoretical IVMO spectra for clusters of different symmetries are proportional to the electron photoemission cross-sections and degeneration factors for different levels (a_1', a_{1g}, a_{2u} are non-degenerate, e' are doubly degenerate, and t_{2g} and t_{1u} are triply degenerate IVMO); thus, they should be typical and substantially different.

In the clusters in question, the interaction of the filled M*np* and L2*s* AO gives rise to bonding (e', t_{1u}) and antibonding (e'^*, t_{1u}^*) IVMO. If the admixtures of the vacant valence Ln4*f*, Ln5*d* and Ln6*s* AO in these IVMO are small, the electrons of these MO should influence only slightly the energy of the chemical bond in the cluster. A significant admixture of these AO in IVMO would weaken the antibonding nature of the $e'^*(t_{1u}^*)$ MO and enhance the bonding nature of the $e'(t_{1u})$ MO. Thus, the formation of these IVMO would result in stronger binding between the neighbouring atoms.[18, 55, 60, 86, 87] The interaction of the M*ns* AO with the L2*s* AO can also give rise to couples of bonding a_1' and a_{1g} and the corresponding antibonding $a_1'^*$ and a_{1g}^* IVMO. Analogous considerations concerning the influence of IVMO electrons on the chemical bonding in clusters are also applicable to these IVMO. Some IVMO such as a_2'', e_g, a_{2u} and t_{2g} are mainly formed by the M*np* and L2*s* AO. However, vacant valence AO can also be admixed to them. If these admixtures are small, the IVMO would be of the quasi-atomic nature.

The limited resolving power of X-ray photoelectron spectrometers and line broadening caused by solid-state effects in the spectral range considered preclude elucidation of all structural details of the IVMO in lanthanide trifluorides. Nevertheless, the most clear-cut changes in the structure of the IVMO spectra compared to the structure of the spectra of the AO of neighbouring atoms are experimentally measurable. It is noteworthy that in a more rigorous approach, the real experimental spectra of lanthanide compounds should be compared with the theoretical spectra calculated using the relativistic approximations taking into account many-body processes that take place during the electron photoemission. However, no calculations of this type are available to date.

When discussing the low-binding energy spectral structure in MF_3 which are characterised by relatively low spin–orbit coupling between the low-energy filled M*np* shells, one can use the data of non-relativistic calculations. This is true for compounds such as, for example, ScF_3, YF_3 and LaF_3; the spin–orbit splittings (ΔE_{so}) for the Sc3*p*, Y4*p* and La5*p* levels are equal to 0.7, 1.3 and 2.3 eV, respectively (see Table 2). The results of non-relativistic SCF X_α DVM calculations of the electronic structures of the ScF_6^{3-} (C_3 symmetry), non-symmetrical YF_9^{6-} and LaF_{11}^{8-} (D_{3h} symmetry) clusters (Fig. 9) [63] are given schematically in Figs 10, 11, 12. The structures of these clusters simulate most closely the environment of scandium, yttrium and lanthanum in ScF_3, YF_3 and LaF_3, respectively.

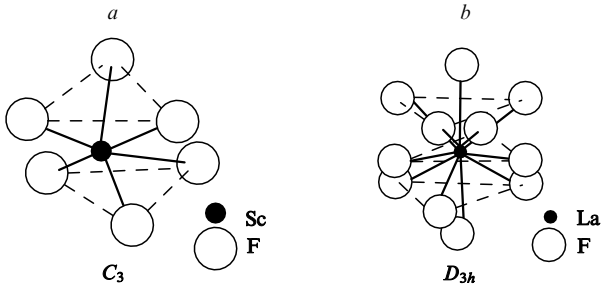


Figure 9. Structure of the ScF_6^{3-} (C_3 symmetry) (*a*) and LaF_{11}^{8-} (D_{3h} symmetry) clusters (*b*). The Sc–F bond length in ScF_6^{3-} is 0.202 nm; in the LaF_{11}^{8-} cluster, the average value over five distances $\bar{R}(La-F)$ = 0.239 nm, and that for the other six distances, $\bar{R}(La-F)$ = 0.272 nm.[63]

The calculations for the electronic structure of the ScF_6^{3-} cluster (C_3 symmetry) were performed using structural data[2] of ScF_3, which indicate that the fluorine atoms are located at approximately equal distances from scandium; the average $\bar{R}(Sc-F)$ value is 0.202 nm, and no inversion centre is present (see Fig. 9).

According to these calculations, the broadened line near the Fermi level in the spectrum of ScF_3 is attributed to OVMO electrons (see Figs 1, 10). The spectral structure in the Sc3*p* and F2*s* binding energy range is due to the IVMO electrons. For the considered Sc–F bond lengths in the ScF_6^{3-} cluster, noticeable mixing of the Sc3*p* and F2*s* AO takes place, resulting in the formation of the $1a_1$ and $3a_1$ IVMO. Therefore, the fine structure in the spectrum of the Sc3*p* and F2*s* electrons is attributable to the formation of these IVMO (see Figs 1, 6).

The resonance energy values $E_\alpha^R(Sc-F)$,[18] which characterise the covalent bonding between scandium and fluorine in ScF_3 imply that the greatest contribution to the stability of ScF_3 is made by the $5a_1$ OVMO and $2a_1$ and $1a_1$ IVMO electrons. Due to mixing

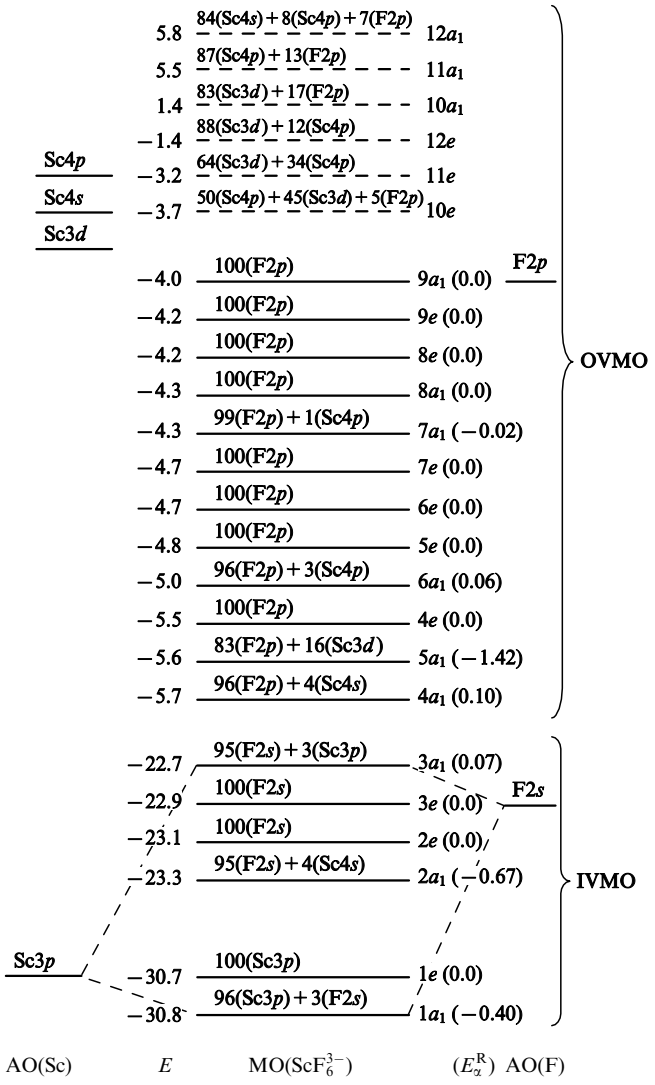


Figure 10. Diagram of the MO in the ScF_6^{3-} cluster [C_3 symmetry, $\bar{R}$(Sc−F) = 0.202 nm] calculated in the SCF X_α-DVM approximation.[63] The MO energies are expressed in eV (the diagram is not scaled). The values in parentheses are the resonance energies E_α^R(Sc−F) in a.u.

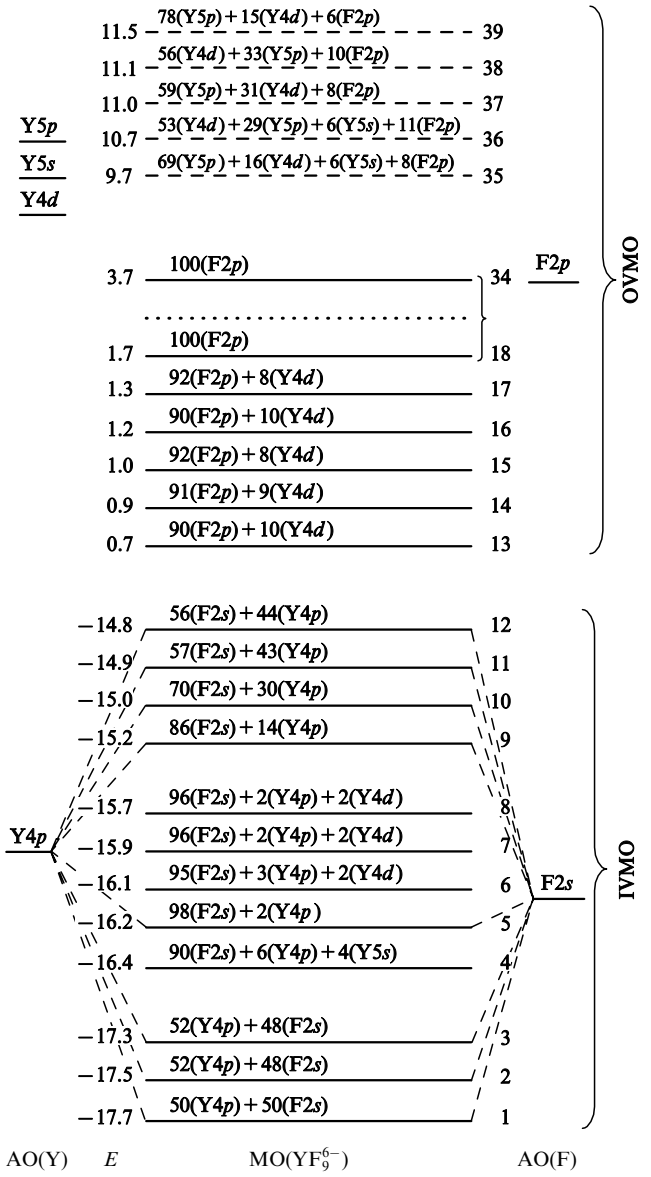


Figure 11. Diagram of MO of the asymmetrical YF_9^{6-} cluster (SCF X_α-DVM) in which the average value over eight bond lengths, $\bar{R}$(Y−F) = 0.229 nm, and for the ninth bond length, R(Y−F) = 0.260 nm.[63] The MO energies are expressed in eV (the diagram is not scaled).

of the outer and inner valence AO, as noted in a number of publications,[18, 52, 55, 85, 86] the contribution of the bonding $1a_1$ IVMO prevails over the contribution of the antibonding $3a_1$ IVMO, and, in total, the electrons of these MO strengthen the bond. If the contribution of the $2a_1$ IVMO is taken into account, the total covalent contribution of the IVMO electrons to the chemical bond energy in the ScF_6^{3-} cluster (C_3 symmetry) would be ~43%. Comparison of the calculated energy levels with the experimental spectra should be done using the data for the so-called transition state rather than for the ground state.[88] However, the energy levels calculated for the transition state in a narrow range of MO energies are known to be shifted relative to those found for the cluster ground state towards greater (in magnitude) E_b by a virtually constant value equal to several electron-volts (see, for example, Ref. 89). For comparison, MO energies for the ScF_6^{3-} cluster (C_3 symmetry) increased (in magnitude) by 2 eV are shown in Fig. 1 as vertical segments below the experimental XPS spectrum of scandium trifluoride. A satisfactory qualitative agreement between the experimental and theoretical results can be noted.

The structure of the yttrium local environment in YF_3 is rather complicated. Therefore, the YF_9^{6-} cluster, which has no symmetry elements and in which the metal environment resembles most closely the yttrium environment in the trifluoride, can be chosen for the electronic structure calculations. In this case, the yttrium atom is surrounded by eight fluorine atoms located at distances $\bar{R}$(Y−F) = 0.229 nm and one fluorine atom located at the distance R(Y−F) = 0.260 nm.[2, 63, 90] The calculation results indicate that the higher occupied OVMO are mainly formed by the F2p AO, while the lower OVMO involve the F2p and Y4d AO (see Fig. 11). The IVMO formation is associated with substantial mixing of the Y4p and F2s AO, which may be as great as 50%.

For comparison of the theoretical results of the electronic structure of the YF_9^{6-} cluster with the structure of the XPS spectrum of YF_3, the magnitudes of the MO energy were increased by 10 eV. These results are given under the XPS spectra of yttrium trifluoride in Fig. 1 as vertical segments. The considered calculation results suggest that the spectrum in the Y4p and F2s binding energy range reflects the IVMO system in YF_3. The appearance of these MO can also account for the additional structure observed in this range of the spectrum of YF_3 as shoulders next to the expected atomic lines.

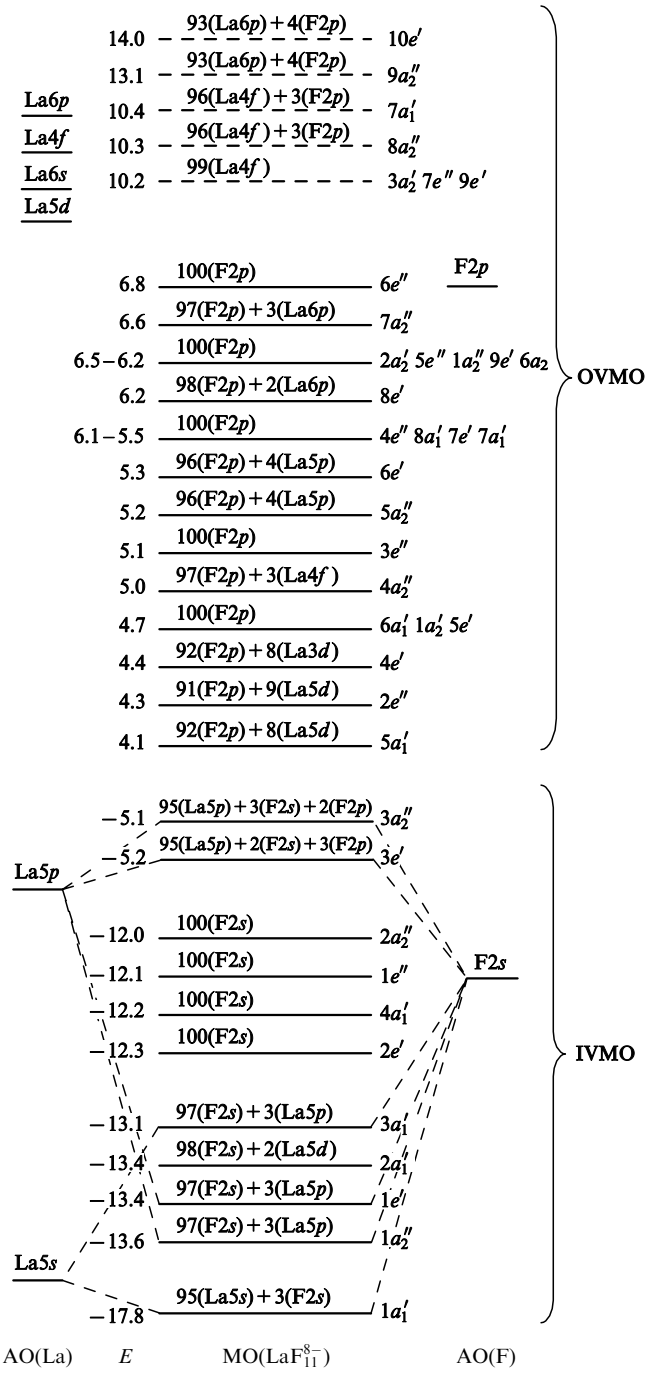


Figure 12. Diagram of MO of the LaF_{11}^{8-} cluster (D_{3h} symmetry) (SCF X_α-DVM) in which the average value over five bond lengths, $\bar{R}(La-F) = 0.239$ nm, and for the other six lengths, $\bar{R}(La-F) = 0.272$ nm.[63] The MO energies are expressed in eV (the diagram is not scaled).

The structure of the low binding energy XPS spectra of lanthanum trifluoride was interpreted using theoretical data for the electronic structures of the LaF_{11}^{8-} cluster (D_{3h} symmetry) obtained by non-relativistic SCF X_α-DV calculations.[5,63] The calculations were based on the crystallographic data for LaF_3,[2,63] which imply that five fluorine atoms in the LaF_{11}^{8-} cluster are located at an average distance $\bar{R}(La-F) = 0.239$ nm away from the lanthanum atom, while the other six fluorines are located at a distance $\bar{R}(La-F) = 0.272$ nm (see Fig. 9). The results of calculations are presented in Fig. 12, which shows that the overlap of the La5*s*, La5*p* and F2*s* AO results in the formation of the $1a'_1 - 3a''_2$ IVMO system. Due to the substantial difference between the La5*p* and F2*s* binding energies [the experimental $\Delta E_b(La5p_{3/2} - F2s)$ value is 10.7 eV] and long La–F bonds, the degree of mixing of the La5*p* and F2*s* AO is not large.

To compare the results of calculations for the electronic structure of the LaF_{11}^{8-} cluster (D_{3h} symmetry) with the structure of the experimental X-ray photoelectron spectrum of LaF_3, the absolute MO energies were increased by 14 eV (see Fig. 1).

As the chemical bond in LaF_3 is formed, the difference between the La5$p_{3/2}$ and La3$d_{5/2}$ binding energies does not change within the error of measurements. For instance, for metallic lanthanum, $\Delta E_b(La5p_{3/2} - La3d_{3/2}) = 818.6$ eV [91] or 818.2 eV,[5] and for LaF_3, this value is 818.7 eV [42] (see Table 1). However, the formation of IVMO of the $3e'$ and $3a''_2$ type is not expected to cause necessarily a significant increase in this energy difference (see Fig. 12) because the mixing of outer and inner valence AO during the IVMO formation may be accompanied by a substantial decrease in the antibonding type of these orbitals.[18] Unfortunately, no theoretical results for the trifluorides of heavier lanthanides using either the non-relativistic or relativistic approximation are currently available. Nevertheless, it follows from the given examples that the results of theoretical calculations agree qualitatively with experimental data. This suggests that the complication of the XPS spectral structure for REE trifluorides in the region of the M*np* and F2*s* binding energies is due to the formation of IVMO.

3. The spectra of core electrons

a. The structures of the spectra of the Ln5s and Ln4s electrons

It follows from theoretical calculations [56–59] that the Ln5*s* AO in lanthanide compounds can be involved in the IVMO formation. However, the concomitant changes in the Ln5*s* spectra observed on passing from metals to compounds are difficult to detect because various effects determining the structure of the XPS spectra can show themselves in this spectral range (Fig. 13). Complication of the spectral structure in the Ln5*s* binding energy range for the compounds considered can be related to the appearance of additional broadened lines caused by electronic Auger transitions. Thus the lines at 63 and 46 eV in the spectra of ErF_3 and TmF_3, respectively, have been attributed [5] to the electronic Auger transitions of the M_5NN type.[92] Nevertheless, in many cases, the basic line for the Ln5*s* electrons, which also has a complex structure, can be distinguished in these spectra. On the side of higher (by 14–16 eV) binding energies, a relatively intense additional structure is observed. A similar, though less intense structure is found in the spectra of electrons of other deep core shells. Therefore, many-body perturbation giving rise to shake-up satellites in the spectra might be a reason for this additional structure (see Fig. 13).

Comparison of the Ln5*p* and Ln5*s* binding energies (see Table 1) shows that the approximate equality $E_b(Ln5s) \approx 2E_b(Ln5p)$ holds for the lanthanide trifluorides considered. It allows the suggestion that a significant complication of the Ln5*s* spectral structure may be caused by the dynamic effect related to the giant Coster-Kronig transitions within the Ln5*s*, Ln5*p* and Ln4*f* shells. As a consequence, photoemission of an Ln5*s* electron gives rise to not only the ground final state ($Ln5s^15p^64f^n$) but also an excited final state ($Ln5s^25p^4f^{n+1}$) with an energy close to that of the ground state. This situation is sometimes considered as the interaction of the configurations of the final states, $Ln5s^15p^64f^n \leftrightarrow Ln5s^25p^4f^{n+1}$. In particular, this might be the reason for some extra peaks in the Ln5*s* spectra (see Fig. 13).

The Ln5*s* spectra of lanthanide compounds exhibit, in the simplest case, a structure related to multiplet splitting (ΔE_{ms}).[44,93,94] In this case, two components arise instead of the expected single line; the splitting is proportional to the number of unpaired Ln4*f* electrons. The greatest multiplet splitting was observed for the lanthanide trifluorides of the middle of the lanthanide row, the maximum value being found for GdF_3: $\Delta E_{ms}(Gd^{3+}) = 3.2$ eV (see Fig. 13). The dependence of the elec-

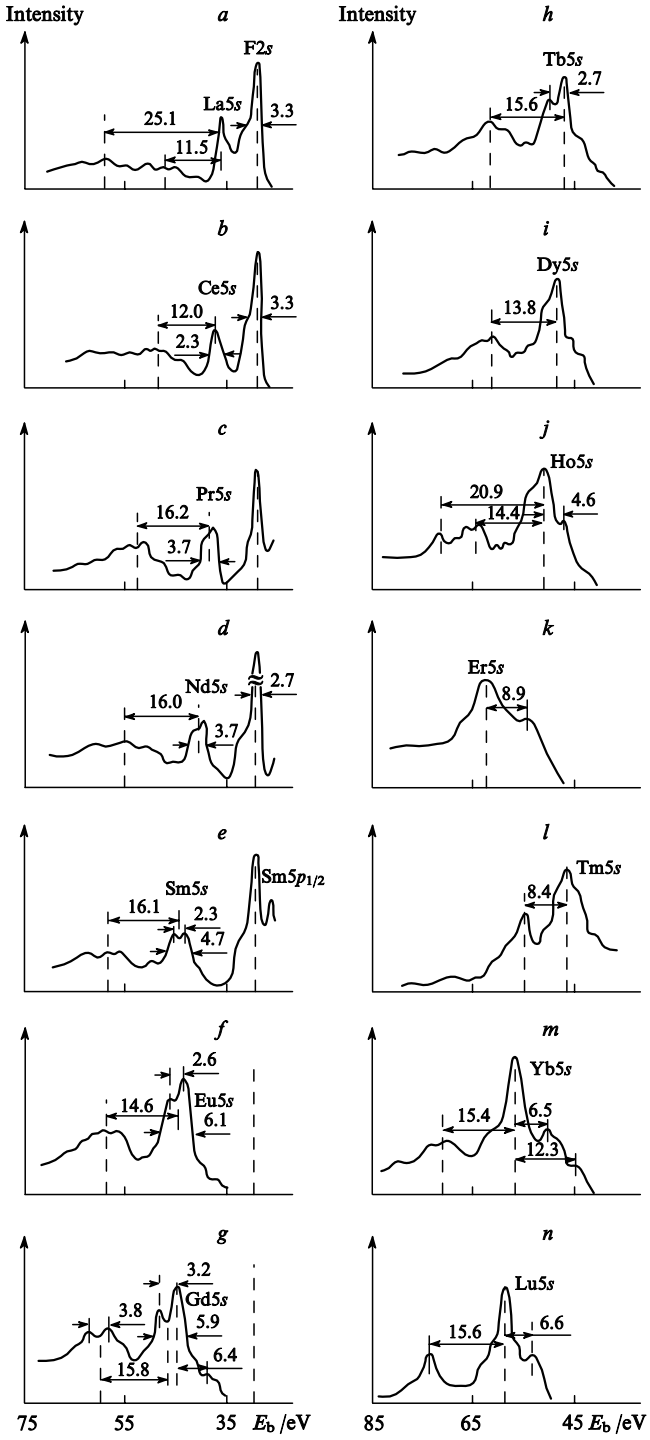


Figure 13. XPS spectra of lanthanide trifluorides in the Ln5*s* binding energy range.[42] (*a*) LaF_3, (*b*) CeF_3, (*c*) PrF_3, (*d*) NdF_3, (*e*) SmF_3, (*f*) EuF_3, (*g*) GdF_3, (*h*) TbF_3, (*i*) DyF_3, (*j*) HoF_3, (*k*) ErF_3, (*l*) TmF_3, (*m*) YbF_3, (*n*) LuF_3.

tron binding energies corresponding to these two components on the lanthanide atomic number is presented in Fig. 14.

A similar structure was observed in the Ln4*s* spectra of lanthanide trifluorides (Fig. 15). In the case of TbF_3, DyF_3, HoF_3 and ErF_3, intense lines caused by the electronic Auger transitions of the $M_5N_{45}O_3$, $M_5N_{45}O_1$, $M_5N_4N_{45}$ and $M_4N_4N_{45}$ types, respectively, appear in the Ln4*s* binding energy range.[92] In the Ln4*s* spectra of these compounds recorded on a spectrometer

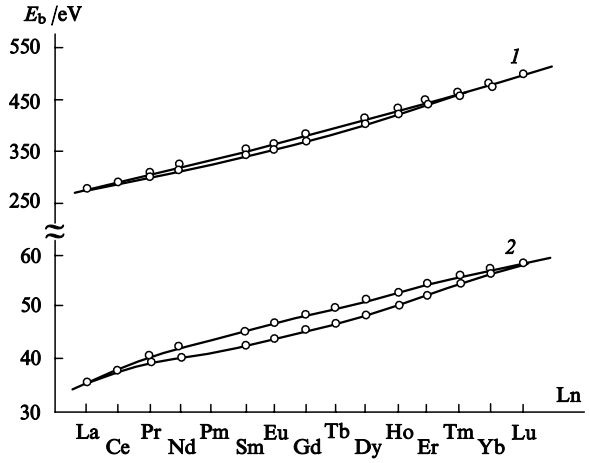


Figure 14. Binding energies (E_b) of the Ln4*s* (*1*) and Ln5*s* electrons (*2*) of lanthanide trifluorides *vs*. the metal atomic number in the La–Lu series.[5] The error of determination of the electron binding energy is ±0.2 eV.

with X-ray $MgK_{\alpha 1,2}$ excitation (1253.6 eV) instead of $AlK_{\alpha 1,2}$ excitation (1486.6 eV), as was to be expected, no Auger lines are observed around the Ln4*s* XPS lines.[44] In this case, the Auger lines are shifted towards the lower binding energy range by the value

$$\Delta E = E(AlK_{\alpha 1,2}) - E(MgK_{\alpha 1,2}) = 233 \text{ eV}.$$

The parameters of the Ln4*s* spectra of TbF_3, DyF_3, HoF_3 and ErF_3 found by Cohen *et al.*[44] allowed interpretation of some of the lines in the previously recorded spectra of these electrons[5] (see Table 1, Fig. 13). The use of $AlK_{\alpha 1,2}$ X-ray excitation provided the possibility of recording the Ln4*s* spectra for the trifluorides of light lanthanides.[42, 52]

Like the spectra of the Ln5*s* electrons, the spectra of the Ln4*s* electrons contain a structure attributable to many-body perturbation on the higher (by ~14–16 eV) binding energy side of the basic lines (see Fig. 15). Since the approximate equality

$$E_b(\text{Ln4}s) \approx E_b(\text{Ln4}p) + 2\,E_b(\text{Ln5}p),$$

holds for the whole lanthanide row, the Ln4*s* spectra are expected to exhibit a structure caused by the dynamic effect, which results in the formation of two final states, $\text{Ln}4s^1 4p^6 5p^6 4f^n \leftrightarrow \text{Ln}4s^2 4p^5 5p^4 4f^{n+2}$.

The above rule holds worst for heavy lanthanides; therefore, the configuration interaction should be manifested in the Ln4*s* spectra of these metals to a lesser extent than in the case of light lanthanides (see Table 1, Fig. 15). This interaction can lead to broadening of the Ln4*s* lines in the spectra of lanthanide trifluorides. For Gd^{3+}, this agrees with the results of theoretical calculations.[95]

In the Ln4*s* spectra of LnF_3, as in the spectra of lanthanide metals,[93] multiplet splitting is about twice as effective as in the Ln5*s* spectra (Fig. 16, see also Fig. 15). The maximum value is reached for GdF_3, in which the Gd^{3+} ion contains the greatest number of unpaired Gd4*f* electrons and occurs in an energy state with the multiplicity $2S + 1 = 8$. The dependence of the multiplet splitting for the Ln4*s* and Ln5*s* lines on the multiplicity ($2S + 1$) of the state of the lanthanide ion in the trifluorides is reflected in Fig. 16, which shows the data of different researchers obtained using both $AlK_{\alpha 1,2}$ and $MgK_{\alpha 1,2}$ excitation types (The data gained with different types of excitation supplement each other.)

The multiplet splitting values (ΔE_{ms}) found by Teterin *et al.*[5, 42] are somewhat lower than the corresponding values determined by Cohen *et al.*[44] Apparently, this is due to the fact that in determining the ΔE_{ms} values, Teterin *et al.*[5, 42] used, whenever possible, the binding energies for the 4*s* and 5*s* electrons found

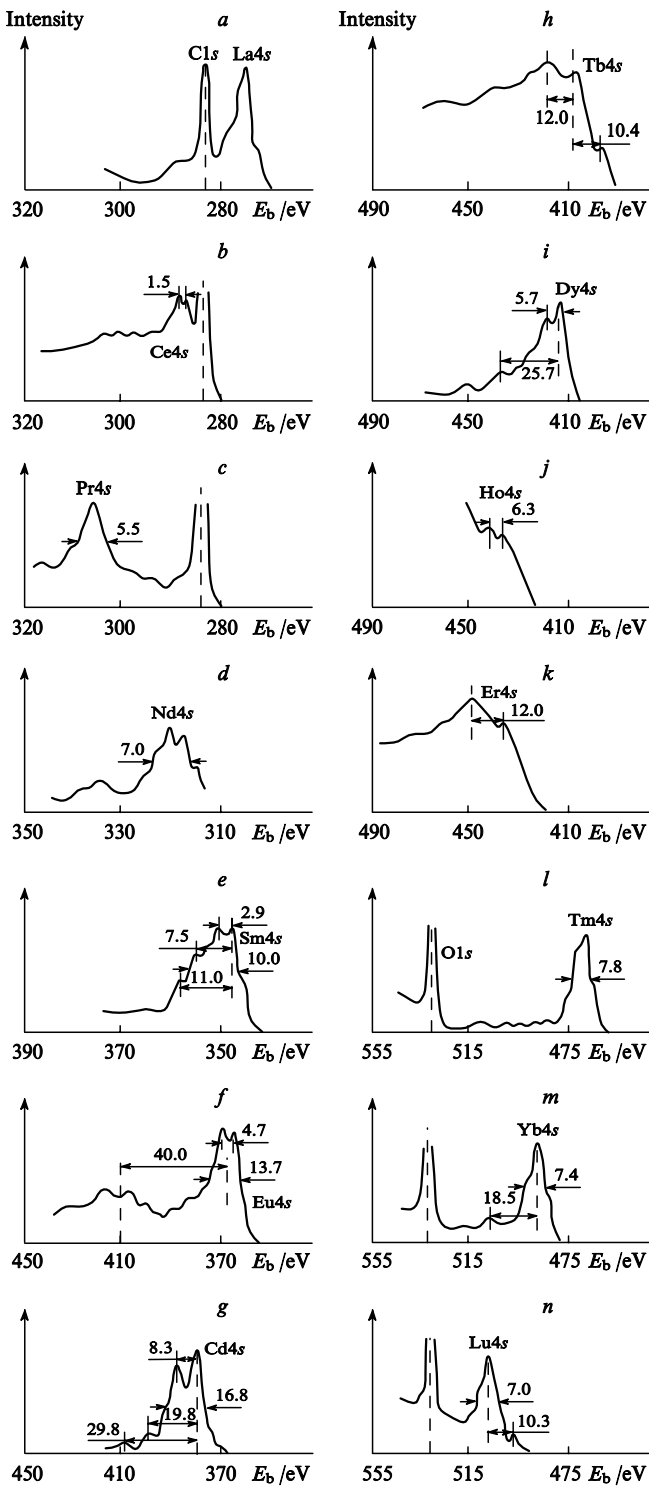


Figure 15. XPS spectra of lanthanide trifluorides in the Ln4*s* binding energy range.[42] (*a*) LaF_3, (*b*) CeF_3, (*c*) PrF_3, (*d*) NdF_3, (*e*) SmF_3, (*f*) EuF_3, (*g*) GdF_3, (*h*) TbF_3, (*i*) DyF_3, (*j*) HoF_3, (*k*) ErF_3, (*l*) TmF_3, (*m*) YbF_3, (*n*) LuF_3.

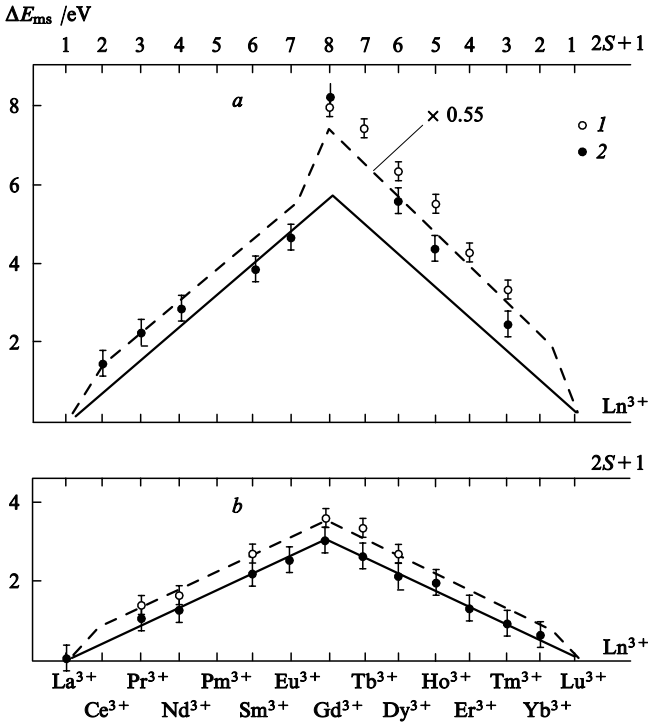


Figure 16. Multiplet splitting (ΔE_{ms}) of the Ln4*s* (*a*) and Ln5*s* (*b*) lines in the XPS spectra of lanthanide trifluorides. (*1*) Data of Ref. 44 ($MgK_{\alpha 1,2}$ excitation); (*2*) data of Ref. 52 ($AlK_{\alpha 1,2}$ excitation); the continuous line shows the results of the SCF X_α-DVM calculations;[69] the dashed line shows the results of *ab initio* calculations;[44,93] the dependence of ΔE_{ms}(Ln4*s*) on the multiplicity ($2S+1$) has been multiplied by 0.55.[93]

from experimental positions of the peaks rather than from the resolution of lines into two components, as was done in the other publication.[44]

The experimental estimates of the ΔE_{ms} values for the Ln5*s* electrons are consistent with the results of calculations carried out in various approximations.[44,69,87,93] In the case of Ln4*s* electrons, to attain agreement with the experimental data, the researchers[93] multiplied the determined ΔE_{ms} values by 0.55 (see Fig. 16). The symmetrical pattern of the calculated E_{ms} – multiplicity plots can be explained by the fact that, as the Ln4*f* shell of the Ln^{3+} ions is being occupied by electrons, the total spin (S) initially increases (from La^{3+} to Gd^{3+}) and then gradually decreases to zero. Thus, it can be seen from Fig. 16 that the magnitude of splitting of the Ln4*s* and Ln5*s* lines characterises the number of unpaired electrons in the lanthanide ions and, as a consequence, the lanthanide oxidation state in the compound. For example, splitting of the Ce4*s* line, ΔE_{ms}(Ce4*s*) = 1.5 eV, in the XPS spectrum points unambiguously to the trivalent state of the cerium ion in the fluoride. The maximum splitting of the Gd5*s* and Gd4*s* lines is also consistent with the fact that gadolinium is trivalent in the fluoride considered (see Fig. 16). In this connection, it should be noted that the structure of the Ln4*s* and Ln5*s* spectra can be useful in the determination of the oxidation and spin states of lanthanides in compounds.

b. The structures of the spectra of the Ln4d electrons

The spectra of Ln4*d* electrons in lanthanide fluorides exhibit a complex fine structure in an energy range of ~40 eV (Fig. 17, see also Table 1). It is noteworthy that the greatest spin–orbit splitting ΔE_{so}(Ln4*d*) over the lanthanide row was found for Lu and was as low as 10 eV. For other lanthanides, the corresponding ΔE_{so}(Ln4*d*) values cannot be determined experimentally due to the complicated structure of the Ln4*d* XPS spectra. In the region of the Dy4*d*, Ho4*d*, and Tm4*d* spectra at 231, 163 and 235 eV, the lines for Auger electrons can arise, caused by L_1MN, L_1MN and $M_5N_5O_3$ type transitions, respectively.[92] The lines observed at 187 and 207 eV in the Yb4*d* spectrum might also be Auger lines caused by the $M_5N_5O_1$ and $M_5N_4O_2$ electronic transitions (see Fig. 17). The spectra can also become complicated due to many-body perturbation accompanied by the formation of shake-up satellites on the higher binding energy side of the basic lines, for example, at ΔE_b = 14–16 eV. As has already been noted with regard to the Ln4*s* and Ln5*s* spectra (see Fig. 13, 15), the

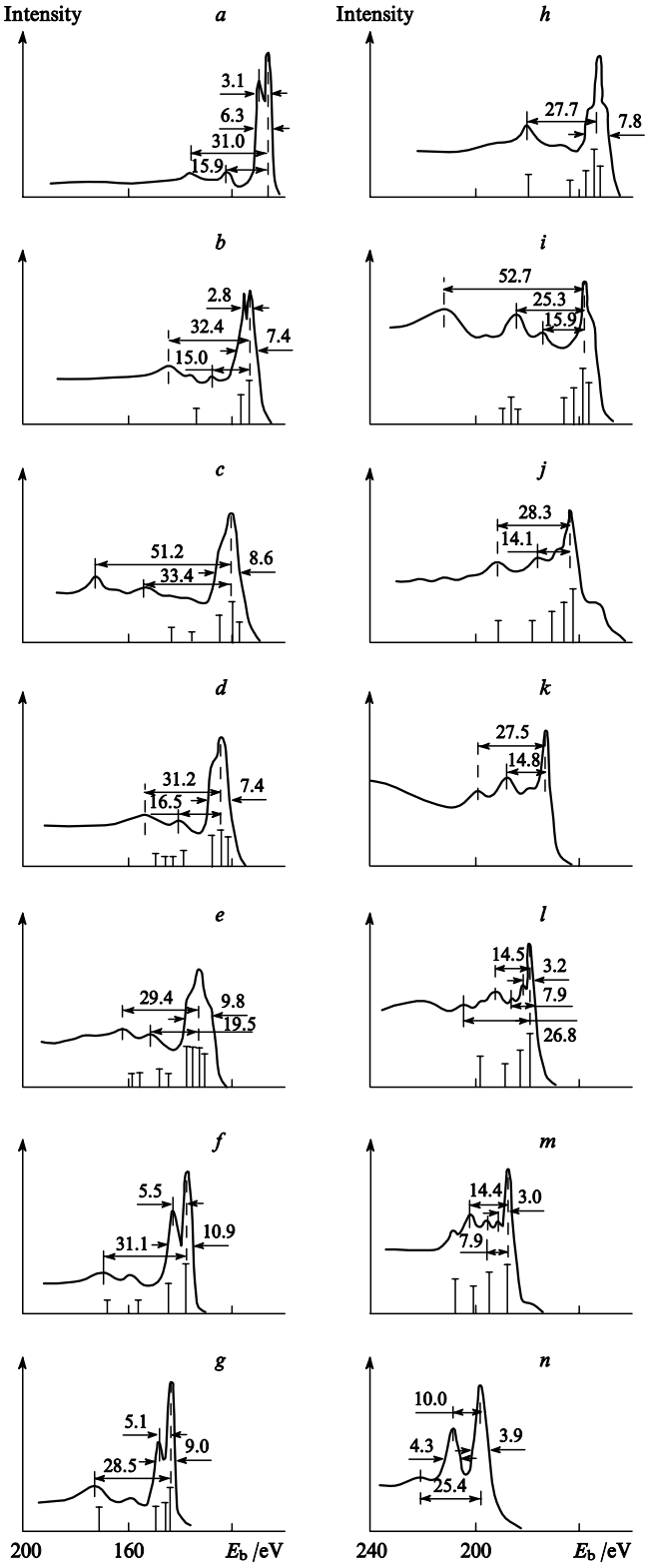


Figure 17. XPS spectra of lanthanide trifluorides in the Ln4*d* binding energy range.[52] (*a*) LaF_3, (*b*) CeF_3, (*c*) PrF_3, (*d*) NdF_3, (*e*) SmF_3, (*f*) EuF_3, (*g*) GdF_3, (*h*) TbF_3, (*i*) DyF_3, (*j*) HoF_3, (*k*) ErF_3, (*l*) TmF_3, (*m*) YbF_3, (*n*) LuF_3. Vertical segments show the calculation results for the spectra of these electrons in the Ln^{3+} ions with allowance for the multiplet splitting.[66]

intensity of these satellites should not be high. Among the lanthanide electronic configurations that can arise after photoemission of the Ln4*d* electrons upon the giant Coster-Kronig transitions between the core and valence shells, the $Ln4d^{9}5s^{2}5p^{6}4f^{n} \leftrightarrow Ln4d^{10}5s^{0}5p^{5}4f^{n+2}$ configurations are the most probable. However, since the approximate equality

$$E_b(Ln4d) \approx 2\,E_b(Ln5s) + E_b(Ln5p)$$

scarcely holds for lanthanides (see Table 1), it has been suggested[42] that the structure related to the dynamic effect would not be pronounced in the Ln4*d* spectra.

The structure of the Ln4*d* spectra depends on the atomic number of the lanthanide (Z), the simplest structures being observed for LaF_3[50,52] and LuF_3. These fluorides contain no unpaired Ln4*f* electrons, and their Ln4*d* spectra exhibit sharp doublets related to the spin–orbit coupling. The spin–orbit splitting markedly increases by the end of the lanthanide row; indeed, it amounts to 3.1 and 10.0 eV for LaF_3 and LuF_3, respectively (see Fig. 17). The extra structure detected in the Ln4*d* spectra of these compounds may also be due to both the many-body perturbation and (to a lesser degree) the dynamic effect.

The Ln4*d* spectra of lanthanides containing the unpaired Ln4*f* electrons are expected to manifest multiplet splitting.[38,45,96] The multiplet splitting was first observed in the spectra of 3*d* elements and europium.[97,98] Unlike the Ln*s* spectra in which the line is split into two components, in the case of Ln4*d* spectra, the final state of the ion after photoemission of these electrons can be rather complicated. In particular, in the Ln4*d* spectra of most lanthanide trifluorides, the multiplet splitting gives rise to a more complicated structure in a binding energy range of ~40 eV (see Fig. 17). The results of calculations[45,66] of the multiplet structure of the Ln4*d* spectra of Ln^{3+} ions are presented in Fig. 17 as vertical segments under the experimental spectra. Qualitative agreement between the theoretical and experimental data can be noted. For example, the Gd4*d* spectra exhibit two most intense lines that seem to resemble in shape a doublet caused by the spin–orbit coupling of these electrons (see Fig. 17). Therefore, in the study,[99] these components in the Gd4*d* spectrum of metallic gadolinium and Gd_2O_3 were misattributed to the $Gd3d_{5/2,3/2}$ components of the doublet. In reality, these are two components of the multiplet structure largely associated with the ^9D and ^7D final states.[96] For the Eu atom[98] and EuO_2 (see Ref. 44), the corresponding peaks in the Eu4*d* spectrum were also unreasonably ascribed to a doublet. This multiplet spectral structure is typical of particular lanthanide fluorides and in some cases, it can be used to determine the oxidation and spin states of lanthanide ions.

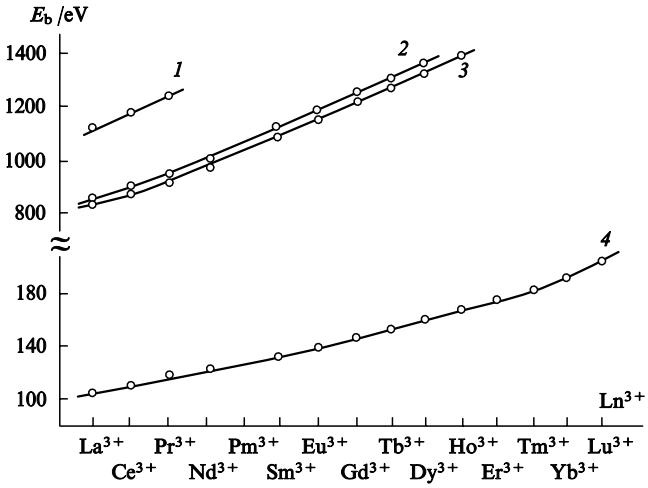


Figure 18. Binding energies (E_b) of the $Ln3p_{3/2}$ (*1*), $Ln3d_{3/2}$ (*2*), $Ln3d_{5/2}$ (*3*) and $Ln4d_{5/2}$ electrons (*4*) of lanthanide trifluorides *vs.* the metal atomic number in the La–Lu series.[5] The $Ln4d_{5/2}$ binding energies were determined for the most intense peaks; the error in the determination of the electron binding energies is ±0.2 eV.

As the lanthanide atomic number increases, the most intense component in the Ln4*d* spectrum shifts regularly towards higher binding energies. This component can formally be matched to the Ln4$d_{5/2}$ electrons. Figure 18 shows the variation of the binding energies of these components *vs*. the lanthanide atomic number; the pattern of variation is the same as observed for the core electrons.[22] The energies of the Ln4$d_{3/2}$ electrons can be estimated taking into account the fact that the spin–orbit splitting ΔE_{so}(Ln4*d*) gradually increases, as noted above, along the lanthanide row (La to Lu) from 3.1 to 10.0 eV.

c. The spectra of the Ln4p and Ln3p electrons

The binding energy range corresponding to the Ln4*p* electrons in the spectra of lanthanide trifluorides may contain, besides the C1*s* line caused by the hydrocarbon molecules absorbed on the sample surface, lines related to the Auger electrons.[20] These lines are broad and often reflect a whole series of Auger transitions (Fig. 19). For example, the increase in the intensity which starts at 350 eV in the Dy4*p* spectrum of disprosium trifluoride may be due, to an extent, to the electrons of the M_5NO type Auger transitions.[92] In the Ho4*p* spectrum, the Auger lines caused by the M_5NO transitions at $E_b > 310$ eV are so intense that the electronic structure of the XPS spectrum can hardly be observed. The broad band at 400 eV occurring in the Tm4*p* spectrum is attributable to the $M_5N_3O_3$ (395.2 eV), $M_5N_4N_5$ (391.1 eV) and $M_5N_4N_4$ (403.2 eV) Auger transitions. The Auger electrons of the $M_5N_2O_2$ (385.8 eV) and $M_5N_1N_7$ (421.7 eV) transitions can be manifested in the Yb4*p* and Lu4*p* spectra, respectively.

Apart from the lines of the Auger electrons, low-intensity shake-up satellites occur at higher binding energies (by 4–16 eV) than the basic spin doublet lines. In this range of the electron binding energies of lanthanide trifluorides containing unpaired Ln4*f* electrons, multiplet splitting can also be observed. Since the LaF_3 and LuF_3 molecules contain no unpaired Ln4*f* electrons, the complex structure arising in the spectra of their Ln4*p* electrons cannot be attributed to this splitting. The Ln4$p_{1/2}$ component in these spectra is diffuse; in the case of the La4$p_{1/2}$ line, the diffusion is pronounced, whereas the Lu4$p_{1/2}$ spectrum deviates to a lesser extent from the expected one.

Comparison of the Ln4*p* and Ln4*d* binding energies (see Table 1) shows that the approximate equality E_b(Ln4*p*) $\approx 2\,E_b$(Ln4*d*) holds satisfactorily for the whole lanthanide row. This fact and the presence of a complex structure in the Ln4*p* spectrum of lanthanum trifluoride suggest that the significant complication of the Ln4*p* spectra for LnF_3 is due to the dynamic effect, which leads to the formation of several final states, Ln4$p^5$4d^{10}4$f^n \leftrightarrow$ Ln4$p^6$4$d^8$4f^{n+1} (see Ref. 20). In the case of LuF_3 in which Lu4*f* is fully occupied, the giant Coster-Kronig transition of an electron from the Lu4*d* shell to the vacant shell next in energy can take place. The probability of such a transition is lower than that of the transition to the Ln4*f* shell; therefore, the structural changes in the Lu4*p* spectrum caused by the dynamic effect are less pronounced than those in the case of the La4*p* spectrum.

The Ln3$p_{3/2}$ spectra for lanthanum, cerium and praseodymium can be analysed in a similar way (Fig. 20). In these spectral ranges, Auger lines can show up.[92] Thus, the Ln3$p_{3/2}$ spectra can be superimposed by the Auger lines of the $M_5N_1N_3$ transitions (1125.6, 1132.0 eV). The Auger transitions of the M_3NO (1184.5 eV), M_3NN (1184.5 eV) and $M_5N_1N_1$ (1202.3 eV) types may be manifested in the Ce3$p_{3/2}$ range in the spectrum of cerium trifluoride; among other factors, this can be responsible for the intense peak observed at 1200 eV in its XPS spectrum. The Auger electrons of the M_3NN (1175.4 eV) and M_5NN_1 transitions (1184.6 eV) may be a reason for the appearance of the intense broad band at 1226 eV in the Pr3$p_{3/2}$ spectrum of praseodymium trifluoride.

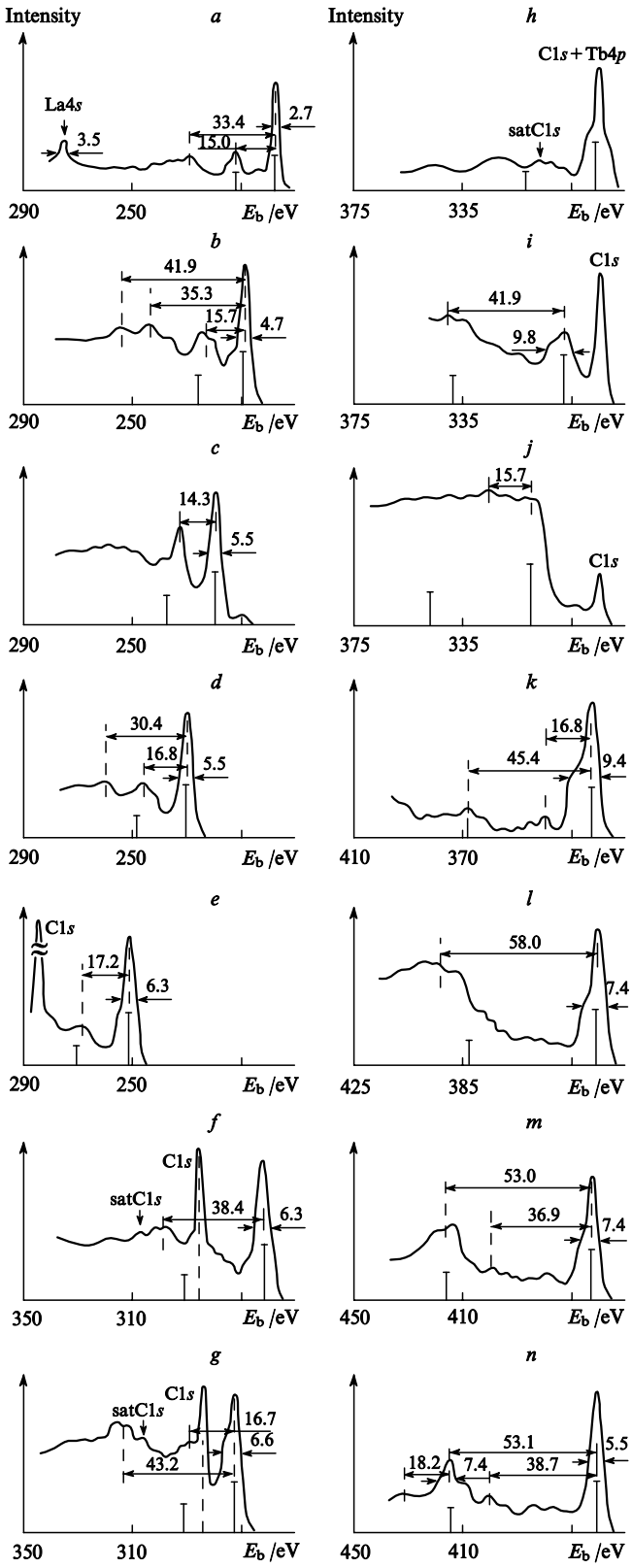


Figure 19. XPS spectra of lanthanide trifluorides in the Ln4*p* binding energy range. (*a*) LaF_3, (*b*) CeF_3, (*c*) PrF_3, (*d*) NdF_3, (*e*) SmF_3, (*f*) EuF_3, (*g*) GdF_3, (*h*) TbF_3, (*i*) DyF_3, (*j*) HoF_3, (*k*) ErF_3, (*l*) TmF_3, (*m*) YbF_3, (*n*) LuF_3.[20] Vertical segments show the expected energies for the atomic components of the Ln4$p_{3/2,\,1/2}$ electrons;[22] sat is satellite.

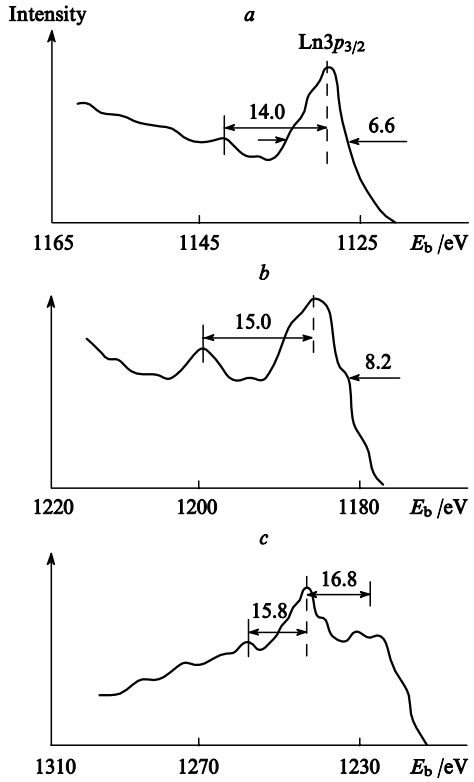


Figure 20. XPS spectra of lanthanum (*a*), cerium (*b*), and praseodymium (*c*) trifluorides in the Ln3$p_{3/2}$ binding energy range.[52]

In these spectra, the peaks located at higher (by 14–16 eV) binding energies than the basic lines may be due to many-body perturbation. Since the approximate equality

$$E_b(\mathrm{Ln}3p) \approx E_b(\mathrm{Ln}3d) + E_b(\mathrm{Ln}4s),$$

is obeyed, a structure related to the dynamic effect, giving rise to the $\mathrm{Ln}3p^5 3d^{10} 4s^2 4f^n \leftrightarrow \mathrm{Ln}3p^6 3d^9 4s^1 4f^{n+1}$ final states, should be expected in the Ln3*p* spectra. By using a different excitation source, the structure due to a dynamic effect can be separated from the Auger lines. However, apart from Al$K_{\alpha 1,2}$ radiation (1486.6 eV), only Mg$K_{\alpha 1,2}$ radiation (1253.6 eV) is currently available but its energy is not sufficient for recording these spectra. In this case, a synchrotron radiation source with variable energy is required. The dependence of the Ln3$p_{3/2}$ binding energy on the lanthanide atomic number for three fluorides is shown in Fig. 18 (curve *1*). The Ln4*p* and Ln3*p* spectra of lanthanide trifluorides are typical of individual compounds and can be used for identification.

d. The structure of the spectra of the Ln3d electrons

In X-ray photoelectron spectroscopy, determination of the oxidation states of elements from the chemical shifts of their core energy levels is normally done using the most intense single lines corresponding to the ground final state of the ion resulting from electron photoemission. In the case of lanthanide compounds, this procedure is faced with problems, because, as noted above, virtually all the spectral lines situated in the binding energy range normally employed in XPS are structured. As a rule, Ln3*d* lines are used for this purpose whenever possible. However, the spectra of these electrons for light lanthanides also have a clear-cut fine structure, while in the case of heavier REE, due to high Ln3*d* binding energies, the relevant lines are highly broadened or cannot be observed at all without using the synchrotron radiation (Fig. 21). The structure of the Ln3*d* spectra of REE related to the spin–orbit splitting has been considered theoretically.[100]

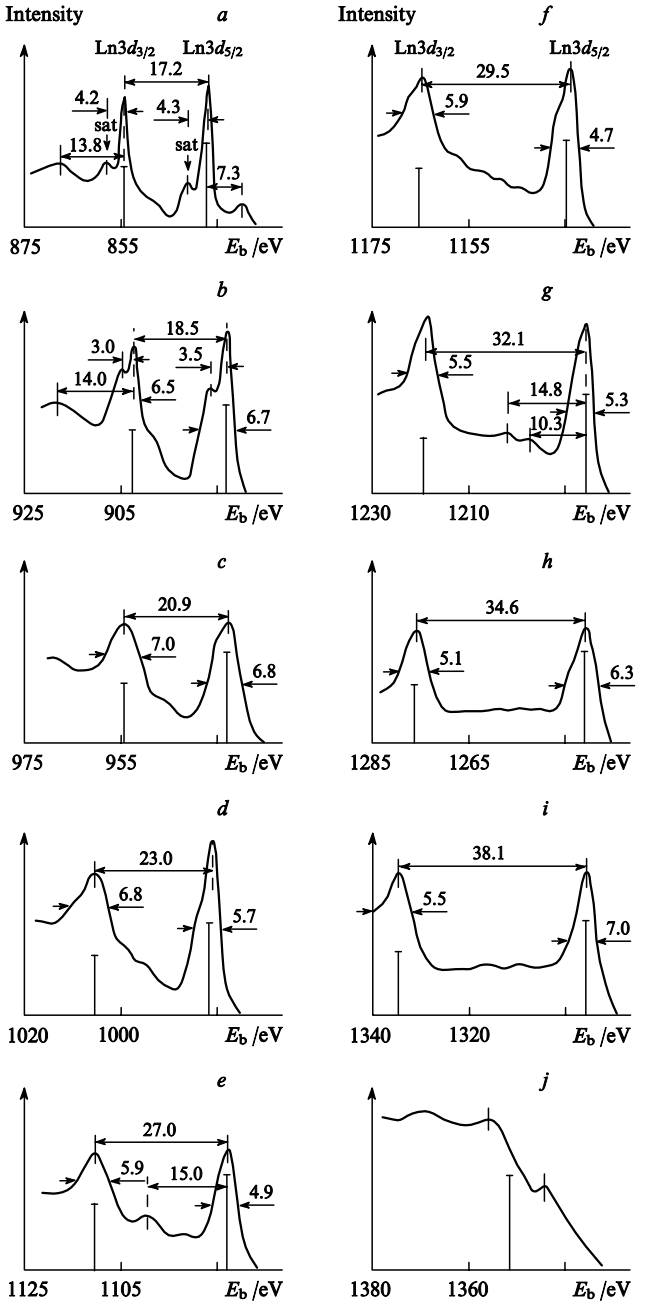


Figure 21. XPS spectra of lanthanide trifluorides in the Ln3*d* binding energy range.[42] (*a*) LaF_3, (*b*) CeF_3, (*c*) PrF_3, (*d*) NdF_3, (*e*) SmF_3, (*f*) EuF_3, (*g*) GdF_3, (*h*) TbF_3, (*i*) DyF_3, (*j*) HoF_3. Vertical segments show the lines of the lanthanide atomic spectra.[22]

The need for determination of the Ln3*d* binding energies in lanthanide compounds has stimulated investigations into the nature of the fine structure observed in these spectra.[41,46,75,101–109] It is worth noting that some Auger electron lines can also occur in this spectral region.[92] Thus the Ln3*d* spectra for lanthanum and cerium exhibit peaks associated with Auger electrons of the $M_5N_3O_3$ (865.6 eV) and $M_5N_1O_2$ (918.3 eV) transitions, respectively (see Fig. 21). The shoulder on the higher binding energy side with respect to the Nd3$d_{3/2}$ line can be partly due to the Auger electrons of the $M_2N_2N_2$ transition (1012.1 eV). Broadening of the Sm3$d_{3/2}$ line can also be related to the superimposition of the Auger line of the M_5N_1N transition (1118.6 eV) onto this spectrum. Due to the Auger N_3OO transition (1341.0 eV), the Ho3$d_{5/2}$ spectrum virtually cannot be observed. A similar complex structure, except for the Auger lines, shows

itself in the binding energy range of Ln3*d* electrons in the spectra of LaF_3 and CeF_3 recorded with $MgK_{\alpha 1,2}$ excitation (1253.6 eV).[46] Hence, the intense extra structure in the spectra of these electrons is not related to Auger transitions.

Comparison of the binding energy of low-energy electrons [$E_b \leqslant E_b$(Ln3*d*)] suggests that the structure caused by the dynamic effect is unlikely in the Ln3*d* spectra. The dependence of the FWHM value (Γ) in the Ln3$d_{5/2}$ spectra on the lanthanide atomic number ($58 \leqslant Z \leqslant 66$) suggests that the multiplet splitting does not play a crucial role in the appearance of the extra structure or line broadening (Fig. 22). If this broadening were largely related to the multiplet splitting, as has been noted in some publications,[101–103] the maximum line width over the Ce^{3+}–Gd^{3+} series would be expected for the Gd3$d_{5/2}$ electrons; this does not agree with the $\Gamma(Z)$ dependence found experimentally (see Fig. 22).

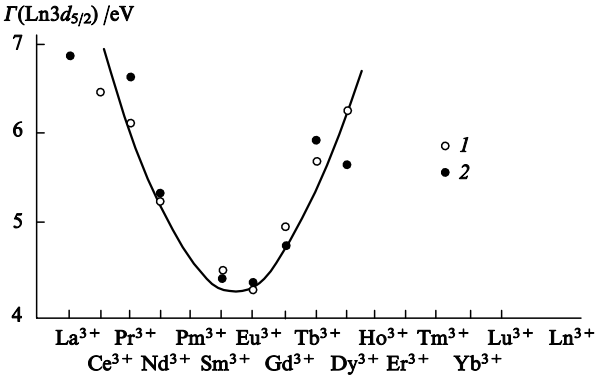


Figure 22. Dependence of the width (Γ) of the Ln3$d_{5/2}$ line on the lanthanide atomic number in the La–Lu series.[42] (*1*) LnF_3, (*2*) Ln_2O_3. The Γ values are referred to Γ(C1*s*) = 1.3 eV.

The Ln3*d* spectra of lanthanide trifluorides exhibit low-intensity shake-up satellites located at a higher binding energy (by 14–16 eV) than the most intense Ln3$d_{5/2}$ lines. The researchers' opinions concerning the nature of the low-energy spectral structure in the vicinity of the basic lines vary. While admitting that for light lanthanides such as La, Ce and so on, the spectral structure in the Ln3*d* binding energy range is mainly due to many-body perturbation, some researchers believe that these extra lines are shake-up satellites,[45,104–107] while others consider them to be shake-down satellites.[75,108,109] A fundamental difference between the two above standpoints is that the line located at a lower binding energy, in the Ln3$d_{5/2}$ range is interpreted as either the basic line or a satellite caused by the many-body perturbation. It is noteworthy that the binding energy of the Ln3*d* electrons of the ground state has to be known for the solution of many problems.

The presumptive mechanism of the appearance of the Ln3*d* satellites in the XPS spectra can be illustrated by means of diagrams shown in Fig. 23. They are based on the results of X_α-SW (scattered wave) calculations for the LaF_3, CeF_3, CeF_3^+ and YbF_3 (D_{3h} symmetry) clusters in which R(La–F) = 0.246 nm, R(Ce–F) = 0.241 nm and R(Yb–F) = 0.226 nm.[47,48] The calculations of the electronic structures of these clusters before and after photoemission of an Ln3*d* electron were performed and MO occupancies in these clusters were analysed. On the basis of these data and using the two-level Larsson's model (see Refs 47 and 110 and references therein), the satellite intensities and energies were estimated with respect to the basic spectral lines in the sudden approximation.[111,112] These results have enabled some qualitative conclusions.[47]

For example, for the LaF_3 cluster (D_{3h} symmetry), the removal of an Ln3*d* electron was found to reduce substantially the energy difference between the system of occupied bonding a_1', e', e'', a_2', a_2'' and e' OVMO, which mainly consist of F2*p* AO, and

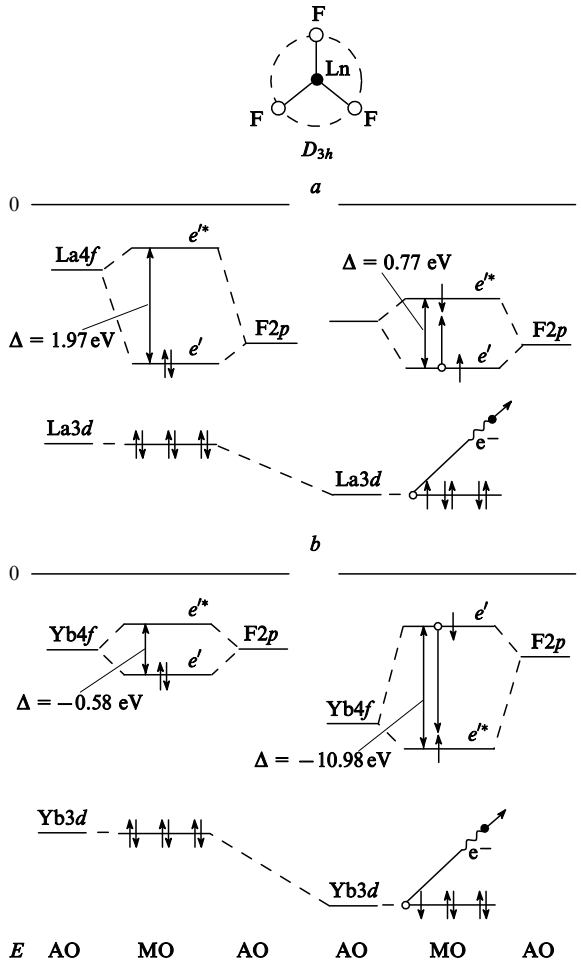


Figure 23. Diagrams illustrating the mechanisms of formation of shake-up (*a*) and shake-down satellites (*b*) in the XPS spectra of Ln3*d* electrons constructed with allowance for the results of X_α-SW calculations for the LnF_3 clusters (D_{3h} symmetry).[47] The left-hand part of the figure presents the initial states of the systems, while the right-hand part shows the final states after electron photoemission.

the system of vacant antibonding e'', a_2'', e'^*, a_2' and a_1' OVMO, which include the Ln4*f* AO. This is due to the fact that the OVMO containing the Ln4*f* AO respond more efficiently to the appearance of a hole in the lanthanum atom than the OVMO containing the F2*p* AO. This is reflected in the diagram for the e' and e'^* OVMO couple in lanthanide trifluorides (see Fig. 23 *a*). In this case, the energy difference (Δ) between these MO decreases from 1.97 to 0.77 eV. Therefore, photoemission of an Ln3*d* electron can induce electron subexcitation within the considered OVMO, reflecting transition from the e' to e'^* OVMO. Since the e' OVMO energy is greater in magnitude than the e'^* OVMO energy, this transition corresponds to a shake-up process. In the Ln3*d* spectrum, the corresponding satellites should occur at higher energies than the basic lines. These results show that most intense low-energy lines observed in the La3*d* spectrum of lanthanum trifluoride should be assigned to the ground final state with a hole in the La3*d* level. The theoretical values for the satellite energy and its intensity with respect to the basic lines ΔE_{sat} = 1.1 eV and I_{sat}/I_o = 0.42 (I_{sat} and I_o are the satellite and basic line intensities, respectively) differ substantially from the experimental values (4.3 eV and 0.30).[42] Similar results were obtained for the CeF_3^+ (ΔE_{sat} = 1.1 eV, I_{sat}/I_o = 0.23) and CeF_3 (1.1 eV and 0.37, respectively) clusters. The experimental ΔE_{sat} and I_{sat}/I_o values for CeF_3 are 3.5 eV and 0.58.[42]

For the YbF_3 cluster (D_{3h} symmetry), the calculations imply that the MO related to the Yb4*f* AO are comparable in energy with

the OVMO caused by the F2*p* AO.[47] The removal of two Yb3*d* electrons entails a very pronounced increase in the energies of these two groups of MO; the energies of the OVMO composed of the Yb4*f* AO are appreciably increased, and the energy levels of these MO become lower than those of the OVMO formed by the F2*p* AO. For instance, for the e'^* and e' OVMO couple shown in Fig. 23 *b*, the energy difference reaches 10.98 eV in magnitude. In this case, transition of an electron from a higher OVMO, for example, e', to the lower e'^* MO can occur simultaneously with the Yb3*d* photoemission. Since the e' MO energy is lower than the e'^* MO energy, this transition, as noted above, is referred to as a shake-down process and the spectral structure caused by this transition is a shake-down satellite. In particular, it follows from the results of calculations[47] that the shake-down satellites in the Yb3*d* spectrum are expected to occur at lower binding energies than the basic lines ($\Delta E_{sat} = -16.0$ eV), their intensity being about 5 times as high as the basic line intensity ($I_{sat}/I_o = 4.81$). It is noteworthy that no experimental data for this electron energy range for ytterbium compounds are available to date for the reasons noted above.

On the basis of the calculation results, it was concluded [47] that an increase in the number of Ln4*f* electrons in the lanthanide fluoride brings about displacement of the satellites in the Ln3*d* spectra from left to right with respect to the basic doublet components. It remains unknown in which lanthanide spectrum in the La – Lu series the sign of the ΔE_{sat} changes.

It is noteworthy that some suggestions concerning the reasons for the appearance of satellites in the Ln3*d* spectra based on the results of theoretical calculations do not contradict the available experimental data. Thus an insignificant shift should be expected for the line of the OVMO formed mainly by the F2*p* AO of fluorides (see Fig. 3) because the F1*s* binding energy (E_b) changes slightly with an increase in the lanthanide number (Z). In the case of LaF_3, the OVMO line is observed at 8.1 eV (see Table 1, Fig. 1). In the LnF_3 spectra, the centre of gravity of the structure caused by the Ln4*f* electrons shifts from the level taken as the reference point toward higher binding energies. Due to this shift, the OVMO related to the Ln4*f* AO and those related to the F2*p* AO can become equal in energy at some Z, which agrees with the theoretical results (see Fig. 3). Hence, on photoemission of an Ln3*d* electron, the Ln4*f* electronic level is expected to be located lower than the corresponding F2*p* electronic levels. This should favour a shake-down electronic transition (see Fig. 23).

As the atomic number of lanthanide increases, at least, in the case of transition from LaF_3 to PrF_3, the Ln3*d* spectra show a decrease in the difference between the electron binding energies of the basic and satellite lines (ΔE_{sat}). Furthermore, with the assumption that one reason for the substantial broadening of the Ln3*d* spectral components is the formation of satellites, the change in the Ln3$d_{5/2}$ FWHM upon an increase in Z (see Fig. 22) can be attributed to migration of the satellite from left to right on passing from La to Lu, as has been suggested on the basis of calculations. In this case, the change in the sign of ΔE_{sat} is to be expected at about $Z = 63$ (Eu) (see Fig. 22).

For identification of lines in the Ln3*d* spectra of the trifluorides of light lanthanides, Teterin and Baev[5] have proposed comparing the differences between the electron binding energies of different shells found for metallic lanthanides and for lanthanide compounds. The following values were found for LaF_3: $\Delta E_b(La5p_{3/2} - Ln3d_{5/2}) = 818.4$ (823.0) eV, $\Delta E_b(La5p_{3/2} - La4d_{5/2}) = 85.8$ eV and $\Delta E_b(La4d_{5/2} - La3d_{5/2}) = 732.6$ (737.2) eV (the energies for weaker lines or shoulders are given in parentheses; see Table 1). The corresponding differences between the electron binding energies for metallic lanthanum are 818.2, 86.0 and 732.2 eV. The value $\Delta E_b(La5p_{3/2} - La3d_{5/2}) = 818.2$ eV coincides within the error of measurement with a value of 818.6 eV, found by Schlapbach and Scherrer.[91]

If one assumes that after the IVMO formation from the La5*p* and F2*s* AO in lanthanum trifluoride, the spectrum in the La5$p_{3/2}$ region does not differ much from the atomic spectrum (see Table 1), the comparison of the ΔE_b values leads to the conclusion that the basic La3*d* line in the spectrum of LaF_3 is located at lower electron binding energies. The satellites recorded at higher (by 4.3 eV) binding energies with respect to the basic lines are due to the shake-up process.

The results of comparison of the binding energy differences $\Delta E_b(Ce5p_{3/2} - Ce3d_{5/2})$ for CeF_3 (865.3, 868.8 eV) (see Table 1) and for metallic cerium (866.3 eV),[113] at least, do not contradict the statement that the satellites in the Ce3*d* spectra are shake-up satellites observed at higher binding energies than the basic lines. The theoretical data do not disprove this either.[114] Comparison of the results of calculations for YbF_3 with the experimental spectra is difficult due to the fact that the Yb3$d_{5/2}$ binding energy ($E_b = 1527$ eV) is beyond the range accessible for measurements as long as X-ray Al$K_{\alpha 1,2}$ excitation is used (1486.6 eV).

The dependence of the Ln3*d* binding energy on the lanthanide atomic number is shown in Fig. 18. On the basis of the binding energies of these electrons, one can draw conclusions concerning the oxidation state of lanthanides from La to Ho. Note that the use of synchrotron radiation provides the possibility of an XPS study of the Ln3*d* electrons and compounds of heavier lanthanides.

III. Lanthanide oxides

Lanthanide oxides are the REE compounds most abundant in nature. They serve as the main raw materials for the production of various technologically important lanthanide compounds. Therefore, despite difficulties associated with experimental and theoretical investigations of the electronic structures of lanthanide oxides, this problem attracts increasing attention. These difficulties are related to the complexity of the lanthanide electronic configurations, low symmetry of the close environment of metal atoms in the crystal lattices, and to the presence of Ln ions in different oxidation states in some oxides. Thus praseodymium and terbium oxides are known[1] to have complex stoichiometric compositions ($Pr_2O_3 \cdot 4\,PrO_2$ and Tb_4O_7). The oxidation state of cerium in the cerium oxide is still open to question. According to data obtained by different researchers, this oxide is either described by the general formula CeO_2 (see Ref. 1), or contains a $CeO_2 \cdot n\,Ce_2O_3$ mixture on the surface,[115] or contains variable-valence cerium.[116] The other lanthanide oxides may have a stoichiometric composition corresponding to Ln_2O_3.

In recent years, the XPS method has been widely used in the study of REE oxides[27, 39, 41, 42, 50, 80, 99, 108, 115, 117–127] and some other oxygen-containing compounds.[19, 28–30, 41, 53, 78, 79, 84, 128] Important information concerning the electronic structures of these oxides can also be drawn from X-ray emission spectra;[129, 130] however, in most cases, studies are carried out for oxide films and separate electronic shells of metals. In a number of publications,[5, 18, 20, 37, 68] lanthanide (except for Pm) oxides were studied as bulk samples (pressed powders). Attention was concentrated on elucidation of the mechanisms of formation of fine structure in the spectra of these compounds and the dependence of the spectral structure on the physicochemical properties and on the nature of chemical bonding in lanthanide oxides. For this purpose, the spectra over the whole energy range accessible for measurements were analysed. The binding energies of various electron shells in the ~0 – 1350 eV range for the oxides under study are presented in Table 3. In all cases, two lines of O1*s* electrons were observed. The component located at a lower binding energy is attributable to the oxide oxygen,[33, 41] while the less intense line at higher binding energies should be ascribed to impurities containing carbonate or hydroxy groups.[19, 131] It has been noted [5, 42] that successful interpretation of the mechanism of appearance of the fine spectral structure requires that the data for the whole REE row be obtained using the same XPS spectrometer under the same conditions. The results of experimental studies that comply with this requirement [20, 37, 68, 79, 132–136] are of special interest.

Table 3. Electron binding energies (E_b /eV) for lanthanide oxides.[5, 59]

Compound	OVMO	IVMO [a]				Ln4$d_{5/2, 3/2}$	Ln4$p_{3/2, 1/2}$	Ln4s	Ln3$d_{5/2}$ (see [b])	O1s (see [b])
		Ln5$p_{3/2}$	Ln5$p_{1/2}$	O2s	Ln5s					
La_2O_3	4.9	17.7	19.4	−; 24.0	35.0	102.8; 105.8	196.3; 199.4; 206.4	274.9	835.1; (888.6)	528.9; (531.4)
CeO_2 (see [c])	5.0	18.0	unknown	unknown	36.8	108.5; 112.0; 114.4	207.1; 214.1	288.8	832.3; (888.8)	529.5; (531.8)
Pr_2O_3 (see [c])	3.7; 5.9	19.3	22.9	−; 24.0	37.4; 38.4	114.0; 116.8; 119.8; 128.2; 131.0	218.5	303.9; 305.9	(929.5); 933.5	528.9; (531.8)
Nd_2O_3	5.3; 9.0	19.4	23.0	−; 24.1	39.1; 40.6	122.0; 125.0	226.4; 229.7; 243.5	319.0; 321.5	(978.0); 981.9	529.4; (531.1)
Sm_2O_3	5.7; 8.2	20.4	24.4	unknown	40.8; 43.3	132.7; 135.1	250.4	348.8; 353.3	1083.1	529.2; (531.6)
Eu_2O_3	−; 7.3	21.5	25.7	the same	43.3; 46.2	136.5; 142.0; 166.4	261.2; 264.2	364.3; 369.8	1134.6	529.2; (531.6)
Gd_2O_3	5.7; 9.0	22.3	27.4	"	44.3; 48.0	142.8; 147.9; 171.8	270.6; 272.6	378.8; 386.7	1187.3	529.3; (531.7)
Tb_2O_3 (see [c])	3.0; 7.6; 9.8	23.0	28.1	19.4	46.2; 48.8	150.1; −; 178.2	284.0; 323.0	unknown	1241.1	529.2; (531.4)
Dy_2O_3	3.4; 6.0; 9.1	23.4	28.5	19.7	47.0; 49.5	154.8; 156.0; 176.5; 178.9; 184.0	292.6; 294.3; 335.5	413.7; 419.6	1296.0	529.1; (531.7)
Ho_2O_3	7.1; 9.7	24.7	30.4	19.5; 21.5	49.0; 50.7	161.9; 167.4; 776.6; 189.0; 198.0	308.2; 314.2	433.8; 438.2	1352.5	529.3; (531.8)
Er_2O_3	6.3; 9.5	25.3	31.1	20.5; 22.5	51.3; 52.8	169.1; 175.0; 163.4; 191.7; 196.0	320.3; 326.1; 362.9	449.5; 453.0	unknown	529.4; (531.3)
Tm_2O_3	6.0; 7.2; 9.1; 10.9	26.0	32.4	20.5; 23.0	53.5; 54.6	176.8; 180.0; 189.7; 192.2; 201.3	333.0; 337.0	468.8; 470.5	the same	529.4; (531.7)
Yb_2O_3	7.6; 11.1	26.7	33.6	21.5; 23.8	55.4; 56.1	185.1; 188.4; 193.2; 199.3; 205.3	346.4; 399.6	488.0; 489.0	"	529.6; (531.8)
Lu_2O_3	7.8; 9.0	27.5	33.9	21.6; 23.5	57.0	196.5; 206.3	359.3; 412.5	506.7	"	529.6; (531.6)
HfO_2	5.7; 7.4; 17.4; 18.4	32.8	40.1	unknown	unknown	213.4; 223.9	unknown		"	530.7
Y_2O_3	4.3; 5.6	25.0 [d]		20.0	45.4 [e]	156.7; 158.5 [f]	299.8; 312.0 [g]	394.0 [h]	"	530.8; (532.2)
Sc_2O_3	6.0	31.5 [i]		21.9	53.4 [j]	unknown	401.9; 406.4 [k]	501.0 [l]	"	530.1; (531.8)

Note. The E_b values are presented for the peaks relative to the C1s binding energy for hydrocarbons on the sample surface [E_b(C1s) = 285.0 eV]. [a] The given energies correspond to IVMO electrons exhibited in the spectral ranges of the valence AO electrons. [b] The values in parentheses are the electron energies for less intense lines or shoulders. [c] The E_b values are given for Ln^{3+} in complex oxides ($Ln_2O_3 \cdot n\,LnO_2$). [d] The Y4p line. [e] The Y4s lines. [f] The Y3$d_{5/2, 3/2}$ lines. [g] The Y3$p_{3/2, 1/2}$ lines. [h] The Y3s line. [i] The Sc3p line. [j] The Sc3s line. [k] The Sc2$p_{3/2, 1/2}$ lines. [l] The Sc2s line.

1. Structure of the spectra of low binding energy electrons

The spectra of low binding energy electrons of lanthanide oxides exhibit two groups of lines with binding energies of $\sim 0-15$ and $\sim 15-50$ eV, attributable to the OVMO and IVMO electrons, respectively (Fig. 24, see Table 3). In the case of lanthanum oxide, the OVMO binding energy range, besides the line at 5.6 eV, mainly due to the La5*d*, La6*s* and O2*p* electrons, can display two weak maxima at $E_b = 11$ eV; these are due to some impurities containing presumably the CO_3^{2-} group (this is also valid for other Ln_2O_3). The corresponding C1*s* line is located at $E_b = 290.8$ eV. In the spectra of lanthanide oxides containing Ln4*f* electrons, the intensity of the corresponding lines gradually increases with an increase in the atomic number (Z) of the metal. The pattern of Ln4*f* spectra of lanthanide oxides generally resembles the corresponding structure of the spectra of Ln4*f* electrons in lanthanide trifluorides (see Fig. 2). The difference lies in the fact that the OVMO line reflecting mainly the O2*p* AO in the XPS spectra of REE oxides is located at binding energies lower in magnitude than the F2*p* line in the lanthanide fluoride spectra. For convenience of the comparison of the OVMO and Ln4*f* binding energies in REE oxides with the corresponding characteristics of lanthanide fluorides, the absolute E_b values for lanthanide oxides were increased by 1.6 eV (see Fig. 3). This is the shift of the XPS lines of lanthanum trifluoride with respect to the lines of La_2O_3 (see Tables 1, 3). Considerations concerning the origin of the structure of the Ln4*f* lines presented above for REE fluorides are also valid for the spectra of these electrons in lanthanide oxides (see Section II). However, the overlap of the OVMO and Ln4*f* lines in the XPS spectra of lanthanide oxides starts at a smaller Z than in the case of LnF_3 (see Fig. 3).

The experimental dependence of the Ln4*f* line intensity (I_{exp}) on the number n_{4f} of electrons in the Ln^{3+} ion found as the ratio of the total intensity $I[(Ln4f) + (\sum OVMO)]$ in the binding energy range of 0–15.5 eV to the total intensity $I(\sum IVMO)$, except for the Ln5*s* lines, is shown in Fig. 25. Using the least-squares method, this dependence for lanthanide oxides was shown to be linear

$$I_{exp} = 0.12n_{4f} + 0.25. \quad (6)$$

By analogy with expression (5) corresponding to LnF_3, the following theoretical dependence was derived for Ln_2O_3:

$$I_{theor} = 0.01n_{4f}^{2.24} + 0.18. \quad (7)$$

It can be seen that, as for lanthanide trifluorides (see Fig. 5), in this case, too, the experimental and theoretical plots for the intensity *vs.* n_{4f} [see Eqns (6), (7) and Fig. 25] are appreciably different.

On passing from Lu_2O_3 to HfO_2, the metal atomic number increases by unity, the number of the M4*f* electrons (14) remains the same, and the intensity of the line under consideration increases jumpwise tending to the corresponding theoretical value (see Fig. 25). The Hf4$f_{7/2}$-electron binding energy, equal to 17.4 eV, also markedly (by 9.6 eV) exceeds the binding energy of the OVMO electrons in lutetium (see Table 3). It follows from these data that the Lu4*f* electrons, which can be regarded in a certain approximation as inner valence electrons, differ markedly in spectral characteristics from the Hf4*f* electrons, which acquire some features of core electrons.

In the Ln5*p* and O2*s* spectral range, fine structure is observed. The structure becomes most intricate by the middle of the row of lanthanide oxides (see Fig. 24). Among other reasons, complication of the spectral structure may be due to the presence of lanthanide ions in different oxidation states in some lanthanide oxides. In this connection it should be noted that, as shown on the basis of analysis of the spectral structure of core electrons, REE oxides, except for cerium, praseodymium and terbium, contain Ln^{3+} ions. In praseodymium and terbium oxides, Pr and Tb in higher oxidation states occur as impurities, their concentrations being not higher than 5%.[5] The spectral structure observed for cerium oxide is more complicated. If one assumes that the additional lines in the Ce3*d* spectrum (36%) are due to Ce^{4+} ions, the contents of Ce^{4+} and Ce^{3+} ions on the surface of the cerium oxide studied should be 36% and 64%, respectively; this would complicate significantly the considered spectral structure (see Fig. 24). Teterin *et al.*[137,138] believe that the additional structure (36%) is caused by many-body perturbation involving the Ce5*s* electrons and does not complicate the structures of the Ce5*p* and O2*s* spectra. Since the O1*s* spectra of the studied REE oxides exhibit in

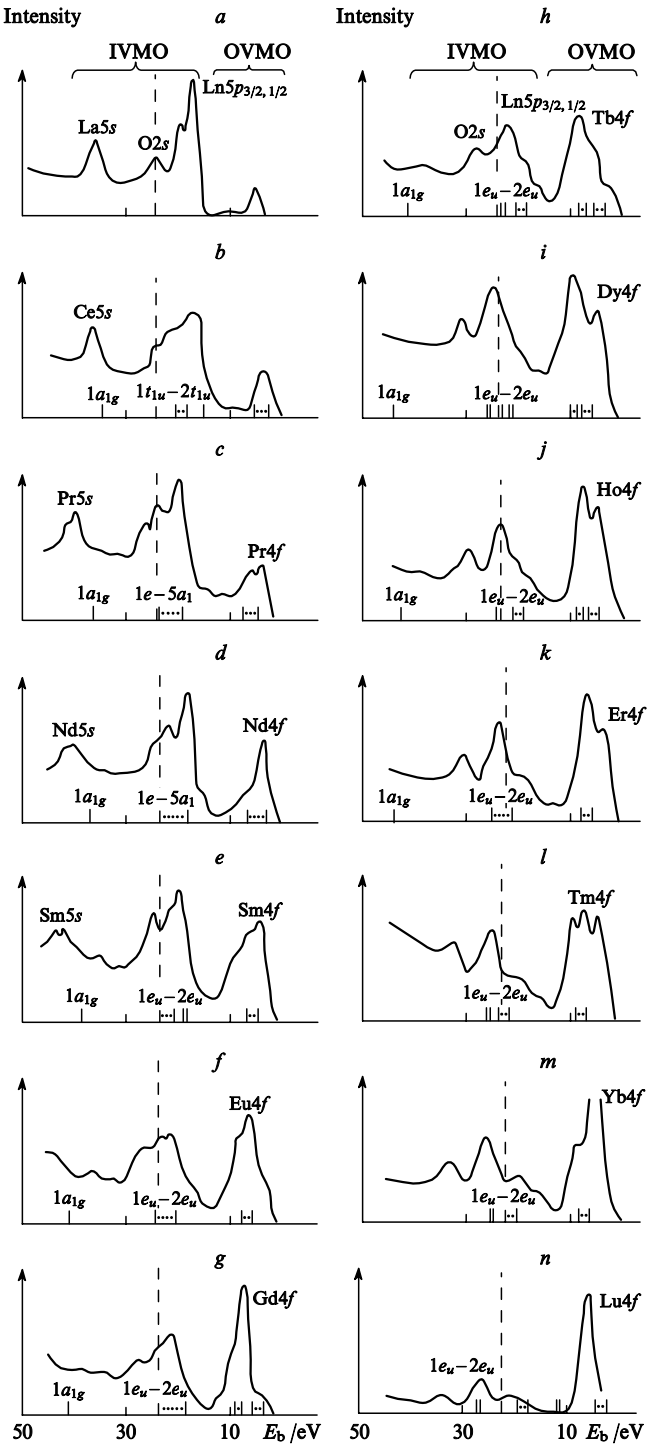


Figure 24. XPS spectra of low binding energy electrons in lanthanide oxides.[132] (*a*) La_2O_3, (*b*) CeO_2, (*c*) Pr_2O_3, (*d*) Nd_2O_3, (*e*) Sm_2O_3, (*f*) Eu_2O_3, (*g*) Gd_2O_3, (*h*) Tb_2O_3, (*i*) Dy_2O_3, (*j*) Ho_2O_3, (*k*) Er_2O_3, (*l*) Tm_2O_3, (*m*) Yb_2O_3, (*n*) Lu_2O_3. Vertical segments show the results of calculations (SCF NR X_α-DVM) of the electronic structure of CeO_8^{12-} (O_h symmetry), PrO_7^{11-} and NdO_7^{11-} (C_2 symmetry), and LnO_6^{9-} (D_{3d} symmetry) for other oxides.[57,58]

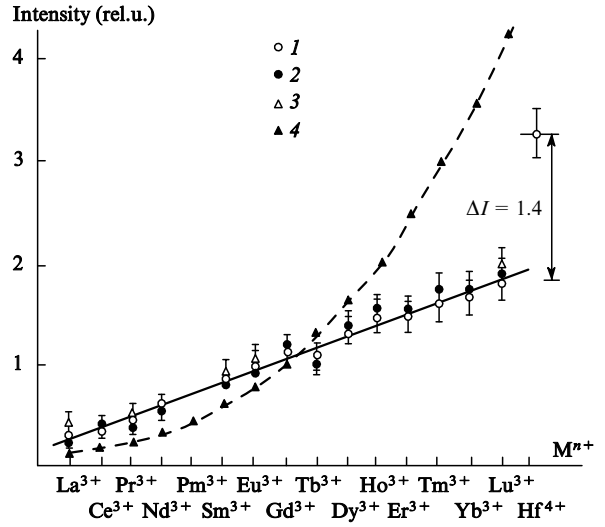


Figure 25. Relative intensity of the XPS lines of the Ln4*f* electrons *vs*. the number of these electrons in lanthanide oxides (*1*, *2*)[134] and orthoniobates $LnNbO_4$ (*3*) [133] and the corresponding theoretical dependence (*4*) [see Eqn (7)]. Two series of oxide samples were used, one provided by the Russian Research Centre 'Kurchatov Institute' (*1*) and one by the Saratov State University (*2*). For comparison, data for HfO_2 are given ($n_{4f} = 14$).

some cases two lines for oxygen, the O2*s* spectrum should also contain two lines. This would complicate the spectral structure in the Ln5*p* and O2*s* binding energy range.

In the Ln5*p* spectra of the oxides of light lanthanides, in particular, lanthanum, the many-body perturbation should be more pronounced than in the spectra of the corresponding fluorides. This suggestion relies on the fact that the Ln3*d* spectra recorded for oxides exhibit more intense satellites than the corresponding spectra of fluorides. The influence of the multiplet splitting and the dynamic effect on the Ln5*p* spectral structure should not be more pronounced in the case of REE oxides than in the case of REE fluorides and should not result in substantial complication of the spectral structure.

Since the E_b value for the O2*s* spectra falls in the middle of the range in which the Ln5*p* binding energy varies with an increase in the lanthanide atomic number, the formation of the inner valence MO may be a reason for the appearance of the fine spectral structure in the Ln5*p* and O2*s* binding energy ranges.[55–59, 61, 62, 78, 79, 83, 84] These IVMO are largely composed of the Ln5*p* and O2*s* AO.[18, 133, 135]

Lanthanide oxides have a complex geometric structure (Fig. 26),[57–59] which accounts for complication of their electronic structures and, hence, of the XPS spectral structure for low-energy electrons and also complicates the corresponding theoretical calculations. The XPS spectra are often interpreted by referring to the results of quantum-chemical calculations for the electronic structures of lanthanide oxides.[55, 59, 79, 84] In particular, theoretical investigation of the PrO_7^{11-} and NdO_7^{11-} clusters (C_2 symmetry), two series of LnO_6^{9-} clusters (Ln = Sm–Lu) (D_{3d} and C_2 groups of symmetry) and the CeO_8^{12-} complex (O_h symmetry) have been carried out in the spin-polarised approximation of the NR X_α-DV method.[57–59] The energy levels found by these calculations are shown in Fig. 24 as vertical segments in the low-energy spectral range. Figures 27, 28 show the MO diagrams for the PrO_7^{11-} (C_2 symmetry) and TbO_6^{9-} (D_{3d} symmetry) clusters.

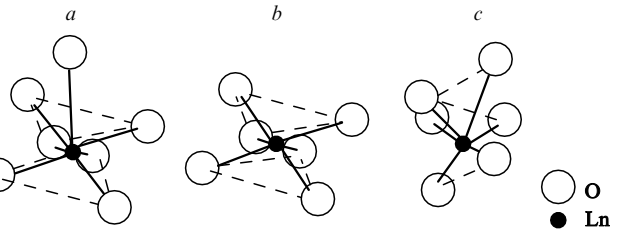


Figure 26. Model clusters of lanthanide oxides in which the structure of the local environment is taken into account.[59] (*a*) LnO_7^{11-} (C_2 symmetry) for La–Nd oxides; (*b*) LnO_6^{9-} (D_{3d} symmetry); (*c*) LnO_6^{9-} (C_2 symmetry) for Sm–Lu oxides.

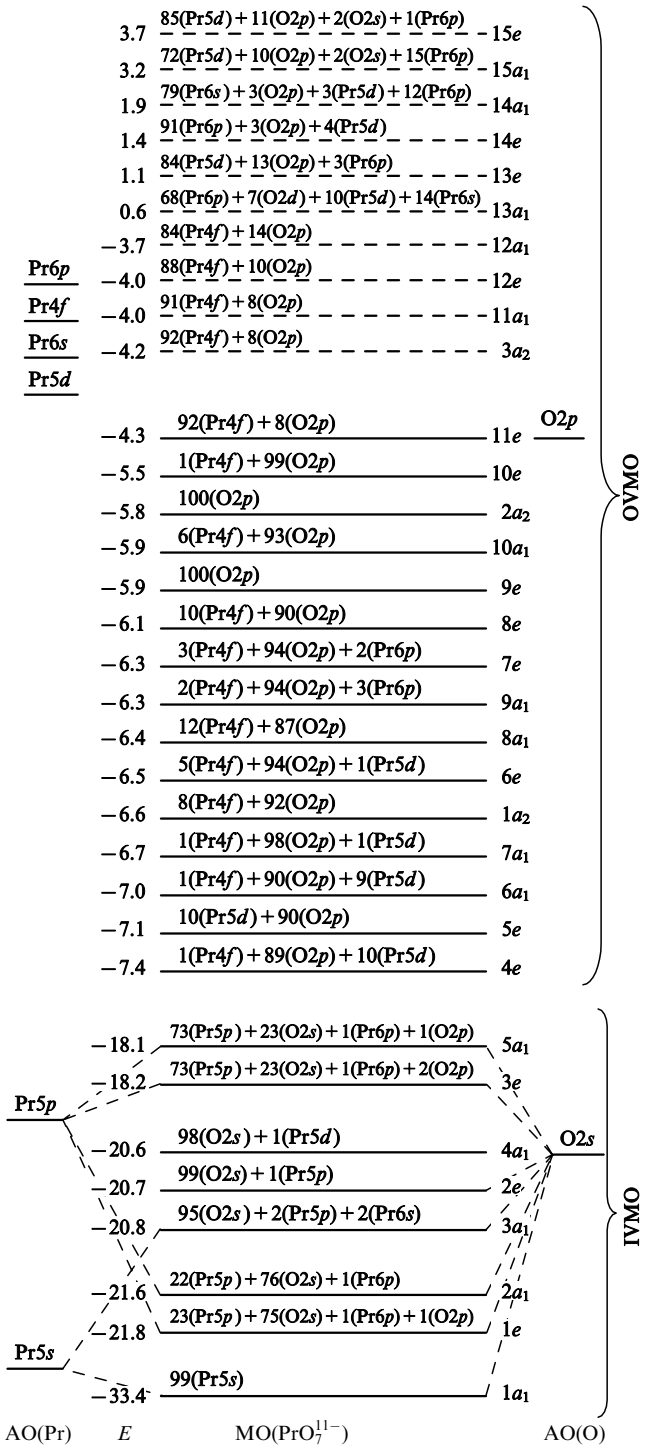


Figure 27. Diagram of the MO of the PrO_7^{11-} cluster [C_2 symmetry, R(Pr–O) = 0.237 nm, R'(Pr–O) = 0.262 nm] determined by the SCF NR X_α-DVM calculations for $\alpha(\uparrow)$.[57] MO energies (eV) and compositions (%) are given (the diagram is not scaled). Unoccupied energy levels are shown by dashed lines.

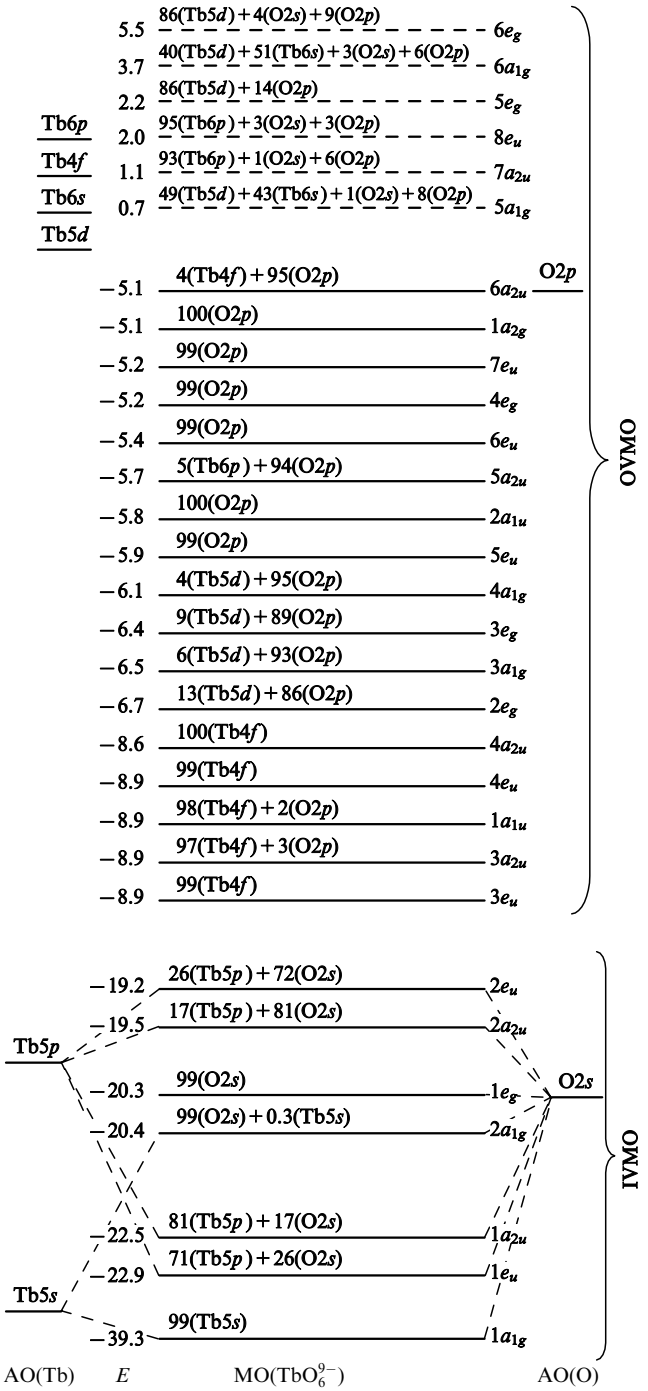


Figure 28. Diagram of the MO for the TbO_6^{9-} cluster [D_{3d} symmetry, $R(Tb-O) = 0.230$ nm] determined by the SCF NR X_α-DVM calculations for $\alpha(\uparrow)$.[58] MO energies (eV) and compositions (%) are given (the diagram is not scaled). Unoccupied energy levels are shown by dashed lines.

As follows from the results of calculations, the PrO_7^{11-} cluster (C_2) has two groups of MO consisting of $4e-15e$ OVMO and $1a_1-5a_1$ IVMO type orbitals (see Fig. 27). On the basis of calculations and the relevant XPS parameters, the conclusion concerning the involvement of the Ln4*f* AO in the formation of OVMO in the lanthanide compounds has been drawn in a number of publications.[56–59, 68, 78, 79, 83, 84, 132]

The inner valence MO ($1a_1-5a_1$) of the PrO_7^{11-} cluster (C_2 symmetry) mainly consist of low-energy occupied AO of the neighbouring praseodymium and oxygen atoms. The greatest mixing of the Pr5*p* and O2*s* AO is found for the $1e$, $2a_1$, $3e$ and $5a_1$ IVMO (see Fig. 27). The inner valence Pr5*s* AO do not participate significantly in the IVMO formation. These results indicate that a substantial overlap of the Pr5*p* and O2*s* AO, favourable for the IVMO formation, takes place in the PrO_7^{11-} cluster.

As the lanthanide atomic number increases, the energy of the Ln5*p* electrons approaches the O2*s* energy or becomes even higher for relatively large Z values; therefore, for the first half of the lanthanide row, the degree of mixing of the Ln5*p* and O2*s* AO increases upon IVMO formation, while on further increase in Z, this degree of mixing gradually decreases.

To illustrate the arrangement of the MO energy levels and the MO composition, the local environments found in the oxides formed by elements of the second half of the lanthanide row were taken into account in the simulation of the structure of the LnO_6^{9-} clusters (D_{3d} symmetry). Figure 28 shows the MO diagram based on the results of the spin-polarised NR X_α-DV calculations of the electronic structure of the TbO_6^{9-} cluster (D_{3d} symmetry).[58, 59] The occupied $3e_u-6a_{2u}$ OVMO of this cluster, like those in PrO_7^{11-}, are formed by participation of the 4*f* AO. However, in this case, unlike PrO_7^{11-}, the molecular orbitals containing the Tb4*f* AO are lower in energy than the OVMO consisting mostly of the O2*p* AO. This is a consequence of the lower position of the Tb4*f* energy level compared to the Pr4*f* level with respect to O2*p* (see Fig. 3).

The IVMO in the TbO_6^{9-} cluster (D_{3d} symmetry) differ in structure from the IVMO of the PrO_7^{11-} cluster (C_2 symmetry). This is due to the different structures of these two clusters. However, in the terbium cluster, as in the praseodymium one, substantial mixing of the Tb5*p* and O2*s* AO takes place in the IVMO formation (see Fig. 28). As the lanthanide atomic number increases, the degree of participation of the Ln5*p* AO in, for example, the $2e_u$ IVMO of these clusters decreases; for LuO_6^{9-} (D_{3d} symmetry), it is as low as 4%.

According to calculations, an increase in the atomic number (Z) of lanthanides in the oxides should entail the displacement of MO energy levels caused by Ln4*f* electrons towards higher values, which is observed in experimental spectra (see Figs 3, 24). Indeed, the structure of the experimental spectra of Ln_2O_3 in the Ln5*p* and O2*s* binding energy ranges becomes much more complicated on approaching the center of the lanthanide row, while the spectral pattern observed for the oxides of elements situated at either the beginning or the end of the row, for example, La_2O_3 and Lu_2O_3, is close to the sum of the atomic spectra of lanthanides and oxygen (see Fig. 24).

The similar energies of the Ln4*f* and O2*p* levels and the relatively short distances between the neighbouring lanthanide and oxygen atoms in the considered oxides may promote an increase in the degree of mixing of the Ln4*f* and O2*p* AO giving the OVMO. It is noteworthy that the involvement of the Ln5*p* and O2*s* AO in the formation of the IVMO is one of the reasons for the appearance of the fine structure in the Ln5*p* and O2*s* spectral range for lanthanide oxides.

2. The core electron spectra of lanthanide oxides

a. The Ln_2O_3 oxides

The spectral structure of the core electrons of lanthanide oxides has much in common with the spectra of the same electrons in lanthanide trifluorides provided that the lanthanide oxidation states in these compounds are equal. The formation mechanisms for the fine structure of these oxides can also be considered in the ionic approximation. Thus the spectra of the Ln5*s* and Ln4*s* electrons in Ln_2O_3, like the spectra of the corresponding electrons in LnF_3, exhibit multiplet splitting characterising the lanthanide spin state in oxides and fluorides (Fig. 29, see also Fig. 16). In some cases, these data can be used to determine the lanthanide oxidation state. For example, comparison of the multiplet splittings for Ln4*s* and Ln5*s* electrons in individual lanthanides and in the oxides indicates that the most pronounced discrepancy is observed between europium and Eu_2O_3 (see Fig. 29). The multiplet splitting ΔE_{ms} for the Eu4*s* electrons in the XPS spectra of

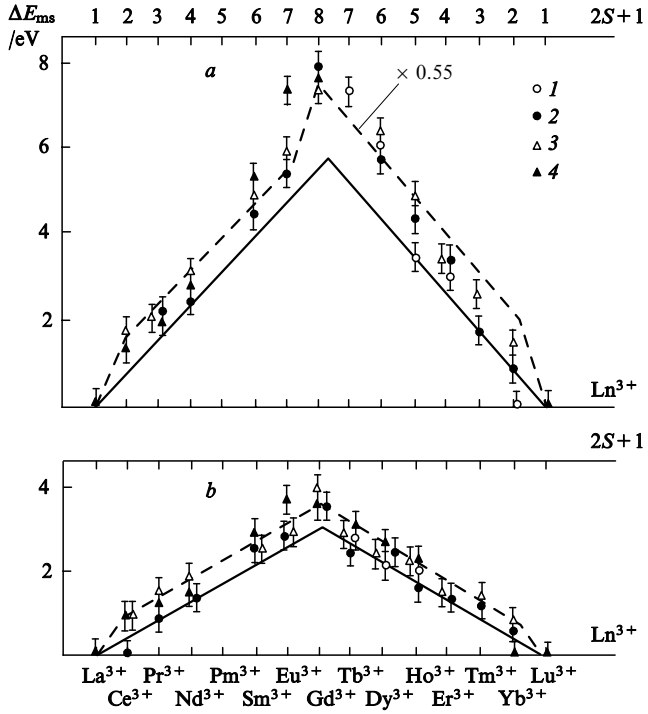


Figure 29. Multiplet splitting (ΔE_{ms}) of the Ln4*s* (*a*) and Ln5*s* lines (*b*) in the XPS spectra of oxygen-containing compounds of lanthanides and individual metals; (*1*) surface oxides;[80] (*2*) Ln_2O_3 oxides; (*3*) LnL_3 (L is the *o*-methoxybenzoic acid residue);[5] (*4*) individual metals;[93] the continuous line shows the results of SCF NR X_α-DVM calculations;[69] the dashed line corresponds to the results of *ab initio* calculations;[44,93] the dependence of ΔE_{ms} on the multiplicity $(2S+1)$ of the Ln4*s* electrons was multiplied by 0.55.[93]

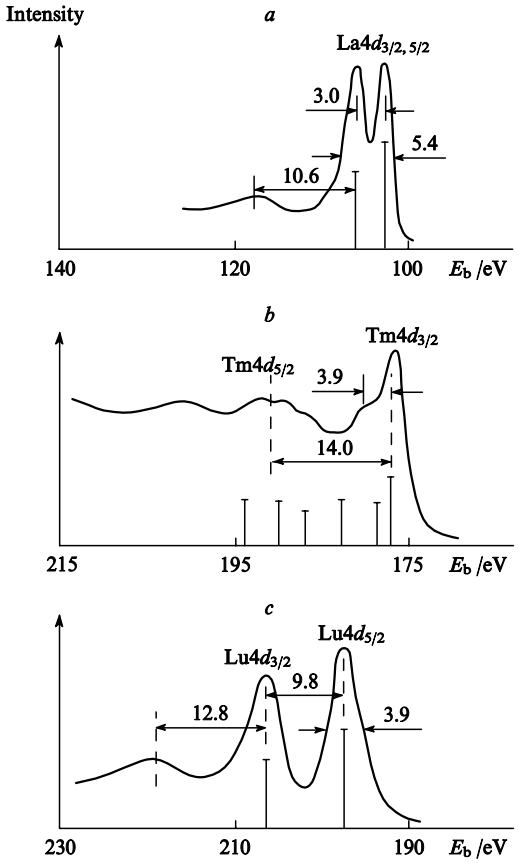


Figure 30. XPS of lanthanum (*a*), tulium (*b*), and lutetium (*c*) oxides in the Ln4*d* binding energy range. The intensity of the La4$d_{3/2}$ component is increased due to the superposition of the shake-up satellite from the La4$d_{5/2}$ line.[83] The vertical segments below the Tm_2O_3 spectrum show the results of calculations with allowance for the multiplet splitting.[66]

europium metal [$\Delta E_{ms}(Eu) = 7.4 \pm 0.2$ eV] differs considerably from the corresponding value for the oxide [$\Delta E_{ms}(Eu_2O_3) = 5.5 \pm 0.2$ eV] and is approximately equal to the multiplet splitting observed in the spectrum of gadolinium oxide [$\Delta E_{ms}(Gd_2O_3) = 7.8 \pm 0.2$ eV]. These results are attributable to the fact that the number n_{4f} of unpaired Eu4*f* electrons in europium atoms is greater in the metal than in the oxide and is equal to the number of these electrons in the gadolinium contained in the oxide. In terms of the ionic approximation, this implies that europium metal contains Eu^{2+} ions, which is a known fact, while the oxide contains Eu^{3+} atoms.

The multiplet splitting in the Ln4*d* spectra of the Ln_2O_3 oxides for $58 \leqslant Z \leqslant 70$ has a more complicated pattern than that in the Ln4*s* and Ln5*s* spectra of the same compounds, the structure caused by this splitting being mainly consistent with the corresponding structure observed in the spectra of the Ln4*d* electrons in LnF_3 (Fig. 30, see also Fig. 17). As an example, Fig. 30 shows the spectrum of the Tm4*d* electrons in Tm_2O_3 . Whereas the complex structure in the spectrum of Tm_2O_3 is mainly related to the multiplet splitting, this splitting is missing from the Ln4*d* spectra of La_2O_3 and Lu_2O_3, because La^{3+} and Lu^{3+} ions in the oxides contain no unpaired Ln4*f* electrons. Indeed, the spectra of these electrons in lanthanum and lutetium oxides contain mainly doublets caused by the spin–orbit splitting: $\Delta E_{so}(La4d) = 3.0 \pm 0.1$ eV and $\Delta E_{so}(Lu4d) = 9.8 \pm 0.1$ eV. These values are in good agreement with analogous values for LaF_3 and LuF_3 (3.1 ± 0.1 and 10.0 ± 0.1 eV, respectively; see Figs 17, 30 and Tables 1, 3). The observed violation of the intensity ratio of the La4$d_{5/2}$ and La4$d_{3/2}$ doublet components in La_2O_3 can be related, as has been noted, for example for $La(OH)_3$ [139,140] and La_2O_3 ,[50] to the superposition of the shake-up satellite from the La4$d_{5/2}$ line on the La4$d_{3/2}$ doublet component. The structures of the Ln4*d* spectra for other Ln_2O_3 oxides in which the lanthanide ions have electronic configurations with Ln4*f* electrons are much more complicated than the spin doublet (see Fig. 30). The spectral structures observed for the bulk samples of lanthanide oxides [5,123] are similar to those in the spectra of surface oxides.[73,80,118,122]

These results can serve as experimental evidence for the fact that the multiplet splitting in the spectra of Ln4*d* electrons of lanthanide oxides gives rise to a complex fine structure the main features of which can be considered in the ionic approximation.[45,66] Replacement of the ligands surrounding the Ln^{3+} ions induces changes in the fine spectral structure, which can be partially due to the many-body perturbation and the dynamic effect in the spectra of these electrons. In other words, fine structure parameters depend on the nature of ligands in lanthanide compounds, *i.e.*, on the type of chemical bonds in them. As a consequence, despite its complexity, the fine structure of the Ln4*d* spectra is characteristic of a given lanthanide compound and can be used as a 'fingerprint' for compound identification.

The fine structure observed in the spectra of the Ln4*p* electrons of lanthanide oxides generally resembles the corresponding spectral structure of lanthanide trifluorides (Fig. 31). Instead of the expected doublet related to the spin–orbit splitting, the Ln4*p* spectra of REE oxides in the series from La to Yb exhibit a structure around the Ln4$p_{3/2}$ line and the component corresponding to the Ln4$p_{1/2}$ electrons is highly smeared.[20,83] Note that for oxides of elements situated at the end of the lanthanide row, in particular, for Yb_2O_3, the structure of the Ln4*p* spectrum is similar to a doublet in shape, while the spectrum of the corresponding electrons of Lu_2O_3 is already mainly a spin doublet (see Fig. 31).

On the basis of the XPS data for lanthanide fluorides, the structure of the Ln4*p* spectra was suggested to be due to the

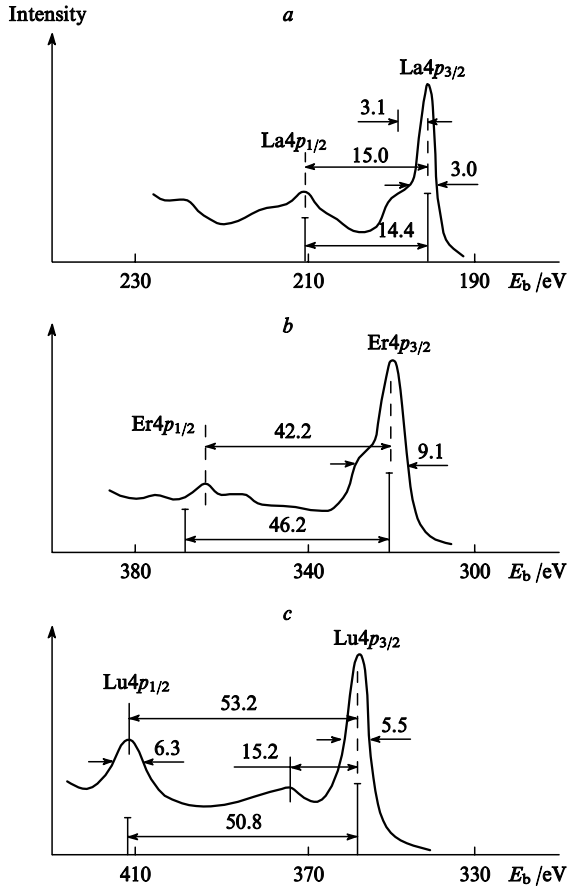


Figure 31. XPS spectra of lanthanum (*a*), erbium (*b*) and lutetium (*c*) oxides in the Ln4*p* binding energy range.[20] Vertical segments show the expected atomic spectra without allowance for the dynamic effect.[22]

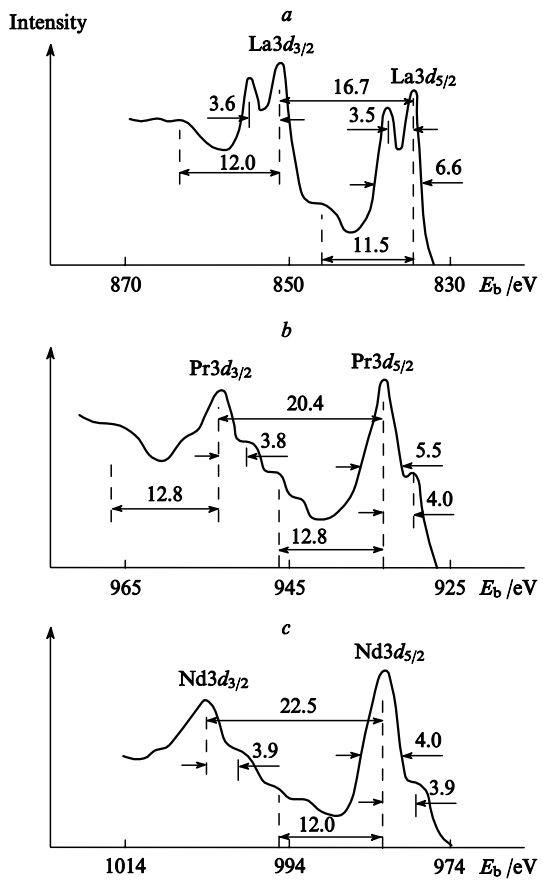


Figure 32. XPS spectra of lanthanum (*a*), praseodymium (*b*) and neodymium (*c*) oxides in the Ln3*d* binding energy range in which many-body perturbation effects are visible.[83]

dynamic effect, inducing the formation of the $Ln4p^5 4d^{10} 4f^n \leftrightarrow Ln4p^6 4d^8 4f^{n+1}$ type final states after photoemission of the Ln4*p* electron.[42] The appearance of an additional final state $Ln4p^6 4d^8 4f^{n+1}$ is possible only in the case where the Ln4*f* shell is not fully occupied. This assumption is in good agreement with the experimental data for REE oxides (see Fig. 31). Indeed, since the electronic configurations of the La^{3+} and Er^{3+} ions are $La4f^0$ and $Er4f^{11}$, respectively, the photoemission of an Ln4*p* electron from La_2O_3 and Er_2O_3 may give, in addition to the ground state, $Ln4p^5 4d^{10} 4f^n$, one more two-hole final state, $Ln4p^6 4d^8 4f^{n+1}$, which would result in the formation of the fine structure in the La4*p* and Er4*p* spectra of these oxides (see Fig. 31). Photoemission of an Lu4*p* electron from Lu_2O_3 cannot produce this additional final state, and the spectrum of the Lu4*p* electrons exhibits a spin doublet and satellites associated with many-body perturbation. These results can serve as yet further proof of the fact that the XPS fine structure in the spectra of the Ln4*p* electrons of REE compounds is mainly due to the dynamic effect. The considered data [20] are at variance with the suggestion [80] that the Ln4*p* spectral structure of REE oxides is mainly determined by multiplet splitting.

The spectra of the Ln3*d* electrons for light lanthanide oxides exhibit a fine structure the characteristics of which differ appreciably from those of the fine structure of other REE compounds (Fig. 32, see also Fig. 21). As noted above in the discussion of the spectra of the Ln3*d* electrons in lanthanide trifluorides, the spectral fine structure is due to the many-body perturbation. The dependence of the FWHM (Γ) of the $Ln3d_{5/2}$ line on the atomic number (Z) for lanthanide oxides resembles a similar dependence for LnF_3 (see Fig. 22). As noted previously, the observed change in the line width cannot be explained by multiplet splitting. The decrease in the Γ value ($Ln3d_{5/2}$) for REE oxides for the beginning of the lanthanide row is due, as indicated by the spectra, to a decrease in the intensity of the low-energy component of the structure containing satellites.

It has been shown for 3*d*-metal compounds [24, 141] that the intensity of satellites in the spectra of electrons of various shells decreases with a decrease in the binding energy. A similar regularity is found in the spectra of La3*d* and La4*d* electrons for $LaNbO_4$.[133] Therefore, a similar pattern could be expected in the spectra of lanthanide compounds, in particular, oxides. In other words, if the fine structure of the Ln3*d* spectra is caused by many-body perturbation, satellites, although less intense, should also appear in the spectra of other, lower binding energy electrons. Their positions with respect to basic lines are expected to be approximately the same as those in the spectra of Ln3*d* electrons. Indeed, the most clear-cut satellites of this type (with an intensity of 43%) are found in the La4*d* spectrum of La_2O_3 (see Fig. 30); they occur on the higher binding energy side of the basic lines and can be classified as shake-up satellites. A similar satellite is recorded in the $La4p_{3/2}$ spectrum (intensity 30%). This serves as experimental evidence for the fact that in the spectra of La3*d* electrons, satellites are located at a higher binding energy than the basic lines.

Comparison of the difference between the core level binding energies for LaF_3, La_2O_3 and metallic lanthanum also leads to the conclusion that the components located at lower binding energies in the spectrum of La3*d* electrons of lanthanum oxide should be identified as the basic lines. The binding energy differences between the $La4d_{5/2}$ and $La3d_{5/2}$ electrons $\Delta E_b(La4d_{5/2} - La3d_{5/2})$ for metallic lanthanum and its oxide and fluoride found with allowance for the low-energy components of the $La3d_{5/2}$

spectra are equal to 732.2 ± 0.4,[5] 732.3 ± 0.4 and 732.9 ± 0.4 eV, respectively (see Tables 1, 3). These values are in satisfactory agreement with one another within the determined error; meanwhile, the $\Delta E_b(La4d_{5/2} - La3d_{5/2})$ values for the $La3d_{5/2}$ high-energy components for La_2O_3 and LaF_3 are equal to 735.8 ± 0.4 and 737.2 ± 0.4 eV, *i.e.*, they markedly exceed the corresponding energy difference (732.2 ± 0.4 eV) for metallic lanthanum (see Tables 1, 3). It is also worth noting that the spectrum of La3*d* electrons for metallic lanthanum exhibits no extra lines [91, 142–144] comparable to the basic lines in intensity; this contradicts the data of another study [145] in which an intense extra structure has been detected in the spectrum of metallic lanthanum.

The data considered above convincingly demonstrate that the satellites observed in the La3*d* spectra of the lanthanum compounds in question are due to a shake-up process which accompanies photoemission of La3*d* electron; this is consistent with the results of other publications.[50, 105, 140]

As noted above, praseodymium and terbium oxides may have a complex stoichiometric composition other than Ln_2O_3. These oxides are supposed [1] to contain lanthanide ions in different oxidation states, for example, Ln^{3+} and Ln^{4+}. The intensity of the extra structure in the spectra of Pr3*d* and Tb3*d* electrons, which can be attributed to Pr^{4+} and Tb^{4+} ions, does not exceed 3%–5% of the basic line intensity corresponding to Pr^{3+} and Tb^{3+} ions.[5] It has been noted [117] that on passing from the Eu^{2+} in the metal to the Eu^{3+} in the Eu_2O_3 oxide, the energy levels of the core electrons shift by about 10 eV. Significant changes in the spectral structure of complex lanthanide oxides with respect to the spectra of Ln^{3+} compounds are also found for cerium oxide.[116, 137]

b. Cerium oxide

In recent years, considerable attention has been devoted to the study of variable valence in lanthanides and their compounds,[146–148] which may be responsible for the fine structure in the XPS spectra. The extra structure in the spectra of the valence and core electrons of rare earth metals,[101, 149, 150] intermetallics [119, 151–156] and lanthanide compounds [157–165] has been attributed to the presence of lanthanide atoms in variable oxidation states. Theoretical calculations of the XPS spectra of rare earth metals [166, 167] and their compounds [116, 168–170] are often carried out using so-called Andersson's impurity model [38, 39, 171] and its various modifications. In particular, this model has been used to interpret the complex structure of the XPS spectra of core electrons in CeO_2.[116, 170]

The structure of the spectrum of the Ce3*d* electrons in cerium oxide contains a number of additional lines that are missing from the corresponding spectra of other oxygen-containing compounds and cerium fluoride (Fig. 33, see also Fig. 21).[137, 138] This extra structure is a doublet the splitting of which (ΔE_b = 18.3 eV) is in good agreement with the spin–orbit splitting of the Ce3*d* line [ΔE_{so}(Ce3*d*) = 18.3 eV][138] and with the data of one more study.[119] For example, it was assumed on the basis of the analysis of cerium spectra in intermetallic compounds [172–174] that the two intense extra lines with $E_b \approx 898.0$ and 916.3 eV are components of a spin doublet corresponding to Ce^{4+} ions, while the low-energy doublet containing a complex structure corresponds to the Ce3*d* electrons of the Ce^{3+} ion. It has been suggested that the presence of two types of cerium ions in the oxide may be due either to variable valence exhibited by cerium in chemical [175] and intermetallic compounds,[155] or to the formation of a mixture of oxides on the sample surface.

Thus on the basis of X-ray CeL_{III} absorption spectra and the Ce4*d* XPS spectra it was concluded [176] that Ce^{3+} and Ce^{4+} ions are formed on the $CeCo_2$ surface. The XPS spectra of the CeO_2 oxide and the theoretical data [177] indicate that a variable valence of cerium in the oxide is impossible, the structure observed in the Ce3*d* spectrum being due to the $Ce3d^94f^0$ and $Ce3d^94f^1$ configurations of the final state. The results of NR X_α-SW calculations suggest [178] that the extra structure in the Ce3*d* and Ce4*d* spectra of

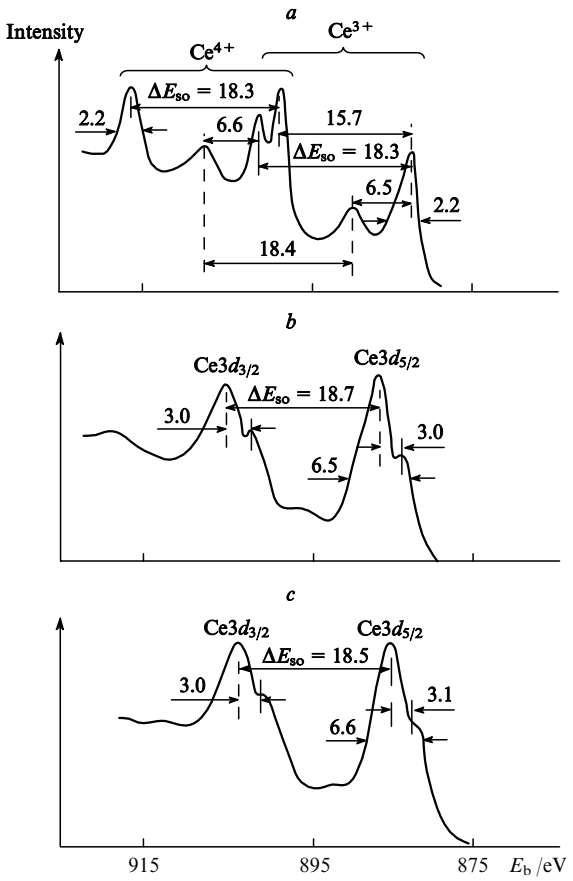


Figure 33. XPS spectra of the $Ce_2O_3 \cdot n\,CeO_2$ oxide (*a*) and the CeL_3^1 (*b*) and $CeL_3^2 \cdot 1.5\,H_2O$ (*c*) cerium complexes in the Ce3*d* binding energy range (L^1 and L^2 are the residues of *o*-methoxybenzoic and diphenylacetic acids, respectively).[137]

CeO_2 is due to shake-up satellites. These satellites in the spectra of the Ce3*d* electrons correspond to the $Ce3d^94f^0$, $Ce3d^94f^1$ and $Ce3d^95p^5(np)$ final states of the cerium ion.

X-Ray photoelectron spectra provide an unambiguous answer to the question as to whether or not the structure of the Ce3*d* spectra is related to a complex initial or final state of the cerium ion in compounds.[137, 138] One of the main suggestions is that the observed spectra of the core electrons of cerium in the oxide result from superposition of the structures related to the $Ce3d^94f^0$, $Ce3d^94f^1$ and $Ce3d^95p^5(np)$ type final states of the cerium ion. [The formation of the unusual final state $Ce3d^95p^5(np)$ is confirmed by the fact that the spectra of the Ce5*p* and OVMO electrons do not exhibit the extra structure characteristic of the Ce3*d*, Ce4*d* and Ce4*p* spectra.] Indeed, comparison of the spectra of the Ce4*d* and Ce4*p* electrons for cerium oxide and the CeL_3 complex (L is the *o*-methoxybenzoic acid residue) shows that three groups of lines corresponding to cerium ions in different final states can be distinguished in these spectra as well as in the spectra of the Ce3*d* electrons of cerium oxide (Fig. 34). In these spectra, the line corresponding to the Ce^{4+} ion is located 13.2 eV away from the corresponding Ce^{3+} line, which is consistent with the calculation results.[179] The intensity ratio of the lines corresponding to the Ce3*d* electrons of cerium ions in different oxidation states indicates that the near-surface layer of the sample studied contained 36% of Ce^{4+} and 64% of Ce^{3+} in the final state.

As expected, the spectrum of 4*d* electrons of the Ce^{4+} ion is a doublet caused by the spin–orbit splitting; ΔE_{so}(Ce4*d*) = 3.4 eV (see Fig. 34 *a*,*b*). This proves experimentally the fact that the complex structure of the 4*d* spectrum of the Ce^{3+} ions with the $Ce5s^25p^64f^1$ final state is due to multiplet splitting.

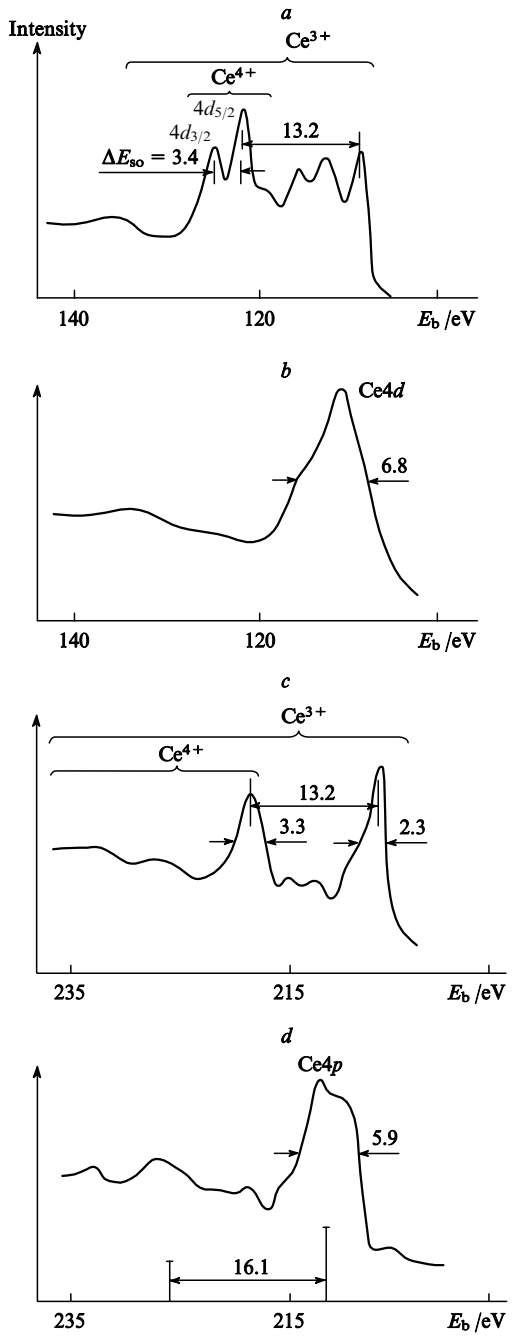


Figure 34. XPS spectra of the $Ce_2O_3 \cdot n\,CeO_2$ oxide and the CeL_3 complex in the Ce4*d* (*a*,*b*) and Ce4*p* (*c*,*d*) binding energy ranges (L is the *o*-methoxybenzoic acid residue).[138] (*a*,*c*) $Ce_2O_3 \cdot n\,CeO_2$; (*b*,*d*) CeL_3.

The structures of the Ce4*p* spectra for Ce^{4+} and Ce^{3+} ions have much in common (see Fig. 34 *c*,*d*). Thus in both cases, the component due to the Ce4$p_{1/2}$ electrons virtually cannot be detected, despite the fact that the electronic configuration of Ce^{4+} is Ce4$p^6$5$s^2$5$p^6$4f^0, *i.e.*, cerium contains no unpaired 4*f* electrons. This proves experimentally the fact that the complex structure in the spectrum of Ce4*p* electrons is mainly due to the dynamic effect.

The spectra of the 3*d* and 4*d* electrons of the Ce^{4+} ion consist of two components of a doublet and contain no complex structure, in particular, no satellites (see Figs 33, 34). This allows one to determine the binding energy difference, $\Delta E_b(4d_{5/2} - 3d_{5/2}) = 776.3$ eV. This value is close to the energy difference between the corresponding low-energy components in the $3d_{5/2}$ and $4d_{5/2}$ spectra of the Ce^{3+} ions ($\Delta E_b = 882.3 - 108.5 = 773.8$ eV, see Table 3). The observed difference between these values ($776.3 - 773.8 = 2.5$ eV) can be due to various reasons. First, the multiplet splitting changes the structure of the 4*d* spectrum of Ce^{3+}; this may displace the most intense peak with respect to the Ce^{3+} $4d_{5/2}$ component. However, the same difference (2.5 eV) is found between the most intense components of the Ce4*p* doublet the structures of which for Ce^{3+} and Ce^{4+} are similar. Second, the chemical shifts of metal ions in different oxidation states are well-known [33] to be different for different energy levels. Comparison of the spectra for the Ce3*d* ($\sim$900 eV), Ce4*p* ($\sim$220 eV) and Ce4*d* ($\sim$120 eV) shells demonstrates that the differences between the electron binding energies corresponding to the most intense lines for individual shells in Ce^{3+} and Ce^{4+} amount to 15.7, 13.2 and 13.2 eV, respectively (see Fig. 33, 34). These data suggest that upon increasing the electron binding energy from 100 to 900 eV, the difference between the chemical shifts of separate levels does not exceed 16%.[137,138]

It follows from the results obtained that the most intense low-energy component in the $3d_{5/2}$ spectra of Ce^{3+} may be identified as the basic line and the components next in energy may be considered as shake-up satellites. The most intense satellites are due to the many-body perturbation involving the Ce5*p* electrons, which gives rise to an ion with a poorly shielded hole at the Ce5*p* level.

The spectra of core electrons also allow the conclusion that the stoichiometric compositions of praseodymium and terbium oxides basically correspond to Ln_2O_3.

IV. General rules for the formation of the XPS spectral structure of lanthanide compounds

The XPS spectral structures observed for different lanthanide compounds are rather similar if the metal ions contained in them all have the same formal oxidation state equal to three. When the lanthanide oxidation state in a compound differs from three, the structure of their XPS spectra substantially changes.

1. Spectral region of low-energy electrons

In the spectral region corresponding to low-energy electrons of various lanthanide compounds, an increase in the atomic number (Z) and the number of Ln4*f* electrons (n_{4f}) entail an increase in line intensity near the Fermi level (see Figs 2, 24). The structure observed in this spectral region for compounds formed by elements of the middle and the end of the lanthanide row is mainly due to Ln4*f* electrons because photoionisation cross-sections of these electrons exceed appreciably the corresponding values of the electrons of the outer valence Ln5*d*, Ln6*s* and L2*p* AO of the lanthanide and the ligand.[76] As noted above, the data obtained in recent years using the SCF NR X_α-DV and X_α-SW calculations for the electronic structures of clusters [56–59] confirm the substantial participation of the Ln4*f* AO in the formation of OVMO. Therefore, attempts have been made [37,68,132] to estimate the degree of participation of the Ln4*f* electrons in the chemical bond on the basis of spectral parameters or, at least, to estimate the degree to which the Ln4*f* electrons can be regarded as outer valence electrons.

On passing from lanthanide oxides to fluorides, the weighted-mean Ln4*f* electron binding energies increase. The chemical shifts of these electron levels observed on passing from one compound to another are comparable to the corresponding values for the core levels.

For example, the chemical shift (ΔE_b) of the Lu4$p_{3/2}$ electron levels in LuF_3 (relative to Lu_2O_3) in which the lutetium ion is formally in the trivalent state amounts to 1.8 eV, and the weighted-mean value for the Lu4*f* level, $\Delta\bar{E}_b$(Lu4*f*), equals 1.7 eV. The binding energy differences ΔE_b(Lu4*f* – Lu4$p_{3/2}$) for lutetium oxide and fluoride coincide within the experimental error and are 350.8 and 350.9 eV for Lu_2O_3 and LuF_3, respectively. It should be noted that the Ln4*f* electrons respond to minor changes in the effective charge of lanthanide nuclei to approximately the

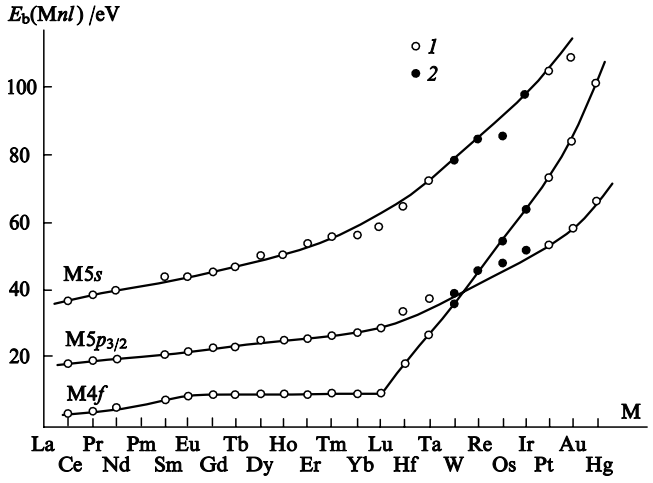


Figure 35. Binding energy of the Mnl electrons [E_b(Mnl)] for metal oxides, except for metallic Au and Pt, *vs.* the metal atomic number in the La – Hg series. (*1*) The results from Ref. 132; (*2*) the data from Ref. 22. For M4*f* and M5*s* electrons, the weighted-mean values of the binding energy are given, and for the Hf – Hg oxides ($Z > 71$), only the energies of the M4$f_{7/2}$ electrons are given.

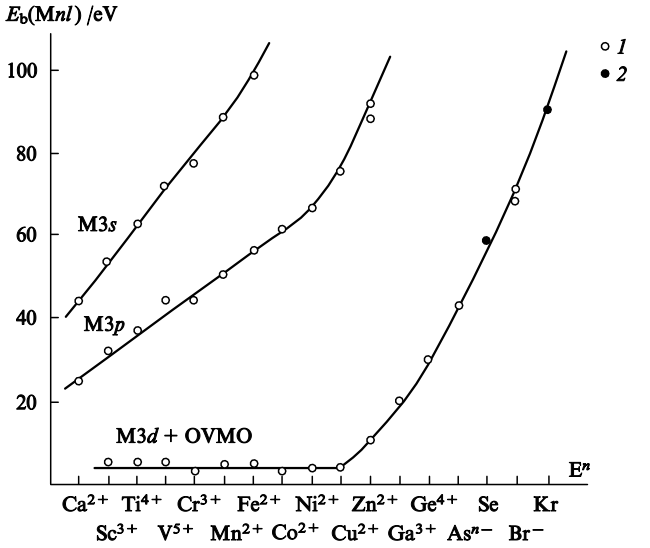


Figure 36. Binding energy (E_b) of the Mnl electrons of CaO, Sc_2O_3, TiO_2, V_2O_5, Cr_2O_3, MnO, FeO, CoO, NiO, CuO, ZnO, Ga_2O_3, GeO_2, and $FeAs_2$, Se, KBr, Kr *vs.* the element (E) atomic number in the Ca – Kr series. (*1*) the results from Ref. 5; (*2*) the data from Ref. 22. For M3*d* electrons, the weighted-mean values for these OVMO electrons are given, and for Zn, Ga, Ge oxides and for As^{n-}, Se, Br^- and Kr ($Z \geqslant 30$), the M3*d* energies are presented.

same extent as the core electrons. For a separate series of lanthanide compounds, a substantial increase in the metal atomic number in the $58 \leqslant Z \leqslant 71$ range causes insignificant variation of the weighted-mean value of the Ln4*f* binding energy. The increase in the binding energy of these electrons over the lanthanide row is 6.8 eV for fluorides and 4.5 eV for oxides (Fig. 35). On further increase in the atomic number, *i.e.*, on passing from Lu to Hg ($Z = 72$), the binding energy of the M4*f* electrons sharply increases. The M5$p_{3/2}$-electron binding energy varies in a similar way, although to a lesser extent. The same trend, even less pronounced, can also be followed for the M5*s* electrons (see Fig. 35).

The dependence of the M4*f* binding energy on *Z* for compounds of lanthanides and heavier metals (see Fig. 35) resembles the corresponding dependences of the M*nd* electrons in transition metals and in the subsequent elements.[22,132] For example, the weighted-mean binding energy for the M3*d* electrons in 3*d*-metal oxides, as in the lanthanide oxides, depends only slightly on *Z* over the $21 < Z \leqslant 29$ range but starting with zinc, it sharply increases (Fig. 36).

The relative intensity of the Ln4*f* line in the lanthanide compounds studied follows an almost linear dependence on the metal atomic number in the $57 < Z \leqslant 71$ range (see Figs 5, 25). A further increase in *Z* results in a sharp change in the pattern of dependence (Fig. 37). For comparison with the experimental dependence,[132] Fig. 37 also shows the relevant data obtained using photoionisation cross-sections.[76] The fundamental qualitative difference between the experimental and theoretical curves cannot be interpreted, for example, by assuming that after photoemission from a substance, the electrons are highly scattered. The extrapolation of the straight section of the theoretical curve to $Z = 57$ (La) shows that the plot for the relative intensity of the M4*f* line *vs.* *Z* is a straight line in the case where all the Ln4*f* shells are fully occupied. The deviation of the Ln4*f* line intensity from a linear dependence occurs for Hf and Ta due to the fact that the outer valence Ln4*f* electrons in these metals become inner electrons. It follows from experimental data that the relative intensity of the M4*f* line for lanthanide oxides increases in proportion with *Z*. For the latter half of the lanthanide row, these values remain lower than the theoretical values but in the $71 < Z \leqslant 78$ range, they rapidly increase and subsequently, they exceed the theoretical values by, on average, 25% – 27%; like theoretical values, they also increase with an increase in *Z*. Thus for Hg ($Z = 82$) in HgO,

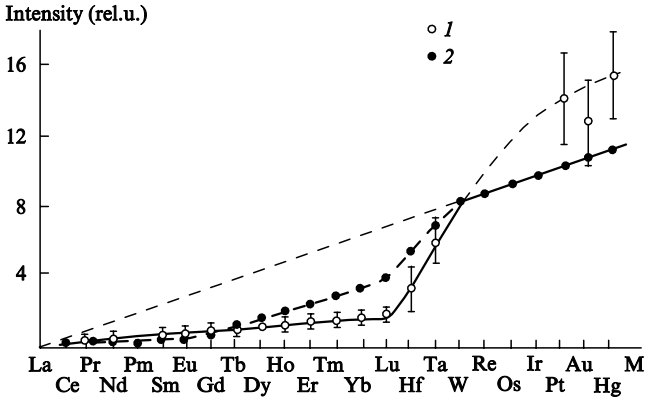


Figure 37. Experimental (*1*) and theoretical (*2*) dependences of the relative intensities of the M4*f* lines for REE and heavier metal oxides, except for metallic Pt and Au, *vs.* the metal atomic number in the La – Hg series.[132]

$I_{exp} = 15.6$, $I_{theor} = 11.4$ and $\Delta I(I_{theor} - I_{exp}) = 4.2$, while for uranium ($Z = 92$) in $K_4UO_2(CO_3)_3$, $I_{exp} = 22.3$, $I_{theor} = 16.9$ and $\Delta I = 5.4$.

This is exemplified in Fig. 38 which shows for comparison the variations of the relative intensities of the OVMO and E3*d* lines in the oxides of Period 4 elements (E). The corresponding theoretical intensities were calculated for atoms E using the data obtained by Scofield.[76] For elements with $Z > 30$, the experimental and theoretical values are presented as the intensity ratios for the lines of 3*d* and 3*p* electrons. This does not introduce a substantial error because the photoionisation cross-sections of the E3*d* and E3*p* shells are much greater than those of the E4*s*, E4*p* or O2*p* shells. If one takes into account the contribution to the intensity of the O2*p* electrons of the oxide oxygen atoms for elements with $20 \leqslant Z \leqslant 29$, the theoretical intensity value would increase by approximately 10%, which provides a better qualitative agreement with the experimental data (see Fig. 38).

It follows from the obtained results that spectral characteristics of the Ln4*f* electrons have much in common with those of the M*nd* electrons in compounds of *nd* transition metals, which can

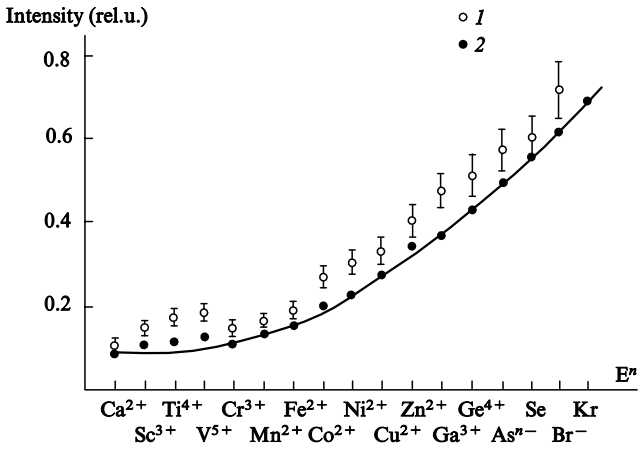


Figure 38. Experimental[132] (*1*) and theoretical[76] (*2*) dependences of the relative intensities of the E3*d* and OVMO lines for CaO, Sc_2O_3, TiO_2, V_2O_5, Cr_2O_3, MnO, FeO, CoO, NiO, CuO, ZnO, Ga_2O_3 and GeO_2 oxides and $FeAs_2$, Se, KBr and Kr on the element (E) atomic number in the Ca–Kr series. For the oxides of elements with $Z \leqslant 30$ (Ca–Zn), the intensities were found as the ratio of the total intensity of the OVMO and E3*d* lines to the intensity of the 3*p*-electron lines, and for $Z > 30$ (Ga–Kr), they were found as the ratio of the 3*d* to 3*p* lines.

efficiently participate in the MO formation. In lanthanides, Ln4*f* is a valence shell, it can be involved in the MO formation in Ln compounds. At least, XPS data do not contradict the assumption, based on calculations, concerning substantial participation of the Ln4*f* AO in the formation of MO in these compounds.[56–59,180] Indeed, the involvement of these electrons in the chemical bond may be the reason for the decrease in the experimental intensity of the Ln4*f* lines compared to the theoretical intensity for the oxides formed by elements of the second half of the lanthanide row.

2. The spectra of the inner valence MO electrons

In order to elucidate the general features of the IVMO formed from the Ln5*p* and O2*s* AO in oxygen-containing lanthanide compounds, model NR SCF X_α-SW calculations both with and without allowance for the electron spin polarisation were carried out for the LnO_3^{3-} clusters (D_{3h} symmetry).[79,84] The R(Ln–O) bond lengths were taken to be equal to the sum of the covalent radii of the lanthanide and oxygen ions.[1] The calculation results are reflected in Fig. 39 and, for the LaO_3^{3-} cluster (D_{3h} symmetry) in which R(La–O) = 0.174 nm, they are also presented in Table 4. The total partial charges (Q_l^j, electron charge units) for this cluster found using the MT (muffin-tin) approximation of the SCF X_α-SW technique[79] are presented below (region II is an asymmetric region within the Watson sphere, and region III is situated outside this sphere[56]).

La				O		Regions
s	*p*	*d*	*f*	*s*	*p*	II, III
1.6	4.0	0.6	0.8	4.3	10.4	10.3

It follows from the data of Table 4 that the occupied low-energy valence Ln5*p* and O2*s* AO can participate substantially in the MO formation in the cluster in question.

Thus in the LaO_3^{3-} cluster (D_{3h} symmetry), the $1a_2''$ IVMO can be regarded, to a certain approximation, as a quasi-atomic MO composed mainly of the La5*p* AO. The $1e'$ and $2e'$ ($1a_1'$ and $2a_1'$) IVMO can formally be attributed to the bonding and antibonding orbitals, respectively (see Table 4). The binding $1a_1'$ IVMO contains 85% of the La5*s* AO and 12% of the O2*s* AO, whereas the antibonding $2a_1'$ IVMO, 17% of the La5*s* AO and 80% of O2*s* AO. In addition, the contributions of the outer valence AO of lanthanum and oxygen to these IVMO couples are quite substantial but different. For example, whereas the bonding $1e'$ MO contains only 2.5% of the O2*p* AO, the antibonding $2e'$ MO

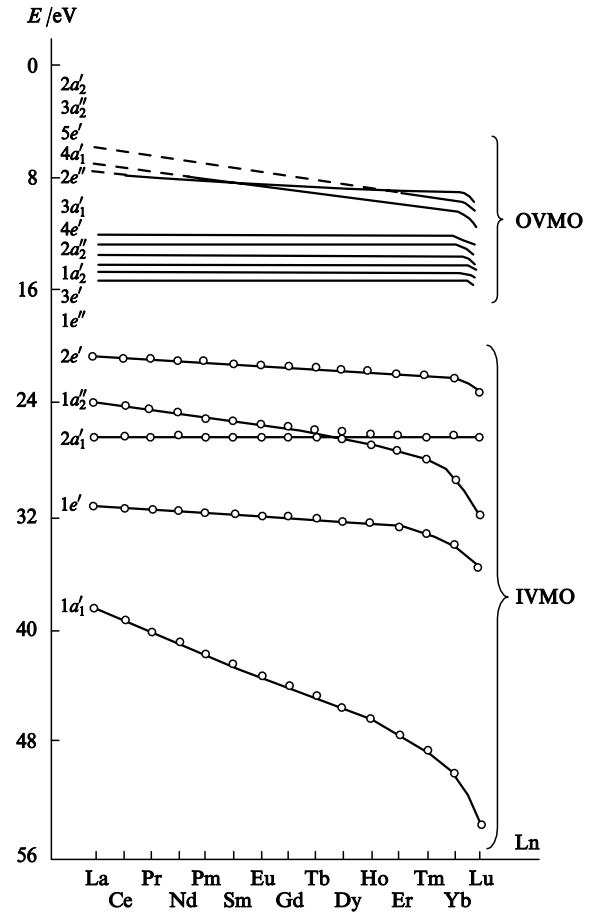


Figure 39. MO energies (E) for the LnO_3^{3-} cluster (D_{3h} symmetry) *vs.* the lanthanide atomic number in the La–Lu series.[79] The $4a_1'$ and $5e'$ OVMO energies are not given. The dashed lines show unoccupied MO.

Table 4. MO energies (E /eV), partial electron contributions (%) to different regions of the LaO_3^{3-} cluster [D_{3h} symmetry, R(La–O) = 0.174 nm] calculated in the SCF X_α-SW approximation.[79]

MO type	Orbital	$-E$	La				O		Regions I, II, III
			s	*p*	*d*	*f*	*s*	*p*	
OVMO	$2a_2'$	6.25	–	–	–	88.0	–	6.3	5.7
	$3a_2''$	6.91	–	1.1	–	84.9	–	3.3	10.7
	$5e'$	7.15	–	0.6	1.2	83.0	–	2.7	12.5
	$4a_1'$	7.35	2.0	–	8.4	25.7	–	–	63.9
	$2e''$	7.38	–	–	2.2	77.9	–	–	19.9
	$3a_1'$ (see [a])	12.29	1.3	–	5.0	15.7	0.3	53.1	24.6
	$4e'$	12.60	–	7.4	5.3	4.0	–	52.2	41.1
	$2a_2''$	13.51	–	6.2	–	4.2	–	57.0	32.6
	$1a_2'$	14.66	–	–	–	6.8	–	57.6	35.6
	$3e'$	14.96	–	2.3	3.0	–	1.5	55.8	37.4
	$1e''$	15.11	–	–	2.8	1.8	–	53.7	41.7
IVMO	$2e'$	20.67	–	40.0	0.7	0.1	20.4	10.2	28.6
	$1a_2''$	24.03	–	59.6	–	–	–	3.0	37.4
	$2a_1'$	26.50	13.1	–	0.9	1.1	61.8	0.3	22.8
	$1e'$	31.23	–	18.2	0.9	0.2	49.5	1.8	29.4
	$1a_1'$	38.87	66.0	–	–	0.1	9.3	2.1	22.5

[a] The upper fully occupied orbital.

contains 14% of the O2*p* AO. Such admixtures of the outer valence AO to the IVMO, as noted in a series of studies of molecules of light elements [18, 55, 61, 86, 87] and in another series of studies [18, 55, 181–183] of molecules of heavy elements, result in weakening of the antibonding nature of the higher MO, in particular, the $2e'$ IVMO. As a consequence, the contributions of the electrons of IVMO couples such as, for example, the $1e'$ and $2e'$, strengthens the chemical bond between the lanthanum and oxygen atoms.

As the lanthanide atomic number in the LnO_3^{3-} cluster grows, the energies and compositions of their MO change significantly. In constructing the dependence of MO energies of these clusters on *Z*, the energy of the quasi-atomic $2a_1'$ MO of oxygen was suggested to be constant and equal to 26.5 eV (see Fig. 39).[79] This energy was chosen as the reference value to compare the results of theoretical calculations with experimental data. Upon an increase in *Z*, the most pronounced changes in energy are observed for the upper $2e''-2a_2'$ OVMO and the $1a_2''$ and $1a_1'$ IVMO. The compositions of the considered MO substantially change. Thus, with an increase in the atomic number *Z*, the $2e''-2a_2'$ OVMO group approaches the O2*p* AO to an increasing extent, while the $1e''-3a_1'$ orbitals become similar to the Ln4*f* AO. The degree of mixing of Ln5*p* and O2*p* AO increases with an increase in *Z* from 57 to ~64. It follows from these data that the degree of mixing of the Ln5*p* and O2*s* AO in the $1e'$ and $2e'$ IVMO in, for example TbO_3^{3-}, is substantially greater than that in LaO_3^{3-}, while the lower $1a_1'$ IVMO becomes a quasi-atomic MO to an increasing extent.

As noted above, the formation of IVMO from the metal Ln5*p* AO and the ligand L2*s* AO in lanthanide can complicate the structure of the XPS spectra of these electrons compared to the sum of the atomic spectra (see Fig. 24). The most pronounced complication of the spectrum in the energy range of these electrons should be expected for the oxygen compounds of lanthanides situated in the middle of the row because for these oxides, the Ln5*p* and O2*s* energies are the closest to each other. The degree of participation of the Ln5*p* and L2*s* AO in the formation of IVMO can be estimated experimentally using the method of binding energy differences between the core and valence electrons.[182, 183]

The oxygen-containing lanthanide compounds have a rather complex structure. The metal atoms are surrounded by a large number of oxygen atoms. However, there is no strong anisotropy for the $R(Ln-O)$ bond lengths in these compounds. Therefore, the IVMO of the $ML_8^{n_2-}$ and $ML_8^{n_3-}$ type clusters (O_h group of symmetry) can be used in qualitative considerations (see Fig. 8 *b*,*c*). The correlation schemes of these IVMO imply that upon the formation of IVMO of the t_{1u}^* type in lanthanide compounds, their energies shift to lower (in magnitude) values with respect to the core levels. In this case, the Δ_1 value (see Fig. 8), which characterises the degree of participation of the Ln5*p* and L2*s* AO in the formation of the t_{1u}^* IVMO, can be estimated experimentally. The $\Delta E_3(Ln5p_{3/2}-Ln3d_{5/2})$ values reflecting the difference between the $Ln3d_{5/2}$ and the t_{1u}^* MO binding energies for various lanthanide compounds are presented in Table 5. To estimate Δ_1 (see Fig. 8), the experimental values for the corresponding energy differences for metallic lanthanides are also presented. If, as has been suggested,[50, 140] the basic line in the Ln3*d* spectra of light lanthanide compounds occurs at higher binding energies, comparison of these data indicates that the Δ_1 value for lanthanum oxygen-containing compounds reaches 2.3 eV, that for cerium, 4.5 eV, and that for praseodymium, 0.6 eV (for the oxide) (see Table 5).

Table 5. Binding energies (E_b, eV) and binding energy differences (ΔE_i /eV) for the electrons of lanthanides and ligands in compounds.[5]

Compound [a]	$-E_b(Ln5p_{3/2})$	$\Delta E_1(Ln5p_{3/2}-Ln5p_{1/2})$	$-E_b(Ln3d_{5/2})$ [b]	$\Delta E_2(Ln3d_{5/2})$	$\Delta E_3(Ln5p_{3/2}-Ln3d_{5/2})$	$\Delta E_4(X2s-X1s)$ [c]
LaF_3	18.6	2.2	837.3 (1.00); 841.6 (0.30)	4.3	818.7; 823.0	655.8
La_2O_3	17.7	1.7	835.1 (1.00); 838.6 (0.83)	3.5	817.4; 820.9	507.4
LaL_3^1	18.3	2.1	835.7 (0.76); 838.8 (1.00)	3.1	817.4; 820.5	–
$LaL_3^2 \cdot 1.5\,H_2O$	18.3	–	836.0 (1.00); 838.8 (1.00)	2.8	817.7; 820.5	506.8
$La_2Ti_2O_7$	17.3	2.0	834.6 (1.00); 838.8 (0.91)	4.2	817.3; 821.5	507.9
$LaNbO_4$	17.2	–	834.8 (1.00); 838.8 (0.72)	4.0	817.6; 821.6	508.2
LaH_3 (see [d]) [91]	19.3	2.4	835.5 (0.48); 839.2 (1.00)	3.7	816.2; 819.9	–
La (see [d]) [91]	17.7	2.3	–; 836.3	–	–; 818.6	–
CeF_3	19.4	3.0	884.7 (1.00); 888.2 (0.58)	3.5	865.3; 868.3	655.9
CeO_2	18.0	–	882.3 (1.00); 888.8 (0.68)	6.5	864.3; 870.8	–
CeL_3^1	18.7	3.0	882.8 (0.32); 885.8 (1.00)	3.0	864.1; 867.1	–
$CeL_3^2 \cdot 1.5\,H_2O$	19.3	2.2	882.3 (0.30); 885.4 (1.00)	3.1	863.0; 866.1	506.6
CeH_3 (see [d]) [113]	19.2	2.6	882.4 (0.36); 886.4 (1.00)	4.0	863.2; 867.2	–
Ce (see [d]) [113]	18.0	2.9	–; 884.3	–	–; 866.3	–
PrF_3	20.1	3.7	–; 934.4	–	–; 914.3	655.7
Pr_2O_3 (see [e])	19.3	3.6	929.5 (0.32); 933.5 (1.00)	4.0	910.2; 914.2	–
PrL_3^1	19.7	2.5	929.0 (0.22); 932.8 (1.00)	3.8	909.3; 913.1	–
$PrL_3^2 \cdot 1.5\,H_2O$	20.2	2.8	929.9 (0.24); 934.1 (1.00)	4.2	909.7; 913.9	506.1
$PrNbO_4$	18.9	–	929.2 (0.25); 933.2 (1.00)	4.0	910.3; 914.3	507.9
PrH_3 (see [d]) [109]	20.2	–	930.4 (0.21); 934.6 (1.00)	4.2	910.2; 914.4	–
Pr (see [d]) [109]	18.8	–	–; 932.4	–	–; 913.6	–
NdF_3	20.7	3.7	–; 982.6	–	–; 961.9	655.7
Nd_2O_3	19.4	3.6	978.0 (0.29); 981.9 (1.00)	3.9	958.6; 962.5	507.0
NdL_3^1	20.3	3.9	978.8 (0.37); 982.8 (1.00)	4.0	958.5; 962.5	–
$NdL_3^2 \cdot 1.5\,H_2O$	20.7	4.2	979.0 (0.35); 982.9 (1.00)	3.9	958.3; 962.2	505.7
$NdPc_2$	20.3	3.0	978.1 (0.35); 982.1 (1.00)	4.0	957.8; 961.8	381.6
$NdPct_2$	19.9	3.9	978.6 (0.38); 982.4 (1.00)	3.8	958.7; 962.5	381.7
Nd (see [d]) [142]	–	–	–; 981.2	–	–	–
SmF_3	22.1	4.3	1084.4	–	1062.3	655.5
Sm_2O_3	20.4	4.0	1083.1	–	1062.7	–

Table 5 (continued).

Compound [a]	$-E_b(Ln5p_{3/2})$	$\Delta E_1(Ln5p_{3/2}-Ln5p_{1/2})$	$-E_b(Ln3d_{5/2})$ [b]	$\Delta E_2(Ln3d_{5/2})$	$\Delta E_3(Ln5p_{3/2}-Ln3d_{5/2})$	$\Delta E_4(X2s-X1s)$ [c]
SmL_3^1	20.8	–	1083.8	–	1063.0	–
$SmL_3^2 \cdot 1.5\,H_2O$	21.3	4.4	1084.5	–	1063.2	505.7
$SmNbO_4$	20.0	4.5	1080.1 (0.18); 1083.1 (1.00)	3.0	1060.1; 1063.1	509.2
EuF_3	22.4	–	1135.3	–	1112.9	655.8
Eu_2O_3	21.5	4.2	1134.6	–	1113.1	–
EuL_3^1	22.0	–	1135.2	–	1113.2	–
$EuL_3^2 \cdot 1.5\,H_2O$	22.6	4.7	1135.3	–	1112.7	507.0
$EuNbO_4$	21.3	–	1134.8	–	1113.5	–
GdF_3	22.9	–	1187.7	–	1164.8	655.6
Gd_2O_3	22.3	5.1	1187.3	–	1165.0	–
GgL_3^1	22.7	5.0	1187.3	–	1164.6	–
$GdL_3^2 \cdot 1.5\,H_2O$	23.3	4.3	–	–	–	506.7
LuF_3	28.4	7.3	197.3 [f]	–	168.9 [g]	–
Lu_2O_3	27.5	6.4	196.5 [f]	–	169.0 [g]	508.1
LuL_3^1	29.0	6.4	197.6 [f]	–	168.6 [g]	–
$LuL_3^2 \cdot 2\,H_2O$	28.5	6.4	197.7 [f]	–	169.2 [g]	–
$LuNbO_4$	27.4	–	196.4 [f]	–	169.0 [g]	508.8
Lu_2O_3 (see [d]) [80]	27.7	–	196.7 [f]	–	169.0 [g]	–
Oxide adsorbed on metallic Lu (see [80])	27.8	6.4	197.4 [f]	–	169.6 [g]	–
Lu (see [d]) [80]	26.6	7.0	196.3 [f]	–	169.7 [g]	–

[a] L^1 is the diphenylacetic acid residue, L^2 is the *o*-methoxybenzoic acid residue, Pc is the unsubstituted diphthalocyanine residue, Pct is the 4-*tert*-butyldiphthalocyanine residue. [b] The intensities of one of the $Ln3d_{5/2}$ lines referred to the line whose intensity is taken to be unity are given in parentheses. [c] X = O, F, N; the binding energy differences are given for those compounds for which the X1*s* spectrum is a single line. [d] The binding energies are referred to the electron binding energy for carbon in adsorbed hydrocarbons, $E_b(C1s) = 285.0$ eV [at $E_b(Au4f_{7/2}) = 83.8$ eV for the standard gold plate, $E_b(C1s) = 284.4$ eV]. [e] The E_b values are given for Ln^{3+}. [f] The $Lu4d_{5/2}$ binding energy. [g] The $\Delta E_3(Lu5p_{3/2}-Lu4d_{5/2})$ values.

The data considered lead to the conclusion that IVMO are actually formed in these compounds, the upper orbitals being antibonding. If the basic lines in the Ln3*d* spectra of light lanthanides occur at lower binding energies, as shown for the Ln compounds studied in a number of publications,[5, 50, 140] the Δ_1 value (see Fig. 8) changes its sign, while its magnitude $|\Delta_1|$ for lanthanum oxygen compounds reaches 1.3 eV (see Table 5). These results confirm the formation of IVMO in these compounds. In addition, they indicate that the upper IVMO is a bonding orbital in this case.

The same conclusion can be drawn by considering the $\Delta E_b(Ln5p_{3/2}-Ln4d_{5/2})$ energy differences for lanthanide compounds. The values for LaF_3, La_2O_3, LaL_3^1, $LaL_3^2 \cdot 1.5\,H_2O$, $La_2Ti_2O_7$, $LaNbO_4$ and metallic lanthanum amount to 85.8, 85.1, 85.4, 86.0, 85.0, 85.7 and 86.1 eV, respectively. These data confirm once again the fact that in the La3*d* spectra of the lanthanide compounds studied, the basic lines are located in the lower binding energy region.

On passing from light to heavy lanthanides, the $Ln5p_{3/2}$ energy level is lowered. In the case of lutetium, it is located below the O2*s* level; thus, the Δ_1 value for the lutetium compounds (see Fig. 8) should change the sign. In other words, the ΔE_3 difference (see Table 5) for oxygen compounds of lutetium should become smaller in magnitude than that for metallic Lu. Indeed, it follows from the data of Table 5 that in some cases, $\Delta E_3(Ln5p_{3/2}-Ln4d_{5/2})$ for atomic lutetium is 1.1 eV higher than these values for Lu in compounds ($\Delta_1 = -1.1$ eV).

It has been noted [184] that the emission spectra [185] of Eu_2O_3 and other 'sesquialteral' lanthanide oxides exhibit peaks related to the Ln5*p* and O2*s* hybrid orbitals. The X-ray $SL_{II,III}$ emission spectra of some sesquialteral REE sulfides [186] and lanthanide monosulfides [187] also contain peaks due to the formation of IVMO consisting of the Ln5*s*, Ln5*p* and S3*s* AO.

3. Multiplet splitting

Multiplet splitting shows itself most clearly in the case of the Ln4*s*, Ln4*d* and Ln5*s* electrons in lanthanide compounds. In the XPS spectra of Ln4*s* and Ln5*s* electrons, this splitting gives rise to two components the distance between which is correlated, along the energy scale, with the number n_{4f} of unpaired Ln4*f* electrons (see Figs 16, 29). These results are in satisfactory agreement with theoretical data,[44, 69, 93] and the multiplet splitting value can be used as a parameter in determining the spin and oxidation states of REE ions in compounds.

The XPS spectra of compounds of lanthanides containing unpaired Ln4*f* electrons in the Ln4*d* binding energy region are due to multiplet splitting and exhibit a complex structure (see Fig. 17, 30). Instead of the expected doublets characterised by a spin–orbit splitting energy not exceeding 10 eV even for heavy lanthanides, the spectrum of these electrons exhibits a fine structure in the energy range of up to ~40 eV. The results of theoretical calculations [45, 66] carried out in the ionic approximation are in satisfactory agreement with experimental data. The fine structure of the XPS spectra of the Ln4*d* electrons is typical of particular REE in compounds and can be used for identification and for determination of the oxidation state of the lanthanide ion. For example, this structure allows one to make the conclusion that the cerium oxidation state in all the compounds studied, except for the oxide, is close to Ce^{3+}. Apparently, in the oxide, cerium forms specific clusters, photoemission of a core electron from which gives rise to three final states including the unusual two-hole $Ce3d^9 5p^5(np)$ state (see Figs 33, 34). The presence of one unpaired Ce4*f* electron in Ce^{3+} results in a pronounced disturbance of the structure of the spin doublet present in the Ce4*d* spectra of the Ce^{4+} ion, which does not contain this Ce4*f* electron. The structure of the Yb4*d* spectra leads to the conclusion that ytterbium exists as Yb^{3+} in all the compounds studied. The Yb^{3+} electronic configuration is $4f^{13}$, which markedly complicates the expected spectral structure. The spectrum of the Yb4*d* electrons of the Yb^{2+} with the $4f^{14}$ configuration (in the $YbCu_2Ge_2$ intermetallic com-

pound [156] and metallic ytterbium [71, 96, 188]) contains a doublet caused by the spin–orbit splitting.

4. Spilitting resulting from the induced charge

Charge inducing on the centres regarded previously as diamagnetic (Ti^{4+}) in the double oxides of the $FeTiO_3$ type was first observed by X-ray emission spectroscopy.[189] The excess electron density on the titanium ion contained in complex oxides of the $MTiO_3$ type arises in the case where the second coordination sphere contains paramagnetic metal ions (M). Analysis of the X-ray emission spectra shows [189–191] that, for example, on passing from TiO_2 to $FeTiO_3$ and, possibly, to $Ln_2Ti_2O_7$,[28, 192, 193] the titanium ions, which are expected to be diamagnetic, are actually paramagnetic. This results in splitting of the emission lines of the titanium ions. A similar situation is also found for niobium compounds. This line splitting is a specific case of multiplet splitting, which is an indirect consequence of the presence of paramagnetic ions connected to the metal ion in question *via* an oxygen bridge.

By using a procedure for recording high-resolution XPS spectra of dielectric materials, Teterin and co-workers [133–136, 194, 195] were able to measure the relative line widths of the spectra and the electron binding energies with an accuracy higher than $\sim$0.1 eV. Thus, it became possible to detect, with a relatively high accuracy, slight changes in the unpaired electron density ($\Delta\rho$) on a metal ion in a dielectric material and to estimate semi-quantitatively the $\Delta\rho$ value using the XPS method. An increase in the number of unpaired electrons in a 3*d*-metal or lanthanide ion in a compound by one electron ($\Delta\rho = 1e^-$) is known [44, 93, 94, 196] to increase the splitting of the M3*s* or Ln4*s* line by approximately 1 eV (see, for example, Fig. 29). Since the binding energies and the line widths for core levels can be measured with an accuracy higher than $\pm$0.1 eV, the change in the $\Delta\rho$ value by $0.1e^-$ can be detected by XPS. Using results reported by Teterin *et al.*,[194] the $\Delta\rho$ value for Ti in $FeTiO_3$ was found to be $\sim 0.5e^-$, while that for Nb in $SmNbO_4$ was found to exceed $1e^-$.

This phenomenon has been studied in more detail by XPS [133, 134, 136] in relation to lanthanide (except for Pm and Tm) orthoniobates. On passing from niobium oxide (α-Nb_2O_5) to orthoniobates ($LnNbO_4$) containing Ln^{3+} paramagnetic ions, characteristics of the XPS spectra of the core electrons of niobium change. Thus the line widths in the Nb3$p_{3/2}$, Nb4*s* and Nb4*p* spectra for $LnNbO_4$ containing lanthanides of the middle of the row are much greater than the corresponding values for the α-Nb_2O_5 oxide. The broadening of the Nb4*s* line becomes so pronounced that at least two components of the complex structure are clearly manifested. The observed line broadening is assumed to be mainly due to charge induction ($\Delta\rho$) onto the Nb^{5+} ion, and, on passing from α-Nb_2O_5 to $LnNbO_4$ (Ln are lanthanides from the medium of the row), the Nb^{5+} ion electronic configuration changes appreciably from $\{4d\}$ to $\{4d^{\Delta\rho}\}$. It has been noted [44, 93, 94, 196] that the multiplet splitting arises with the highest probability in the spectra of core electrons having the same principal quantum number as the unpaired electrons. In this case, the most pronounced multiplet splitting should be expected in the spectra of the Nb4*s* electrons. This was actually observed in experiments. However, Lebedev *et al.*[136] do not rule out the possibility that the dynamic effect may also be manifested in these spectra, although it is less pronounced than the multiplet splitting.

The excess unpaired electron density ($\Delta\rho$) has been estimated [133, 134, 136] using data on the multiplet splitting of the Ln4*s* lines for Ln_2O_3 oxides,[80] which indicate that the presence of one unpaired 4*f* electron in a lanthanide ion induces splitting of the Ln4*s* line by $\Delta E_{ms}(Ln4s) \approx 1.1$ eV. In this case, for $GdNbO_4$, it was found that $\Delta\rho_1 > 1e^-$. The appearance of the extra electron density $\Delta\rho$ on the niobium ion on passing from α-Nb_2O_5 $\{4d^0\}$ to $GdNbO_4$ $\{4d^{\Delta\rho}\}$ results in a shift of the core electron lines towards low binding energies; for example, for the Nb3$p_{3/2}$ electrons, this shift is $\Delta E_b(Nb3p_{3/2}) = 0.8$ eV. Since a change in the formal oxidation state of a metal in compounds by unity results in a change of the chemical shift of the core levels by approximately one electron-volt (see, for example, Ref. 33), the excess electron density ($\Delta\rho_2$) found from the chemical shift of the Nb3$p_{3/2}$ level is smaller than the $\Delta\rho_1$ value determined from splitting of the Nb4*s* lines, and equals $\sim 0.8e^-$. This difference between the considered values may be due, in particular, to the fact that $\Delta\rho_1$ is the sum of two contributions ($\Delta\rho_1 = \Delta\rho_2 + \Delta\rho_3$), one of them ($\Delta\rho_2$) being due to the excess charge directly on the $Nb^{\Delta\rho_2}$ ion and the other ($\Delta\rho_3$) being related to polarisation (for example, polarisation of the valence-shell electrons).

The results obtained represent one of the first steps in the study of the appearance of excess unpaired electron density on the ionic centres that have previously been considered diamagnetic. Since double oxides possess ferroelectric ($LnNbO_4$), antiferromagnetic ($FeTiO_3$) and other important physical properties, further investigation of the charge induction mechanism may shed light on the nature of these phenomena and favour the development of methods for the preparation of substances with *a priori* specified useful properties. The use of characteristics of the spectral fine structure allows efficient utilisation of the XPS method in a study of charge induction caused by indirect exchange interaction between metal ions in valuable complex materials.

5. Dynamic effect

Experimental data show that the fine structure associated with the dynamic effect is manifested most clearly in the spectra of those atomic levels the energies of which are divisible by the energies of the nearest upper levels (see above). This shows itself as an individual structure in the spectra of the Ln4*p* electrons for all lanthanide compounds that obey most closely the approximate equality $E_b(Ln4p) \approx 2\,E_b(Ln4d)$ (see Figs 19, 31, 34). Common features of the spectra of these electrons in various lanthanide compounds are that the Ln4$p_{3/2}$ component has a fine structure and that the intensity of the Ln4$p_{1/2}$ component is most often substantially suppressed.

The structure of the Ln4*p* spectra of lutetium compounds is much less complicated. This led to the suggestion that [5, 20] one of the possible final configurations of lanthanide ions resulting from photoemission of the Ln4*p* electron is due to the Ln4*d*-to-Ln4*f* electron migration: $4p^54d^{10}4f^n \leftrightarrow 4p^64d^84f^{n+1}$. The resulting data contradict the suggestion made by Padalia *et al.*[80] that the structure of the Ln4*p* spectra is due to multiplet splitting but are consistent with the results of a calculation for X-ray $LnL\gamma_{II,III}$ emission spectra [197] and other X-ray spectra of lanthanides.[198, 199]

The structure caused by the dynamic effect giving rise to the final states of the type

$$Ln5s^15p^64f^n \longleftrightarrow Ln5s^25p^44f^{n+1},$$

$$Ln4s^14p^65p^64f^n \longleftrightarrow Ln4s^24p^55p^44f^{n+2},$$

$$Ln3p^53d^{10}4s^24f^n \longleftrightarrow Ln3p^63d^94s^14f^{n+1},$$

can markedly complicate the Ln5*s*, Ln4*s* and Ln3*p* spectra of lanthanides in compounds.[5, 200]

Study of the nature of generation of the XPS spectral structure associated with the dynamic effect may clarify the role of the secondary electron processes that accompany the photoemission of electrons from individual shells. In particular, analysis of the XPS spectra stimulates the theoretical investigation of these processes,[168, 200] while the spectra can serve as a criterion for the validity of the models chosen for calculations.

6. Many-body perturbation

When manifested to a substantial extent, many-body perturbation gives rise to satellites in the spectra of electrons of various shells. As shown for 3*d* transition metal [23, 122] and lanthanide [44, 48, 135] compounds, the most intense satellites should be manifested in the spectra of low-lying electron levels because these electrons possess a relatively low kinetic energy after photoemission. For com-

pounds of light lanthanides, the problem of the mechanism of satellite formation is especially acute for several reasons.

As noted in the Introduction, in the binding energy range used normally in investigations, virtually all the XPS spectra of various electron shells in lanthanide compounds exhibit complex structures. The structure present in the spectra of core electrons hampers the measurement of binding energies, which are traditionally used to determine the relative oxidation states of lanthanides in compounds. In the case of light lanthanides, one component of the Ln3$d_{5/2,3/2}$ spin doublet is considered to be suitable for this purpose. However, both the Ln3$d_{5/2}$ and Ln3$d_{3/2}$ spectra in lanthanide compounds can contain at least two intense lines. Study of the reasons for the appearance of complex structures in the spectra of Ln3*d* electrons of rare earth metals [201] and light lanthanide compounds [177] has attracted considerable attention.

An important problem arising in the analysis of the Ln3*d* spectral structure in lanthanide compounds is to find out which of the two lines reflects the main final state with the hole in the Ln3*d* level formed upon photoemission of an electron. On the one hand, clarification of this item is needed for measuring the relative binding energies of these electrons and, on the other hand, this would enable the use of the method of binding energy difference between the core and valence MO when analysing the nature of individual MO.

In a number of studies,[45, 50, 105, 178] it has been suggested that the spectral structure of the Ln3*d* electrons in lanthanide compounds is due to many-body perturbation giving rise to shake-up satellites, which can be more intense than the basic lines. The results obtained for individual light lanthanides [108, 109, 155, 201] indicate that the Ln3*d* spectra do not exhibit the highly intense satellites observed by Shabanova *et al.*[126] The low-intensity extra lines ($\sim 10^{-2}$%) observed in the Ln3*d* spectra of metallic lanthanides on the lower binding energy side of the basic lines may be due to a shake-down process.[201] By analogy, it has been suggested [75, 108, 109] that the intense extra lines recorded in the Ln3*d* spectra of light lanthanide hydrides, oxides and hydroxides are also due to many-body perturbation with the formation of shake-down satellites. In other words, the lines in the spectra of Ln3*d* electrons that have previously [45, 50, 178] been classified as satellites have also been proposed [75, 108, 109] to be basic lines. These lines should occur at higher binding energies than satellites (see Figs 21, 33).

As an argument supporting the formation of shake-down satellites in the spectra of the Ln3*d* electrons of light REE, the researchers [108, 109] proposed the fact that the electron binding energy corresponding to the high-energy component of lanthanide compounds is greater than the Ln3*d* energy in individual metals (see Table 5). However, to measure the Ln3*d* binding energy in lanthanide compounds more rigorously, one should take into account the whole structure of the spectrum of these electrons.[202] In this case, the Ln3*d* binding energy can be determined using the weighted-mean value found from the complex spectrum. Moreover, if the extra structure in the spectra of these electrons is due to shake-down satellites, similar satellites (although less intense) should also occur in the spectra of electrons characterised by lower binding energies than the Ln3*d* electrons. Unfortunately, in none of the studies [75, 108, 109] in which a shake-down process has been proposed to interpret the Ln3*d* spectral structure, was such an analysis performed.

In elucidation of the reasons for the appearance of highly intense satellites in the Ln3*d* spectra of light lanthanides,[51, 64, 135] three spectral parameters have been used: (i) the chemical shift of the electronic energy level corresponding to the considered component relative to the Ln3*d* energy level in the metal; (ii) the presence of satellites in the spectra of other electronic energy levels; (iii) binding energy differences between lanthanides in compounds and in metals for various electrons the spectra of which exhibit no intense satellites of this type.

When considering the spectral structure for the La3*d* electrons in lanthanum compounds from this standpoint, one can detect shake-up satellites. Indeed, the weighted-mean values of the La3*d* binding energies in lanthanum compounds are about 0.3 eV higher than the corresponding values for metallic lanthanum, E_b(La3$d_{5/2}$) = 836.6 eV (see Table 5). The spectra of other electrons of lanthanum compounds also display satellites at higher binding energies relative to the basic lines, the satellite intensity decreasing with a decrease in the binding energies of these electrons (Table 6). This statement is also in agreement with the relationship between the binding energy difference $\Delta E_3(5p_{3/2} - 3d_{5/2})$ in the lanthanum compounds and metallic La. For example, the increase in ΔE_3 for the high-energy component of the spectrum by 4.4 eV on passing from metallic lanthanum to the trifluoride can hardly be explained by the assumption that the basic line for the La3*d* electrons occurs in the spectrum at higher electron binding energies (see Table 5). Meanwhile, the concomitant increase in ΔE_3 for the low-energy component by 0.1 eV can be easily explained by the fact that the upper IVMO in the formation of the La – F bond is an antibonding orbital. The slight participation of the La5*p* and F2*s* AO in the formation of IVMO in LaF_3 is also confirmed by calculations (see Fig. 12). However, to estimate more rigorously the character of the IVMO on the basis of binding energy differences, it is necessary to use the La3*d* binding energies found as the weighted-mean ΔE_b values for the electrons reflecting the whole spectral structure.

Table 6. Intensities of the shake-up satellites $I = I_{sat}/I_o$ (%) and their energies (ΔE_{sat}, eV) relative to the basic lines in the XPS spectra of various lanthanum shells in compounds.[20, 79, 84, 135]

Compound [a]	$I(3d_{5/2})$	$\Delta E_{sat}(3d_{5/2})$	$I(4p_{3/2})$	$I(4d_{5/2})$
LaF_3	30	4.3	18	13
$LaNbO_4$	72	4.2	34	27
La_2O_3	83	3.5	29	22
$La_2Ti_2O_7$	91	4.2	27	–
$LaL^2_3 \cdot 1.5\,H_2O$	100	2.8	–	24
LaL^1_3	132	3.1	–	55

Note. The errors in the determination of I values are ±10%, ΔE_{sat} is ±0.2.
[a] L^1 is the diphenylacetic acid residue, L^2 is the *o*-methoxybenzoic acid residue.

This assumption is in good agreement with the results of the study [140] which illustrates the formation of shake-down satellites in the spectra of the La3*d* electrons for metallic lanthanum and shake-up satellites in the spectra of these electrons in the dielectric $La(OH)_3$ (Fig. 40). Upon the formation of a hole in a core level of lanthanum, the energy of the empty La4*f* AO levels decreases. In a metal, these levels can be filled due to transition of an electron from the conduction band, which corresponds to a shake-down process. In a dielectric having the valence band rather than the conduction band at a higher binding energy, these 4*f* levels can be occupied due to transition of an electron from this band, which implies a shake-up process.

In reality, the satellite formation is a more complex process.[41, 203, 204] The structure and intensity of these satellites are highly sensitive to the variation of a stoichiometric composition of the substance and the nature of the ligands surrounding the lanthanide. Thus it has been noted [45, 46] that an increase in the covalent nature of the bond, for example, in the series of lanthanum halides LaF_3, $LaCl_3$, $LaBr_3$, entails a decrease in the binding energies of shake-up satellites relative to the La3*d* basic lines, while the satellite intensity markedly increases. Hence, the spectral characteristics of the satellites may allow one to estimate the degree of ionicity (covalence) of the La – L chemical bonds in lanthanum compounds. For example, it follows from XPS spectra that the ionic type of the La – O bond markedly increases over the series LaL^1_3, $LaL^2_3 \cdot 1.5\,H_2O$, La_2O_3 (see Table 6). Similar consid-

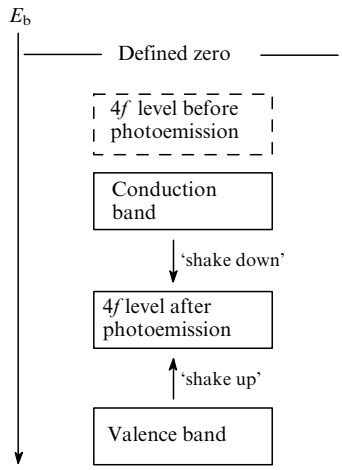


Figure 40. Diagram representing the positions of the 4*f* energy level in compounds of the light lanthanides before and after photoemission of a core electron.[140] The conduction band in a dielectric, for example, in La_2O_3, is empty.

erations concerning the nature of satellites are also valid for cerium compounds.[137, 138, 205] However, it follows from the low-energy spectra in which the Ln4*f* states are shifted relative to the OVMO energy and from the pattern of variation of the Ln3$d_{5/2}$ FWHM for lanthanide trifluorides following an increase in the Ln atomic number (see Figs 23, 22) that shake-down satellites may be expected in the spectra of compounds formed by heavier elements.[206] This is also consistent with the results of theoretical calculations.[47, 114]

The data considered above make it possible to draw the conclusion that determination of the lanthanide oxidation state based on the Ln3*d* XPS spectral characteristics of lanthanide compounds should be done using the weighted-mean value for the binding energy found with allowance for the whole complex structure of the spectrum.

V. Conclusion

The variation of the binding energy and the relative line intensity for the Ln4*f* electrons *vs*. the atomic number of lanthanide in lanthanide oxides shows that the Ln4*f* electrons largely resemble in spectral characteristics the M*nd* electrons of *nd* transition metals. These data are consistent with the results of theoretical calculations pointing to a substantial participation of the Ln4*f* AO in the formation of MO in lanthanide compounds. In all the studied compounds of scandium, yttrium and lanthanides, IVMO are efficiently formed by participation of occupied Sc3*p*, Y4*p*, Ln5*p* and L2*s* AO; this is supported by the results of theoretical calculations. This allows experimental evaluation of the type (either bonding or antibonding) of some IVMO.

The dependences on the multiplet splitting (ΔE_{ms}) of the Ln4*s* and Ln5*s* lines of lanthanide trifluorides, oxides and other compounds on the number of unpaired Ln4*f* electrons have been established; they make it possible to determine spin population on the Ln atom in compounds. It was found that, due to the multiplet splitting, the spectrum of Ln4*d* electrons for lanthanide compounds extends over a range of $\sim$40 eV, which is several times greater than the spin – orbit splitting of the lines of these electrons. The mechanism of satellite formation in the spectra of Ln3*d* electrons was analysed. For LnF_3 and Ln_2O_3, the theoretical concept concerning the change of the sign of the binding energy difference $\Delta E_{sat} = |E_{sat}| - |E_o|$ between the satellite and the basic line (from 'plus' to 'minus') with an increase in the atomic number (Z) over the lanthanide row was confirmed experimentally. It was shown that the structure of the Ln4*p* spectra and, in some cases, the Ln3*p* spectra is largely determined by the dynamic effect, resulting in the $Ln4p^5 4d^{10} 4f^n \leftrightarrow Ln4p^6 4d^8 4f^{n+1}$ and $Ln3p^5 3d^{10} 4s^2 4f^n \leftrightarrow Ln3p^6 3d^9 4s^1 4f^{n+1}$ final states, respectively.

The electron density induction on ions previously considered diamagnetic has been studied by X-ray electron spectroscopy in relation to the lanthanide-containing titanium and niobium double oxides.

Interpretation of the reasons for the formation of fine structure in the XPS spectra of lanthanides and elucidation of the relationships between the structure parameters and the physicochemical properties of these compounds markedly extends the scope of application of the XPS method for the investigations of these compounds. In this case, X-ray electron spectroscopy becomes the most adequate method for determination of the elemental and ionic composition of lanthanide compounds, electronic configurations and magnetic characteristics of lanthanide ions, for investigations into the nature of the chemical bond and secondary electronic processes that accompany photoemission of electrons, and for determining the structure of the local environment of metal ions.

This provides the possibility of more efficient use of expensive advanced equipment and synchrotron radiation in diverse investigations of compounds of lanthanides and other elements.

This work was supported by the International Science and Engineering Centre (Project No. 1358) and the Russian Foundation for Basic Research (Project Nos 00-03-32138, 00-15-97289).

References

1. F A Cotton, G Wilkinson *Basic Inorganic Chemistry* (New York: Wiley, 1976)
2. D Brown *Halides of the Transition Elements. Halides of the Lanthanides and Actinides* (London: Wiley-Interscience, 1968)
3. G A Bandurkin, B F Dzhurinskii, I V Tananaev *Osobennosti Kristallokhimii Soedinenii Redkozemel'nykh Elementov* (Features of the Crystal Chemistry of Compounds of Rare Earth Elements) (Moscow: Nauka, 1984)
4. V I Spitsyn, G V Ionova *Usp. Khim.* **53** 1249 (1984) [*Russ. Chem. Rev.* **53** 725 (1984)]
5. Yu A Teterin, A S Baev *Rentgenovskaya Fotoelektronnaya Spektroskopiya Soedinenii Lantanoidov* (X-Ray Photoelectron Spectroscopy of Lanthanide Compounds) (Moscow: TsNIIatominform, 1987)
6. I N Shabanova, A I Efimenko, V A Trapeznikov *J. Electron Spectrosc. Relat. Phenom.* **10** 197 (1977)
7. J Mitome, E Aceves, U S Ozkan *Catal. Today* **53** 597 (1999)
8. Z Zhang, W Liu, Q Xue *Thin Solid Films* **330** 120 (1998)
9. Yu A Teterin, L D Shustov, in *Sverkhprovodimost': Fizika. Khimiya. Tekhnika* (Superconductivity: Physics. Chemistry. Engineering) (Moscow: TsNIIatominform, 1988) Vol. 4, p. 12
10. Yu A Teterin, M I Sosulnikov, V I Ozhogin, T M Senchenkova, N S Tolmacheva, L D Shustov *Physica C* **185 – 189** 837 (1991)
11. Yu A Teterin, M I Sosulnikov, L D Shustov *J. Electron Spectrosc. Relat. Phenom.* **68** 453 (1994)
12. D S-L Law, M N Mikheeva, V G Nazin, A V Svishchev, M B Tsetlin, N Hayes, S Downes *Physica C* **272** 233 (1996)
13. S M Butorin, V R Galakhov, L D Finkelstein, E Z Kurmaev, Yu A Teterin, M I Sosulnikov, S M Cheshnitsky, S A Lebedev, A I Akimov *Physica C* **177** 8 (1991)
14. Yu A Teterin, M I Sosulnikov *Appl. Supercond.* **1** 457 (1993)
15. Yu A Teterin, M I Sosulnikov *Physica C* **212** 306 (1993)
16. L D Finkelstein, V R Galakhov, V V Fedorenko, L V Elokhina, A A Samokhvalov, E Z Kurmaev, S M Butorin, J Nordgren, B V Slobodin, Yu A Teterin, M I Sosulnikov *J. Electron Spectrosc. Relat. Phenom.* **68** 431 (1994)
17. L D Finkelstein, V R Galakhov, V V Fedorenko, L V Elokhina, A A Samokhvalov, E Z Kurmaev, S M Butorin, J Nordgren, B V Slobodin, Yu A Teterin, M I Sosulnikov *Solid State Commun.* **90** 769 (1994)
18. Yu A Teterin, S G Gagarin *Usp. Khim.* **65** 895 (1996) [*Russ. Chem. Rev.* **65** 825 (1996)]

19. D F Mullica, C K C Lok, H O Perkins, G A Benesh, V Young *J. Electron Spectrosc. Relat. Phenom.* **71** 1 (1995)
20. Yu A Teterin, A Yu Teterin, A M Lebedev, I O Utkin, A S Nikitin *Zh. Strukt. Khim.* **39** 1059 (1998) [a]
21. L V Gurvich, Yu N Dmitriev, L A Kaledin, A N Kobylyanskii, A N Kulikov, E A Shenyavskaya *Izv. Akad. Nauk SSSR, Ser. Fiz.* **48** 721 (1984)
22. K Siegbahn, C Nordling, A Fahlman, R Nordberg, K Hamrin, J Hedman, G Johansson, T Bergmark, S-E Karlsson, I Lindgren, B Lindberg *ESCA Atomic, Molecular and Solid State Structure Studied by Means of Electron Spectroscopy. Ser. IV* Vol. 2 (Uppsala: Nova Acta Regiae Societatis Scientiarum Upsaliensis, 1967)
23. V M Kulakov, Yu A Teterin *Priroda* (2) 78 (1977)
24. Yu A Teterin, A N Baranov, V M Kulakov, L N Nikolenko, N S Tolmacheva *Koord. Khim.* **4** 1860 (1978) [b]
25. S Suga, A Sekiyama *J. Electron Spectrosc. Relat. Phenom.* **114 – 116** 659 (2001)
26. B W Veal, A P Paulikas *Phys. Rev. B* **31** 5399 (1985)
27. M J Capitán, M A Centeno, P Malet, I Carrizosa, J A Odriozola, A Márquez, J F Sanz *J. Phys. Chem. B* **99** 4655 (1995)
28. D A Pawlak, K Wozniak, Z Frukacz, T L Barr, D Fiorentino, S Hardcastle *J. Phys. Chem. B* **103** 3332 (1999)
29. D A Pawlak, K Wozniak, Z Frukacz, T L Barr, D Fiorentino, S Seal *J. Phys. Chem. B* **103** 1454 (1999)
30. K Yoshida, H Sasakura, S Tsukui, R Oshima, Y Mizokawa *Physica C* **329** 292 (2000)
31. J-S Kang, Y Onuki, C G Olson, B I Min *Physica B* **281 – 282** 731 (2000)
32. J-S Kang, C G Olson, M Hedo, Y Inada, E Yamamoto, Y Haga, Y Ōnuki, S K Kwon, B I Min *Phys. Rev. B* **60** 5348 (1999)
33. V I Nefedov *Rentgenoelektronnaya Spektroskopiya Khimicheskikh Soedinenii* (X-Ray Electron Spectroscopy of Chemical Compounds) (Moscow: Khimiya, 1984)
34. J J Joyce, A J Arko, J Lawrence, P C Canfield, Z Fisk, R J Bartlett, J D Thompson, J L Smith *J. Alloys Compd.* **181** 161 (1992)
35. O Eriksson, M S S Brooks, B Johansson *Phys. Rev. B* **41** 7311 (1990)
36. E Z Kurmaev, M A Korotin, V R Galakhov, L D Finkelstein, E I Zabolotzky, N N Efremova, S Stadler, D L Ederer, A Moewes, S Bartkowski, M Neumann, J Matsuno, T Mizokawa, A Fujimori, J Mitchell *J. Electron Spectrosc. Relat. Phenom.,* **101 – 103** 793 (1999)
37. Yu A Teterin, A S Baev, A Yu Teterin, L Vukchevich, in *Proceedings of Yugoslav Nuclear Society Conference (YUNSC'96)* (Ed. D P Antic) (Belgrade: VINCA Institute of Nuclear Sciences, 1997) p. 457
38. A Kotani *J. Electron Spectrosc. Relat. Phenom.* **100** 75 (1999)
39. A Kotani, H Ogasawara *J. Electron Spectrosc. Relat. Phenom.* **86** 65 (1997)
40. J D Lee, O Gunnarsson, L Hedin *Phys. Rev. B* **60** 8034 (1999)
41. M Takahashi, C Suzuki, H Adachi, J Kawai, T Mukoyama, A M Vlaicu *Chem. Phys.* **253** 27 (2000)
42. Yu A Teterin, A S Baev, S G Gagarin *Radiokhimiya* **28** 318 (1986) [c]
43. G K Wertheim, A Rosencwaig, R L Cohen, H J Guggenheim *Phys. Rev. Lett.* **27** 505 (1971)
44. R L Cohen, G K Wertheim, A Rosencwaig, H J Guggenheim *Phys. Rev. B* **5** 1037 (1972)
45. A J Signorelli, R G Hayes *Phys. Rev. B* **8** 81 (1973)
46. S Suzuki, T Ishii, T Sagawa *J. Phys. Soc. Jpn.* **37** 1334 (1974)
47. J Weber, H Berthou, C K Jørgensen *Chem. Phys. Lett.* **45** 1 (1977)
48. J Weber, H Berthou, C K Jørgensen *Chem. Phys.* **26** 69 (1977)
49. G K Wertheim, M Campagna *Solid State Commun.* **26** 553 (1978)
50. W-Y Howng, R J Thorn *Chem. Phys. Lett.* **56** 463 (1978)
51. R J Thorn *J. Phys. Chem. Solids* **43** 393 (1982)
52. Yu A Teterin, A S Baev, S G Gagarin, in *Tezisy Dokladov XIV Vsesoyuz. Soveshch. po Rentgenovskoi i Elektronnoi Spektroskopii, Irkutsk, 1984* (Abstracts of Reports of the XIVth All-Union Meeting on X-Ray and Electronic Spectroscopy, Irkutsk, 1984) p. 77
53. Z Hu, G Kaindl, H Ogasawara, A Kotani, I Felner *Chem. Phys. Lett.* **325** 241 (2000)
54. V A Gubanov, M V Ryzhkov *Zh. Strukt. Khim.* **27** 123 (1986) [a]
55. Yu A Teterin, S G Gagarin *Vnutrennie Valentnye Molekulyarnye Orbitali i Vliyanie ikh Elektronov na Kharakter Khimicheskoi Svyazi Soedinenii* (Inner Valence Molecular Orbitals and Influence of Their Electrons on the Type of Chemical Bond of Compounds) (Moscow: TsNIIatominform, 1985)
56. V A Gubanov, E Z Kurmaev, A L Ivanovskii *Kvantovaya Khimiya Tverdogo Tela* (Quantum Chemistry of Solids) (Moscow: Nauka, 1984)
57. M V Ryzhkov, V A Gubanov, Yu A Teterin, A S Baev *Z. Phys. B, Condens. Matter* **59** 1 (1985)
58. M V Ryzhkov, V A Gubanov, Yu A Teterin, A S Baev *Z. Phys. B, Condens. Matter* **59** 7 (1985)
59. M V Ryzhkov, V A Gubanov, Yu A Teterin, A S Baev *Zh. Neorg. Khim.* **30** 2475 (1985) [d]
60. Yu A Teterin, S G Gagarin, Yu P Dikov, G L Gutsev, V V Nemoshkalenko *Teor. Eksp. Khim.* **19** 259 (1983) [e]
61. Yu A Teterin, A S Baev, V M Kulakov, A G Zelenkov, in *Voprosy Atomnoi Nauki i Tekhniki (Ser. Obshchaya i Yadernaya Fizika)* [Problems of Nuclear Science and Technics (Series of General and Nuclear Physics)] (Khar'kov: Khar'kov Physical Engineering Institute, 1982) Vol. 2 (20), p. 68
62. Yu A Teterin, in *Proceedings of the 5th Seminar on Electron Spectroscopy of Socialist Countries* (Dresden: Technische Universitat, 1984) p. 145
63. M V Ryzhkov, N I Medvedeva, A F Golota, M Ya Khodos, V A Gubanov *Zh. Strukt. Khim* **26** (6) 76 (1985) [a]
64. F R McFeely, S P Kowalczyk, L Ley, D A Shirly *Phys. Lett. A* **45** 227 (1973)
65. P O Hedén, H Löfgren, S B M Hagström *Phys. Rev. Lett.* **26** 432 (1971)
66. V F Demekhin, S A Yavna, Yu I Bairachnyi, V L Sukhorukov *Zh. Strukt. Khim.* **18** 644 (1977) [a]
67. Yu A Teterin, A S Baev, A Yu Teterin *Radiokhimiya* **38** 403 (1996) [c]
68. Yu A Teterin, A Yu Teterin, A M Lebedev, L Vukchevich *Poverkhnost'* **8** 40 (1997)
69. F W Kutzier, D E Ellis, D J Lam, B W Veal, A P Paulikas, A T Aldred, V A Gubanov *Phys. Rev. B* **29** 1008 (1984)
70. J K Lang, Y Baer, P A Cox *J. Phys. F, Met. Phys.* **11** 121 (1981)
71. W A Svensson, M O Krause, T A Carlson, V Radojevic, W R Johnson *Phys. Rev. A* **33** 1024 (1986)
72. Y Baer, G Busch *J. Electron Spectrosc. Relat. Phenom.* **5** 611 (1974)
73. W C Lang, B D Padalia, D J Fabian, L M Watson *J. Electron Spectrosc. Relat. Phenom.* **5** 207 (1974)
74. A Platau, A Callenas, S E Karlsson *Solid State Commun.* **37** 829 (1981)
75. A Fujimori, N Tsuda *Phys. Status Solidi B* **114** K139 (1982)
76. J H Scofield *J. Electron Spectrosc. Relat. Phenom.* **8** 129 (1976)
77. I M Band, Yu I Kharitonov, M B Trzhaskovskaya *At. Data Nucl. Data Tables* **23** 443 (1979)
78. A S Baev, Yu A Teterin, V M Kulakov, N B Nevzorov, S B Pirkes, T A Krasovskaya, in *Fizicheskie i Matematicheskie Metody v Koordinatsionnoi Khimii* (Physical and Mathematical Methods in Coordination Chemistry) (Kishinev: Shtiintsa, 1980) p. 75
79. Yu A Teterin, A S Baev, V M Kulakov, A L Gubskii, A P Kovtun, S B Pirkes, G N Makushova, T A Krasovskaya *Dokl. Akad. Nauk SSSR* **259** 416 (1981) [f]
80. B D Padalia, W C Lang, P R Norris, L M Watson, D J Fabian *Proc. R. Soc. London, A Math. Phys. Sci.* **354** 269 (1977)
81. V L Sukhorukov, S A Yavna, V F Demekhin *Fiz. Tv. Tela* **26** 2172 (1984) [g]
82. J F Herbst *Phys. Rev. B* **30** 3020 (1984)
83. Yu A Teterin, A Yu Teterin, A M Lebedev, I O Utkin, in *Sbornik Dokladov Natsional'noi Konferentsii po Primeneniyu Rentgenovskogo, Sinkhrotronnogo Izlucheniya, Neitronov i Elektronov dlya Issledovaniya Materialov (RSNE'97)* (Collection of Reports of the National Conference on Application of X-Ray, Synchrotron Radiation, Neutrons and Electrons for Investigation of Materials) (Dubna: Joint Institute of Nuclear Investigations, 1997) Vol. 2, p. 442
84. Yu A Teterin, A S Baev, V M Kulakov, A L Gubskii, A P Kovtun, S B Pirkes, G N Makushova, in *Fizicheskie i Matematicheskie Metody v Koordinatsionnoi Khimii* (Physical and Mathematical Methods in Coordination Chemistry) (Kishinev: Shtiintsa, 1980) p. 75

85. B F Ormont *Struktura Neorganicheskikh Veshchestv* (The Structures of Inorganic Compounds) (Moscow; Leningrad: Gostekhteorizdat, 1950)
86. Yu A Teterin, S G Gagarin, Yu P Dikov, G L Gutsev *Dokl. Akad. Nauk SSSR* **268** 921 (1983) [f]
87. Yu A Teterin, A S Baev, S G Gagarin, A P Kovtun *Dokl. Akad. Nauk SSSR* **273** 156 (1983) [f]
88. J C Slater, K H Johnson *Phys. Rev. B* **5** 844 (1972)
89. T Mukoyama, H Nakamatsu, H Adachi *J. Electron Spectrosc. Relat. Phenom.* **63** 409 (1993)
90. M Piotrowski, H Ptasiewcz-Bak, A Mukrasik *Phys. Status Solidi A* **55** K163 (1979)
91. L Schlapbach, H R Scherrer *Solid State Commun.* **41** 893 (1982)
92. F P Larkins *At. Data Nucl. Data Tables* **20** 311 (1977)
93. F R McFeely, S P Kowalczyk, L Ley, D A Shirley *Phys. Lett. A* **49** (4) 301 (1974)
94. V Prabhawalkar, B D Padalia *Solid State Commun.* **49** 805 (1984)
95. V F Demekhin, V L Sukhorukov, T V Shelkovich, S A Yavna, V A Yavna, Yu I Bairachnyi *Zh. Strukt. Khim.* **20** 38 (1979) [a]
96. S P Kowalczyk, N Edelstein, F R McFeely, L Ley, D A Shirley *Chem. Phys. Lett.* **29** 491 (1974)
97. C S Fadley, D A Shirley, A J Freeman, P S Bagua, J V Mallow *Phys. Rev. Lett.* **23** 1397 (1969)
98. C S Fadley, D A Shirley *Phys. Rev. A* **2** 1109 (1970)
99. K Wandelt, C R Brundle *Surf. Sci.* **157** 162 (1985)
100. J F Herbst, J W Wilkins *Phys. Rev. B* **20** 2999 (1979)
101. G K Wertheim, G Crecelius *Phys. Rev. Lett.* **40** 813 (1978)
102. N Spector, C Bonnelle, G Dufour, C K Jørgensen, H Berthou *Chem. Phys. Lett.* **41** 199 (1976)
103. S A Yavna, V L Sukhorukov, V F Demekhin *Fiz. Tv. Tela* **26** 2300 (1984) [g]
104. C K Jørgensen *Struct. Bonding (Berlin)* **24** 1 (1975)
105. D J Lam, B W Veal, D E Ellis *Phys. Rev. B* **22** 5730 (1980)
106. C K Jørgensen, H Berthou *Chem. Phys. Lett.* **13** 186 (1972)
107. H Berthou, C K Jørgensen, C Bonnelle *Chem. Phys. Lett.* **38** 199 (1976)
108. B E Koel, G Praline, H I Lee, J M White *J. Electron Spectrosc. Relat. Phenom.* **21** 31 (1980)
109. A Fujimori, J Osterwalder *J. Phys. C, Solid State Phys.* **17** 2869 (1984)
110. S A Prosandeev, Yu A Teterin, R V Vedrinskii, V M Kulakov *Preprint IAE-3206* (Moscow: Kurchatov Institute of Nuclear Energy, 1979)
111. V P Sachenko, V F Demekhin *Zh. Eksp. Teor. Fiz.* **49** [3(9)] 765 (1965) [h]
112. T Ålberg *Ann. Acad. Sci. Fenn.* **308** 1 (1969)
113. L Schlapbach, J Osterwalder *Solid State Commun.* **42** 271 (1982)
114. A Fujimori *Phys. Rev. B* **27** 3992 (1983)
115. G Praline, B E Koel, R L Hange, H I Lee, J M White *J. Electron Spectrosc. Relat. Phenom.* **21** 17 (1980)
116. A Fujimori *Phys. Rev. B* **28** 4489 (1983)
117. C S Fadley, S B M Hagström, M P Klein, D A Shirley *J. Chem. Phys.* **48** 3779 (1968)
118. W C Lang, B D Padalia, L M Watson, D J Fabian *J. Electron Spectrosc. Relat. Phenom.* **7** 357 (1975)
119. P Burroughs, A Hamnett, A F Orchard, G Thornton *J. Chem. Soc., Dalton Trans.* 1686 (1976)
120. L P Kazanskii, A S Saprykin, A M Golubev, V I Spitsyn *Dokl. Akad. Nauk SSSR* **233** 405 (1977) [f]
121. A F Orchard, G Thornton *J. Electron Spectrosc. Relat. Phenom.* **10** 1 (1977)
122. B D Padalia, W C Lang *Indian J. Phys. A* **52** 463 (1978)
123. A F Orchard, G Thornton *J. Electron Spectrosc. Relat. Phenom.* **13** 27 (1978)
124. I N Shabanova, E I Zabolotskii *Fiz. Tv. Tela* **21** 2147 (1979) [g]
125. J C Fuggle, M Campagna, Z Zolnierek, R Lässer, A Platau *Phys. Rev. Lett.* **45** 1597 (1980)
126. I N Shabanova, A A Samokhvalov, B A Gizhevskii *Fiz. Tv. Tela* **22** 246 (1980) [g]
127. W-D Schneider, C Laubschat, I Nowik, G Kaindl *Phys. Rev. B* **24** 5422 (1981)
128. T N Bondarenko, V V Nemoshkalenko, V N Uvarov, S V Borisenko, A I Senkevich *J. Electron Spectrosc. Relat. Phenom.* **88–91** 385 (1998)
129. T M Zimkina, A S Shulakov, A P Braiko *Fiz. Tv. Tela* **23** 2006 (1981) [g]
130. A S Shulakov, T M Zimkina, V A Fomichev *Izv. Akad. Nauk SSSR, Ser. Fiz.* **49** 1495 (1985)
131. D F Mullica, C K C Lok, H O Perkins, V Young *Solid State Commun.* **52** 775 (1984)
132. Yu A Teterin, A S Baev, A Yu Teterin, V M Kulakov *Dokl. Akad. Nauk* **347** 359 (1996) [f]
133. Yu A Teterin, T N Bondarenko, A Yu Teterin, A M Lebedev, I O Utkin *Radiokhimiya* **40** 103 (1998) [c]
134. Yu A Teterin, T N Bondarenko, A Yu Teterin, A M Lebedev, I O Utkin *J. Electron Spectrosc. Relat. Phenom.* **88–91** 267 (1998)
135. Yu A Teterin, T N Bondarenko, A Yu Teterin, A M Lebedev, I O Utkin *J. Electron Spectrosc. Relat. Phenom.* **96** 221 (1998)
136. A M Lebedev, Yu A Teterin, T N Bondarenko, A S Nikitin, A Yu Teterin, K E Ivanov, I O Utkin *Kondens. Sredy Mezhfaz. Granitsy* **2** 324 (2000)
137. Yu A Teterin, A Yu Teterin, A M Lebedev, I O Utkin *Radiokhimiya* **40** 97 (1998) [c]
138. Yu A Teterin, A Yu Teterin, A M Lebedev, I O Utkin *J. Electron Spectrosc. Relat. Phenom.* **88–91** 275 (1998)
139. K Tatsumi, M Tsutsui, G W Beall, D F Mullica, W O Milligan *J. Electron Spectrosc. Relat. Phenom.* **16** 113 (1979)
140. D F Mullica, C K C Lok, H O Perkins, V Young *Phys. Rev. B* **31** 4039 (1985)
141. M S Ioffe, Yu G Borod'ko *J. Electron Spectrosc. Relat. Phenom.* **11** 235 (1977)
142. G Crecelius, G K Wertheim, D N E Buchanan *Phys. Rev. B* **18** 6519 (1978)
143. J F Herbst, J M Burkstrand, J W Wilkins *Phys. Rev. B* **22** 531 (1980)
144. L Schlapbach *Solid State Commun.* **38** 117 (1981)
145. I Nagakura, T Ishii, T Sagawa *J. Phys. Soc. Jpn.* **33** 754 (1972)
146. M Campagna, G K Wertheim, E Bucher *Struct. Bonding (Berlin)* **30** 99 (1976)
147. D I Khomskii *Usp. Fiz. Nauk* **129** 443 (1979) [i]
148. A N Kocharyan, D I Khomskii *Zh. Vsesoyuz. Khim. O-va im. D I Mendeleeva* **26** 639 (1981) [j]
149. G K Wertheim, M Campagna *Chem. Phys. Lett.* **47** 182 (1977)
150. Å Fäldt, H P Myers *Phys. Rev. B* **33** 1424 (1986)
151. I Nowik, M Campagna, G K Wertheim *Phys. Rev. Lett.* **38** 43 (1977)
152. J C Fuggle, F U Hillebrecht, Z Zolnicrek, R Lässer, Ch Freiburg, O Gunnarsson, K Schönhammer *Phys. Rev. B* **27** 7330 (1983)
153. C Laubschat, B Perscheid, W-D Schneider *Phys. Rev. B* **28** 4342 (1983)
154. S Raaen, R D Parks *Phys. Rev. B* **32** 4241 (1985)
155. G Krill, L Abadli, M F Ravet, J P Kappler, A Meyer *J. Phys. (France)* **41** 1121 (1980)
156. C N R Rao, D D Sarma, P R Sarode, E V Sampathkumaran, L C Gupta, R Vijayaraghaven *Chem. Phys. Lett.* **76** 413 (1980)
157. A Franciosi, J H Weaver, N Martensson, M Croft *Phys. Rev. B* **24** 3651 (1981)
158. J-N Chazalviel, M Campagna, G K Wertheim, P H Schmidt *Phys. Rev. B* **14** 4586 (1976)
159. J-N Chazalviel, M Campagna, G K Wertheim, P H Schmidt *Solid State Commun.* **19** 725 (1976)
160. J-N Chazalviel, M Campagna, G K Wertheim, P H Schmidt, Y Yafet *Phys. Rev. Lett.* **37** 919 (1979)
161. F Iga, Y Takakuwa, T Takahishi, M Kasaya, T Kasuya, T Sagawa *Solid State Commun.* **50** 903 (1984)
162. G Krill, J P Senateur, A Amamou *J. Phys. F, Met. Phys.* **10** 1889 (1980)
163. C N R Rao, D D Sarma *J. Solid State Chem.* **45** 14 (1982)
164. A Fujimori *Phys. Rev. B* **28** 2281 (1983)
165. W-D Schneider, B Delley, E Wuillound, J-M Imer, Y Baer *Phys. Rev. B* **32** 6819 (1985)
166. S H Liu, K-M Ho *Phys. Rev. B* **26** 7052 (1982)
167. A Fujimory, J H Weaver *Phys. Rev. B* **32** 3422 (1985)
168. O Gunnarsson, K Schönhammer *Rhys. Rev. B* **28** 4315 (1983)
169. R V Vedrinskii, E V Vinnikov, S A Prosandeev, M I Buleev, A P Dement'ev, V I Zaporozhchenko *Izv. Akad. Nauk SSSR, Ser. Fiz.* **49** 1555 (1985)
170. T Jo, A Kotani *J. Magn. Magn. Mater.* **52** 396 (1985)

171. P W Anderson *Phys. Rev.* **124** 41 (1961)
172. G Krill, J P Kappler, A Meyer, L Abadli, M F Ravet *J. Phys. F, Met. Phys.* **11** 1713 (1981)
173. B D Padalia, V Prabhawalkar, P D Prabhawalkar, E V Sampathkumaran, L C Gupta, R Vijayaraghaven *J. Phys. C, Solid State Phys.* **14** L93 (1981)
174. L Schlapbach, S Hüfner, T Riesterer *J. Phys. C, Solid State Phys.* **19** (4) L63 (1986)
175. A Fujimori, J H Weaver *Phys. Rev. B* **31** 6345 (1985)
176. C N R Rao, D D Sarma, P R Sarode, R Vijayaraghavan, S K Dhar, S K Malik *J. Phys. C, Solid State Phys.* **14** L451 (1981)
177. E Wuilloud, B Delley, W-D Schneider, Y Baer *Phys. Rev. Lett.* **53** 202 (1984)
178. G Thornton, M J Dempsey *Chem. Phys. Lett.* **77** 409 (1981)
179. J F Herbst, J W Wilkins *Phys. Rev. Lett.* **43** 1760 (1979)
180. D W Lynch, R D Cowan *Phys. Rev. B* **36** 9228 (1987)
181. Yu A Teterin, M V Ryzhkov, V A Gubanov, S G Gagarin, in *Kvantovaya Khimiya Tverdogo Tela* (Preprint of Urals Scientific Centre of Academy of Sciences of the USSR) (Ed. V A Gubanov) (Sverdlovsk: Institute of Chemistry, 1984)
182. Yu A Teterin, M V Ryzhkov, V A Gubanov, S G Gagarin *Dokl. Akad. Nauk SSSR* **284** 915 (1985) [f]
183. Yu A Teterin, A S Baev, S G Gagarin, V D Klimov *Radiokhimiya* **27** 3 (1985)
184. V A Gubanov, D E Ellis, A J Freeman *Fiz. Tv. Tela* **19** 409 (1977) [g]
185. J A Bearden *Rev. Mod. Phys.* **39** 78 (1967)
186. A V Soldatov, A N Gusatinskii, M G Karin, K K Sidorin, O A Sadovskaya *Izv. Akad. Nauk SSSR, Neorg. Mater.* **19** 1052 (1983) [k]
187. A V Soldatov, A N Gusatinskii, G I Al'perovich *Fiz. Tv. Tela* **27** 3423 (1985) [g]
188. S B M Hagström, P O Hedén, H Löfgren *Solid State Commun.* **8** 1245 (1970)
189. R L Barinskii, I M Kulikova, E P Shevchenko *Izv. Akad. Nauk SSSR, Ser. Fiz.* **46** 724 (1982)
190. R L Barinskii, E P Shevchenko, I M Kulikova, A I Likhtenshtein *Dokl. Akad. Nauk SSSR* **274** 562 (1984) [f]
191. I M Kulikova, R L Barinskii *Izv. Akad. Nauk SSSR, Ser. Fiz.* **49** 1476 (1985)
192. T N Bondarenko, V N Uvarov, S V Borisenko, Yu A Teterin, V P Dzeganovski, A M Sych, Yu A Titov *J. Korean Phys. Soc.* **32** 65 (1998)
193. T N Bondarenko, S V Borisenko, V N Uvarov, Yu A Teterin, A N Yaresko, V P Dzeganovski, A M Sych, Yu A Titov, A I Senkevich *Ferroelectrics* **223** 91 (1999)
194. Yu A Teterin, A S Baev, T N Bondarenko, in *Voprosy Atomnoi Nauki i Tekhniki (Ser. Obshchaya i Yadernaya Fizika)* [Problems of Nuclear Science and Technics (Series of General and Nuclear Physics)] (Moscow: TsNIIatominform, 1987) Vol. 4 (40), p. 8
195. T N Bondarenko, Yu A Teterin, A S Baev *Dokl. Akad. Nauk SSSR* **279** 109 (1984) [f]
196. Yu A Teterin, A S Baev, Yu P Dikov, A I Gorshkov *Dokl. Akad. Nauk SSSR* **263** 610 (1982) [f]
197. V F Demekhin, V L Sukhorukov, Yu I Bairachnyi *Izv. Sib. Otd. Akad. Nauk SSSR, Ser. Khim.* **9** (4) 68 (1975)
198. C Bonnelle, G Giorgi *Phys. Rev. B* **50** 16255 (1994)
199. M Ohno, R E LaVilla *Phys. Rev. B* **39** 8852 (1989)
200. G Wendin *Struct. Bonding (Berlin)* **45** 1 (1981)
201. J F Herbst, D N Lowy, R E Watson *Phys. Rev. B* **6** 1913 (1972)
202. R V Vedrinskii, S A Prosandeev, I I Geguzin, Yu A Teterin *Preprint IAE-3200* (Moscow: I V Kurchatov Institute of Nuclear Energy, 1979)
203. V I Matveev, E S Parilis *Usp. Fiz. Nauk* **138** 573 (1982) [i]
204. E-J Cho, S-J Oh, S Suga, T Suzuki, T Kasuya *J. Electron Spectrosc. Relat. Phenom.* **77** 173 (1996)
205. D R Mullins *J. Electron Spectrosc. Relat. Phenom.* **114–116** 333 (2001)
206. R Vercaemst, D Poelman, L Fiermans, R L van Meirhaeghe, W H Laflere, F Cardon *J. Electron Spectrosc. Relat. Phenom.* **74** 45 (1995)

[a] — *J. Struct. Chem. (Engl. Transl.)*
[b] — *Russ. J. Coord. Chem. (Engl. Transl.)*
[c] — *Radiochemistry (Engl. Transl.)*
[d] — *Russ. J. Inorg. Chem. (Engl. Transl.)*
[e] — *Theor. Exp. Chem. (Engl. Transl.)*
[f] — *Dokl. Chem. (Engl. Transl.)*
[g] — *Phys. Solid State (Engl. Transl.)*
[h] — *J. Exp. Theor. Phys. (Engl. Transl.)*
[i] — *Physics-Uspekhi (Engl. Transl.)*
[j] — *Mendeleev Chem. J. (Engl. Transl.)*
[k] — *Inorg. Mater. (Engl. Transl.)*